Food and Agriculture Organization of the United Nations

UNESCO IHE DELFT

REMOTE SENSING FOR WATER PRODUCTIVITY

WATER ACCOUNTING SERIES

Water Accounting in the Niger River Basin

Water Accounting in the Niger River Basin

REMOTE SENSING FOR WATER PRODUCTIVITY

WaPOR water accounting series

Published by
the Food and Agriculture Organization of the United Nations
and
IHE Delft Institute for Water Education

Required citation:

FAO and IHE Delft. 2020. *Water Accounting in the Niger River Basin.* FAO WaPOR water accounting reports. Rome. https://doi.org/10.4060/cb1274en

ISBN 978-92-5-133378-5 [FAO]

Cover photo: Yann Fauché

Contents

Tables

Figures

Acknowledgements

This report was prepared by Bich Tran, Solomon Seyoum and Marloes Mul through a collaboration between IHE Delft Institute for Water Education and the Food and Agriculture Organization of the United Nations, with contributions from Claire Michailovsky, Bert Coerver, Quan Pan, Elga Salvadore, and Abebe Chukalla.

This report is an output of project on "using remote sensing in support of solutions to reduce agricultural water productivity gaps" (http://www.fao.org/in-action/remote-sensing-for-water-productivity/en/) funded by the Government of The Netherlands. Water Accounting Plus is an approach which is based on open access data sets and information. The validation of the water accounts for the Niger River Basin depends on observed data. Though not having direct contact, we appreciated all the institutions that publish their database openly, which are all valuable for this water accounts study. These institutions and research groups include, but not limited to, the Niger Basin Authority (ABN), the World Protected Area Database, NASA's Goddard Space Flight Center (GSFC), and the International Groundwater Resources Assessment Centre (IGRAC). We are also grateful to Frank van Weert (Wetlands International) for sharing his insights into the Inner Niger Delta and Office du Niger, and Eddy Wymenga (Altenburg & Wymenga ecological consultants) for sharing the digital modelled flood maps and insights into the research work in the Inner Niger Delta.

Abbreviations and acronyms

ΔS	Total Water Storage Change
ABN	Niger Basin Authority
AETI	Actual Evapotranspiration and Interception
CHIRPS	Climate Hazards Group InfraRed Precipitation with Stations
DGIS	Ministry of Foreign Affairs of the Government of The Netherlands
ET_a	Actual Evapotranspiration (Total)
ET_{incr}	Incremental Evapotranspiration
ET_{rain}	Rainfall Evapotranspiration
FAO	Food and Agricultural Organization of the United Nations
GWF	Grey Water Footprint
GRACE	Gravity Recover And Climate Experiment
GRanD	Global Reservoir and Dam Database
IWMI	International Water Management Institute
LCC	Land Cover Classification
MLU	Modified Land Use
MWU	Managed Water Use
P	Precipitation
PLU	Protected Land Use
TWSA	Total Water Storage Anomalies
ULU	Utilized Land Use
WA+	Water Accounting Plus
WaPOR	FAO portal to monitor Water Productivity through Open access of Remotely sensed derived data
WDPA	World Database on Protected Areas

Executive summary

The Niger River Basin is one of the largest transboundary river basins globally, with 9 riparian countries joining the Niger Basin Authority. Covering a wide range of latitudes and longitudes, the climate over its area is diverse with extreme spatially variable rainfall and evapotranspiration and, thus, variable water generation and consumption. The water availability is affected by high inter-annual rainfall variability, with long periods of drought and damaging floods. There are many opportunities for water resources development in the basin, however, their realization maybe challenged by socio-economic limitations and lack of an overview of the state of the water resources of the basin. Moreover, limited or lack of up-to-date ground observations, in terms of duration, completeness and quality of hydro-meteorological records, makes it difficult to draw an appropriate picture of the water resources conditions. A rapid Water Accounting Plus (WA+) system which was designed by IHE Delft with its partners FAO and IWMI using open-access spatial data has been applied to gain insights into the state of the water resources in the basin.

This report describes the rapid water accounting study for the Niger River Basin using mainly open access remotely sensed data from FAO's data portal to monitor Water Productivity through Open access of remotely sensed derived data (WaPOR v2.0) database. For this study, the WaPOR datasets for the period from 2009 to 2018 was used. The WaPOR version 2.0 level 1 data of precipitation with 5km resolution and reference evapotranspiration with 20km resolution and level 2 with 100m resolution data of actual evapotranspiration, interception and land cover classification layers were used for WA+ analyses. Additional open access data were used in the analysis including the Gravity Recovery and Climate Experiment (GRACE) data to assess changes in total water storage, the World Database on Protected Areas and the Global Reservoir and Dam Database to reclassify the WaPOR land cover classification layers to WA+ classes. Following the water accounts, a detailed analysis using WaPOR data and WA+ results assessed the impact of irrigation water consumption in the Office du Niger irrigation scheme on the maximum flood extent in Inner Niger Delta, which is an important ecosystem function within the Delta.

The results of the rapid Water Accounting Plus for the Niger River Basin showed that though there is still uncertainty in amount and distribution of precipitation and evapotranspiration, at river basin level, the water budget is balanced over the period 2009-2015, with only a small error (1%). Further investigation on the quality of WaPOR data shows that there are anomalies in the Evapotranspiration data in specific years and for specific land covers. With consideration to these uncertainties, the result of the study suggests that the managed water is 3.7% of available water and 5% of exploitable water, out of which 59% is incremental consumption of irrigated crops, suggesting potential for augmenting future agricultural water withdrawals. However, the possibility of irrigation extension, for example in the Office du Niger irrigation scheme, depends greatly on the local seasonal water availability and can have undesirable impacts on the precious downstream ecosystem. The impacts on the ecosystem might not be visible in a short period of time (such as the duration used for this study). Therefore, possible impact of any future irrigation expansion should be thoroughly assessed using data of longer duration. Moreover, the irrigation efficiency of Office du Niger was evaluated to be rather low and did not change much since the study

by Vandersypen et al. (2006). This is mainly due to the fact that the water supply to this irrigation scheme is continuous regardless of irrigation demand (Vandersypen et al., 2006). Thus the water use efficiency from this diversion has a lot of space for improvement. It is strongly recommended that any agriculture development and water withdrawal expansions take place in combination with foremost improvement of water productivity, sustainable management of groundwater storage, sustainable landscape management, and consideration of seasonal and climate variability and the impacts on the people and the ecosystems downstream where water is withdrawn and/or released.

1. Introduction

1.1. Case Study description

The Niger River Basin is one of the selected pilot basins for Rapid Water Accounting Plus using the WaPOR database. It is a transboundary basin, which covers an area of 2,137,000 km2 (between 11035'W, 4013'N and 15052' E, 23057'N). The nine riparian and member states of the Niger Basin Authority (NBA) are Benin, Burkina Faso, Cameroon, Chad, Ivory Coast, Guinea, Mali, Niger, and Nigeria (NBA, 2019). However, the delineated boundary of the basin also includes Algeria and Mauritania, where there are no perennial rivers (Figure 1-1). The Niger River is the third longest river in Africa (4,180km) after the Nile and Congo. It originates from the Guinea Highland in south-eastern Guinea. The river flows northeast through Mali, where it forms a vast flood plain known as the Inner Niger Delta. Then, the river turns southeast through Niger and along the border with Benin. After that, it enters Nigeria where it is merged with its main tributary, the Benue River, near Lokoja. Finally, the river flows through the Niger Delta and discharges into the Gulf of Guinea in the Atlantic Ocean.

The climate in Niger Basin is very diverse, varying almost all possible ecosystem zones in West and Central Africa, from arid and seasonally arid to humid equatorial climates (Andersen et al., 2005; UNEP, 2010, p. 61). Though most parts of the basin receive between 500-1,000 mm/year of rainfall, the mean annual precipitation varies from zero in the Sahara to above 3,000 mm/year near the coast. Rainfall in the Niger River Basin is strongly seasonal with non-uniform pattern throughout the basin and usually peaks in August or September (Amogu et al., 2010). This seasonality, in combination with the variability in topography, diversifies the flow conditions spatially in the Niger River water system. The Niger River Basin can be divided into 4 regions: the Upper Basin, the Inner Delta, the Middle Basin, and the Lower Basin (Figure 1-1):

- **The Upper Basin** is covered with an extensive network of tributaries in Guinea, Mali and Ivory Coast. The tributaries upstream of Bamako city are steep and yield a high level of annual mean runoff due to abundant rainfall (Andersen et al., 2005, p. 32). The Bani River, which is an important tributary joining the Niger before the Inner Delta, receives less rainfall and contribute less runoff than the upstream watersheds.
- **The Inner Delta** is characterized by a large lateral expansion of the river and high evaporation with about 60% of the inflow is evaporated or seeped in the delta (Welcomme and Dumont, 1986). It is a fertile alluvial floodplain that is connected with an extensive network of shallow lakes, which help slow the pace of flow and spread out the flood over its area (Andersen et al., 2005, p. 41).
- **The Middle Basin** is shared by Niger, Mali and Burkina Faso. The Northern side of the riverbank in this region is mostly inactive as there are mostly intermittent rivers in the Sahara. Along this segment, the Niger River is mostly fed by a series of tributaries on the Southern side of the river bank. There are two seasonal peak flows: the white flood in September after the local rainy season and the black flood in December from the delayed upstream flood (Andersen et al., 2005, p. 42).
- **The Lower Basin** is shared by Nigeria, Benin, Cameroon, and Chad. In the East of Lokoja is the Benue River, where there is only one high-flow season from May to October. In the West side, the Niger

River receives water from a network of tributaries in Nigeria and Benin. Downstream Lokoja is the Niger Delta where rainfall is typically high (3,000 mm/year), which adds about 20% of the total discharge into the Gulf of Guinea (Andersen et al., 2005, p. 46).

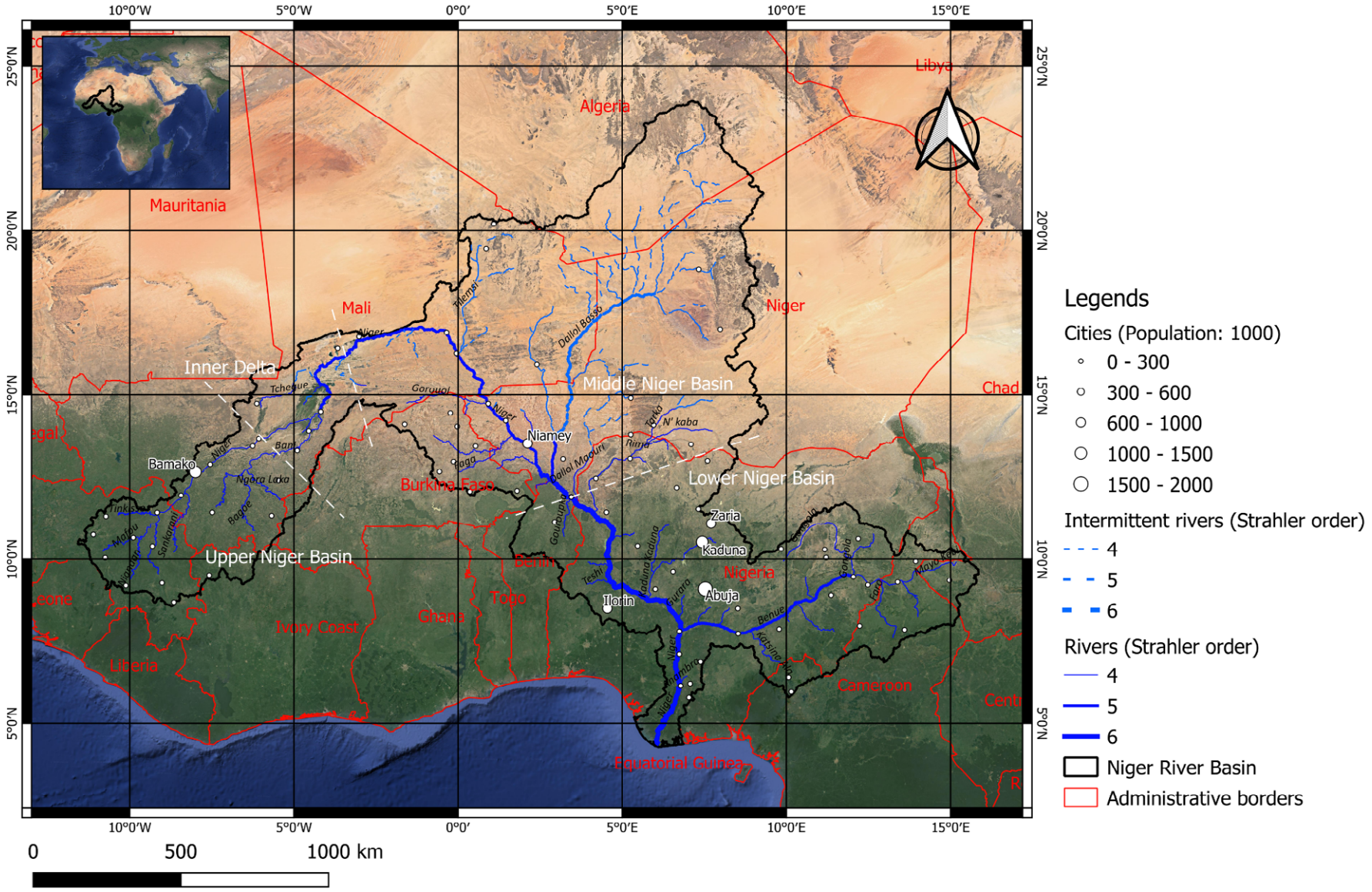

Figure 1-1. The Niger River Basin. (Sources: River basin (HydroSHED), River network (FAO AQUAMAP) and cities (NatureEarthData))

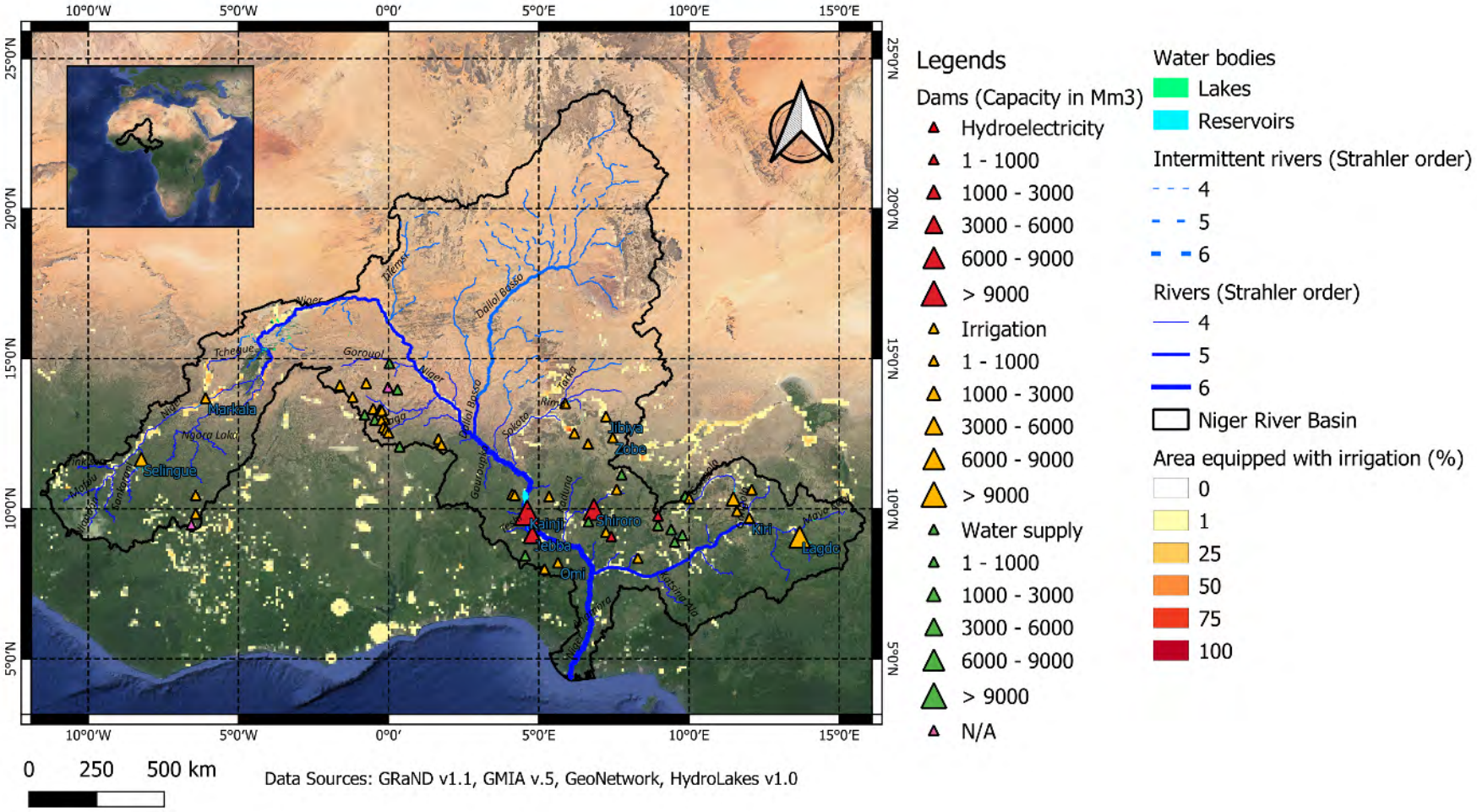

Figure 1-2: Overview of surface water resources developments in the Niger River Basin: Location, capacity, and use of dams, and area equipped with irrigation facility (in percentage of grid area).

1.2. Water resources developments and challenges in the Niger River Basin

1.2.1. Overview of water resources developments

Several dams have been built on the Niger River and its tributaries for hydropower generation, irrigation and water supply. Most of the Niger River large dams are in Nigeria, while Burkina Faso has many small dams (Figure 1-2). The existing dams in the Niger River Basin are substantial to electricity generation and irrigation in the main riparian countries (UNEP, 2010, p. 62). Almost all of the rice cultivation in Mali is accounted to large-scale rice-based irrigation schemes upstream of the Inner Delta, such as Office du Niger, which is supplied by the Markala Dam (Liénou et al., 2010). On one hand, the Niger River Basin, especially in the Upper and Middle Basin, was still considered relatively pristine with limited dams controlling the water resources, thereby sustaining the natural dynamics of the Inner Niger Delta (Liénou et al., 2010). On the other hand, dams constructed on the Niger River has caused reduction in flow and sediment delivered to the coastal delta, thus, causing shifts in the ecological equilibrium (Abam, 1999). Moreover, interdisciplinary studies in the Upper Niger Basin suggested that building new dams was not as efficient to increase economic growth and reduce poverty in the region as focusing on improving the existing infrastructures and economic activities (Zwarts et al., 2006, 2005).

The exploitation rate of the groundwater resources in the Niger River Basin is relatively small. Though there are some aquifers with large water resources in the middle and lower parts of the Niger River Basin (Figure 1-3), the lack of groundwater data was considered to hinder the practices of exploration, exploitation, and management of the groundwater resources (UNEP, 2010, p. 62). In Nigeria, these resource was estimated to be 8 billion times the national domestic water consumption (Akujieze et al., 2003). Moreover, investigation of long-term changes in terrestrial water storages from satellite gravity data from GRACE mission showed that groundwater resources have been increasing in most parts of the basin in the recent years, except for the upper basin in the Guinean highlands (Werth et al., 2017). This rise in groundwater table may be attributed to the increase in rainfall in the upper basin (Werth et al., 2017) in recent years. However, in the middle and lower basin, it was mainly attributed to the increase in recharge caused by land-use changes (Descroix et al., 2009; Leblanc et al., 2008). Increase in recharge may also raise the concentration of salts and fertilizer in groundwater (Favreau et al., 2009). Therefore, it was recommended that groundwater needs to be assessed and included in the water resources management of the Niger River Basin, for it can be an alternative water source during dry years (Werth et al., 2017).

1.2.2. Water resources management challenges

The challenges to water resources management in the Niger River Basin are: (1) growing demands for water, (2) underdeveloped infrastructure, and (3) extreme water hazards due to climate variability.

According to UNEP (2010, p. 61), the Niger River Basin was inhabited in 2010 by approximately 100 million people, 67% of which is in Nigeria, less than 8% is in Mali, and just over 8% is in Niger. The population growth rate was estimated to be approximately 3% per year, which means there will be growing demands on water as well as other water-related resources to meet the needs of the population in the basin. The development of water infrastructures in the basin is not parallel to the population growth. Since the nine member countries of the Niger Basin Authority are among the poorest in the world (Andersen et al., 2005, p. 58), poverty reduction is of higher priority. On the other hand in the Inner Niger Delta, the rural population is highly dependent on the seasonal fluctuations of the flow, which could be adversely affected by upstream developments (Zwarts et al., 2005) Therefore, cooperative investment and development are crucial for the future water resources management in the Niger River Basin.

The great challenge for the Niger River Basin is the intra- and inter-annual variability of the water resources due to climate variability and change. Though the region is traditionally known for its droughts rather than its floods (Mahé and Paturel, 2009; UNEP, 2010, p. 62), recently, the frequency and intensity of flood events in the city of Niamey, Niger has increased dramatically and three damaging floods (2010, 2012 and 2013) were observed in the last decade (Casse et al., 2015). Moreover, hydrological modelling suggests future climate and land-use changes will increase floods of the Niger (Aich et al., 2016). Though the climatic future of the Niger River Basin remains uncertain, the consensus is that increasing in climatic variability is expected, which will affect water resources availability, thus, the livelihood of millions (Goulden and Few, 2011). To tackle this challenge, monitoring fluxes and stocks of water temporally and spatially as well as the development of robust socio-eco-hydrologic models for better understanding, scenario projection and prediction is foreseen important.

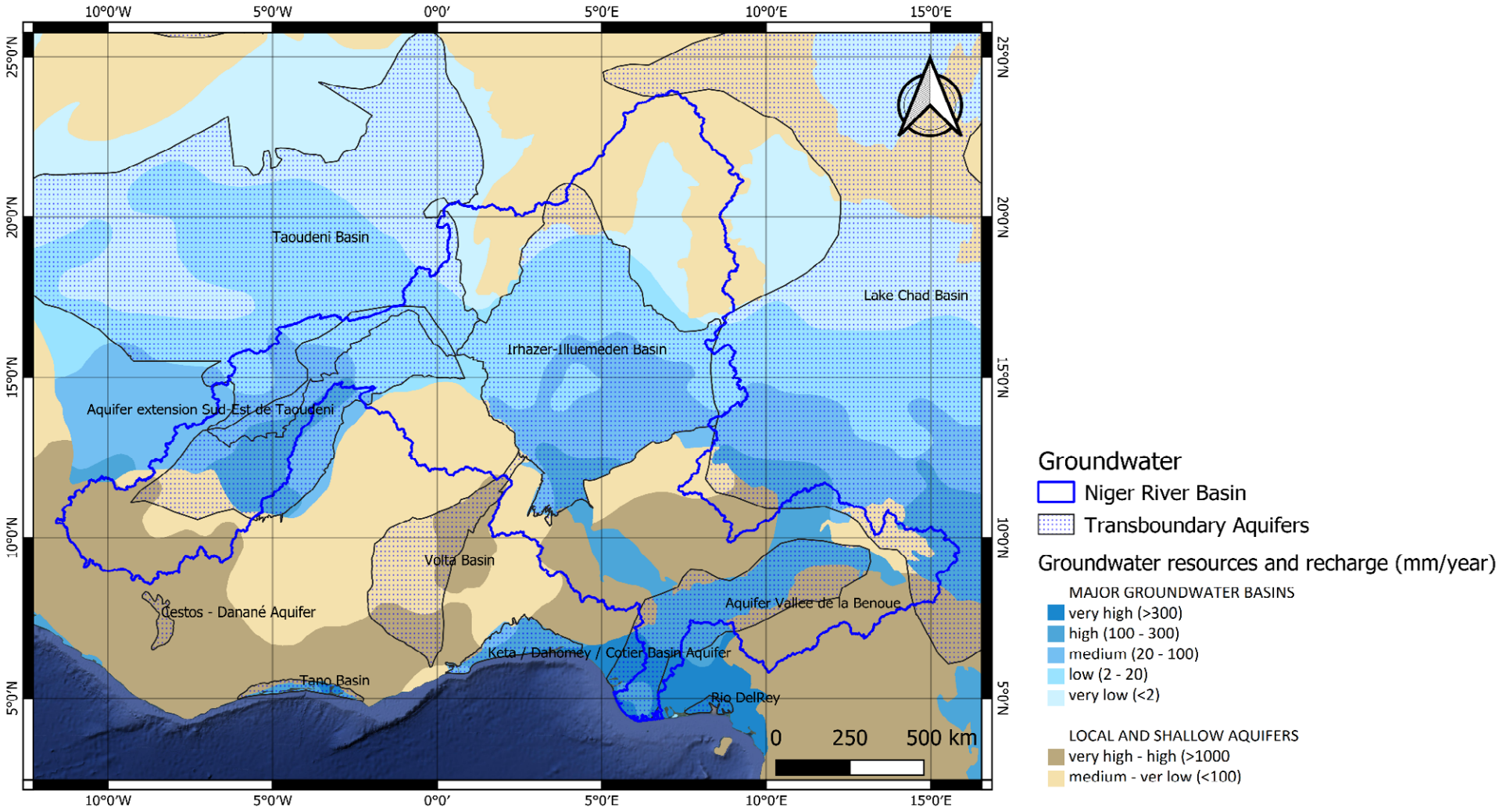

Figure 1-3: Overview of groundwater resources in the Niger River Basin: transboundary aquifers and groundwater recharge rate. Sources: IGRAC and WHYMAP.

1.2.3. Office du Niger

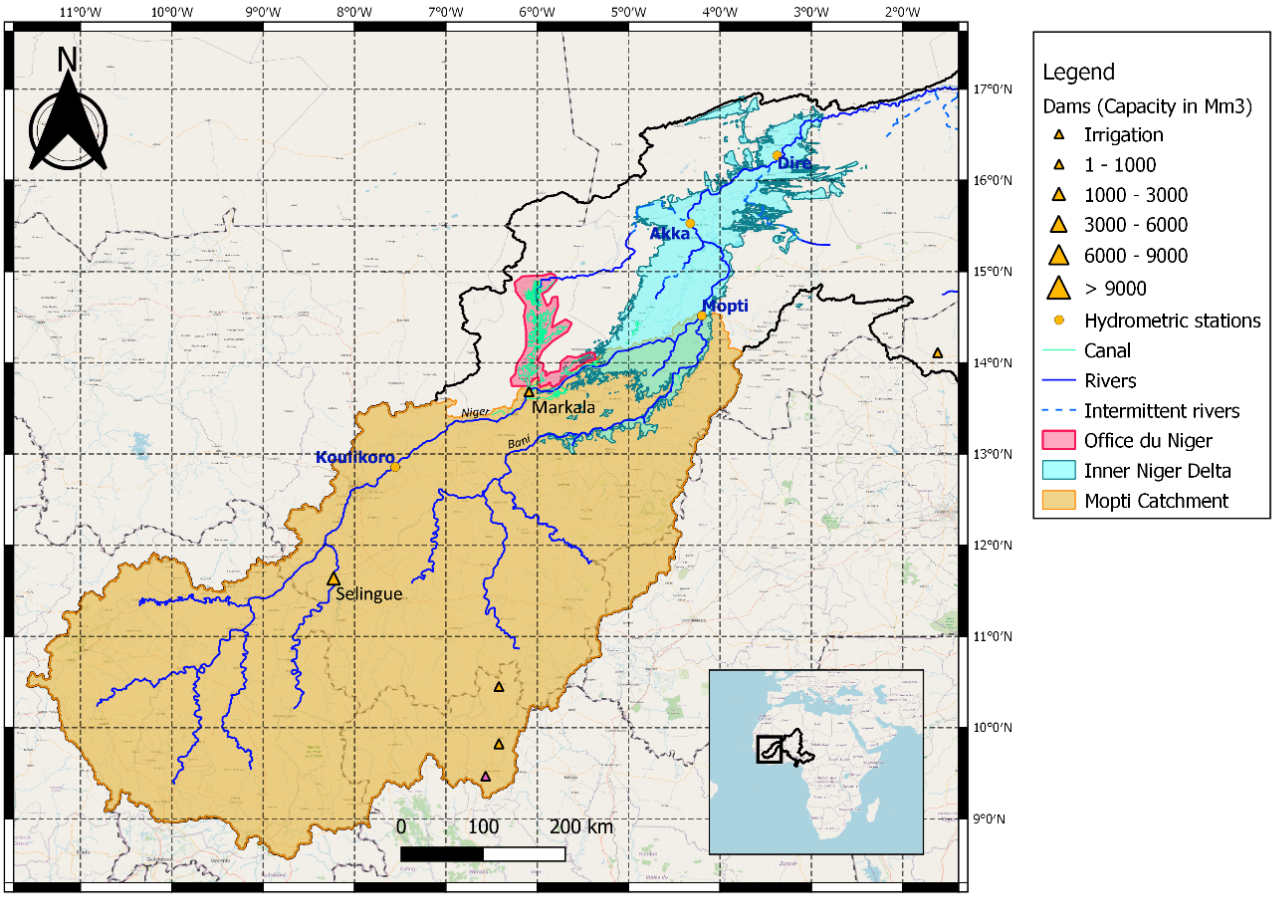

Figure 1-4: Upper Niger Basin and the boundaries of the Inner Niger Delta floodplain and Office du Niger. The boundary of Office du Nigewas delineated based on the map of its production zones (Annex I).

Founded in 1932 by the French Empire to supply cotton to its textile industry and produce rice for its colonized Sahelian region, the Office du Niger (Figure 1-4) is one of the oldest and largest irrigation schemes in Sub-Sahara Africa. The original plan was to develop about one million hectares (ha) in 50 years equipped with modern and commercial production system (Aw and Dejou, 1996). Nowadays, the total developed area is about 117,382 ha (Annex I), which is only about 10% of the original plan. Since the production of cotton ceased in 1970 (Aw and Dejou, 1996), the main production in Office du Niger became rice. Rice is cultivated in two seasons: the main rice growing season from June to December (la Saison) and a very hot season from March to June (Saison Sèche chaude), which is the beginning of the off-season culture (la Contre-saison). Vegetables are cultivated in the relatively cold period of la Contre-saison from January to March (Saison Sèche froide) (Zwart and Leclert, 2010). More recently sugarcane is being cultivated in the Office du Niger by sugar companies (Hertzog et al., 2012; Kassambara et al., 2018). The peak irrigation demand occurs in September at the end of the rainy season and the middle of the main rice growing season, when over 90% of the cultivated surface is irrigated (Vandersypen et al., 2006).

Directly downstream of the Markala dam is the third biggest Ramsar site in the world (Ramsar, 2004; Zwarts et al., 2009), the Inner Niger Delta, which is considered a biodiversity hotspot (Ramsar, 2020). The river discharge at the Mopti gauging station, located on the main Niger River within the Inner

Niger Delta boundary, is about 28 km^3/year varying seasonally from 0.2 km^3/month in dry months and peak flow varies between 4 to 9 km^3/month (Annex VI). The Inner Niger Delta area is semi-arid with annual precipitation of 200–500 mm/year, which is highly seasonal and with large inter-annual variation (Liersch et al., 2013). With low precipitation amounts in the area, the flood in the Inner Niger Delta depends on the river flow, which is generated by precipitation upstream (Liersch et al., 2013; Zwarts et al., 2005). The rainy season peaks between June and September, followed by the flood peak, which occurs between September and December due to propagation lag times (Ogilvie et al., 2015). The flood propagates gradually from the south-western part to the north-eastern part of the inner delta during the flooding season (September-December), and the two parts are often not flooded simultaneously. The maximum flood levels translated to flood extent and permanent water bodies are crucial to the state of wildlife habitats and biodiversity, and also influence fish production in the delta (Davies, 1996; Zwarts et al., 2009, 2005).

From the 1970s to 2000s, a major boost in paddy production in the Office du Niger was achieved thanks to the physical rehabilitation of irrigation network and economical and institutional reforms (Aw and Dejou, 1996; Vandersypen et al., 2006). However, as water was diverted from the Markala dam into the Office du Niger (1995-2004) continuously, regardless of irrigation demand, thereby systematically over-supplying the scheme, resulting in very low irrigation efficiencies was expected (Vandersypen et al., 2006). A more recent remote sensing-based irrigation performance assessment also found low average water productivity throughout the whole scheme and decreasing rice yields from the head to the end of the irrigation network, which could be attributed to failing irrigation and drainage infrastructure (Zwart and Leclert, 2010).

Meanwhile, the diversion to the irrigation scheme reduces the river flow, and thus, the flood level and extent in the Inner Niger Delta. Zwarts et al. (2005) estimated the diversion from the Markala dam into the Office du Niger to be about 2.7 km^3/year for the total irrigated area of 700 km2, which translates to about 3,800 mm/year of supply. Hertzog et al. (2012) reported this supply is between 2,000 and 2,500 mm/year, which is still more than twice the crop requirements (Vandersypen et al., 2006). This supply varies between seasons, around 100-140 m3/s of water from August to November and around 40-80 m3/s from December to April, which is equivalent to only a small fraction in the flood period (3-5% compared to peak flow in Mopti), but up to 50-60% of river flow in the dry period (Zwarts et al., 2005; Zwarts and van der Kamp, 2013). Using a wide range of historical hydro-climatic conditions, Liersch et al. (2019)'s model showed that the future irrigation demand could increase from currently 7% to one-third of mean annual discharge in 2045. Though there might be sufficient water for extending of irrigated agriculture during the wet season, it will have an impact on discharge peaks, which may decrease by up to 40%, thereby, reducing the inundated area in the Inner Niger Delta by as much as 21% (Liersch et al., 2019). Extension of irrigation in the dry season can be realised by reduction of water demand per area or provision of new dams in addition to the major existing Sélingué dam to increase river discharge. However, the dry-season cropping extension would be compromised during dry years even with additional dams, thus, improving water use efficiency of the irrigation schemes would be more sustainable in the long-term (Liersch et al., 2019).

1.3. Objective of water accounts

The purpose of this study is to assess water availability, consumptive use, and non-consumptive use in the Niger River Basin using remote sensing derived data from FAO WaPOR database in conjunction with other open-access data sources. In particular, the study seeks to investigate:

- What is the current water resources availability in the Niger River Basin?
- How much water is being consumed by different land covers/land use and in particular by agriculture in the Niger River Basin?
- What are the safe caps of water withdrawals for the agricultural sector in the Niger River Basin?

A system referred to as Water Accounting Plus (WA+) has been designed by IHE Delft with its partners FAO and IWMI using spatial data from earth observations and various other open-access databases. It aims to complement the lack of routine water resources data collection and incorporates spatially distributed water consumption. The WA+ framework is a reporting mechanism that summarizes the state of the water resources conditions through customized sheets. While the WaPOR database does not contain all the input data required for fully implementing the WA+ framework, key data is provided, such as precipitation, actual evapotranspiration, the breakdown between transpiration, evaporation and interception (FAO, 2018a).

Thus, the present study implements a rapid WaPOR-based WA+ framework, which used WaPOR v2.0 level 2 data (100m resolution), for the Niger River Basin which is available between 2009 and 2018. It focusses on the basin-wide analyses (WA+ Resource Base, as described in Chapter 2 – Section 2.3) as an initial analysis of the state of the water resources utilisation in a river basin. Finally, this report reflects on the quality of the WaPOR v2.0 data for WA+.

In addition, the water accounts will be followed by an analysis focusing on the Office du Niger to assess the consequences and sustainability of possible increases in water productivity in this irrigation scheme using remote sensing derived data from FAO WaPOR database in conjunction with other open-access data sources. In particular, this analysis seeks to investigate:

- What is the current irrigation water consumption in the Office du Niger and how has it changed over the 10-year period from 2009-2018? Can this explain the discrepancy between observed discharge and WaPOR water balance estimations of the Upper Niger Basin (the catchment of the Mopti gauging station)?
- How is the flood extent in the Inner Niger Delta changing over the last 10 years? And can WaPOR data be used to estimate flood extent?
- Is there a correlation between changes in water consumption in the Office du Niger and the flood extent in the Inner Niger Delta?

2. Materials and Methods

In this chapter, we describe: [2.1] key datasets from WaPOR database used for WA+; [2.2] preliminary assessment of WaPOR data using other global datasets and available observations; [2.3] the rapid assessment procedure for WA+ Resource Base Sheet; and [2.4] the methodology used to assess the impacts of irrigation in the Office du Niger on the Inner Niger Delta using WaPOR data and WA+.

2.1. WaPOR datasets

The WaPOR v2.0 database contains information at three different spatial resolutions. At continental level, data is available at 250m resolution (Level 1). For selected countries and basins, data is available at 100m resolution (Level 2). For detailed crop water productivity analyses for selected irrigation systems, 30m resolution data is available (Level 3). In this study, we used the Level 1 Precipitation data (5km resolution) and Level 2 Land Cover Classification (LCC) and Actual Evapotranspiration and Interception (AETI) data (100m resolution). The AETI data is further indicated as ET_a in this report.

2.1.1. Precipitation

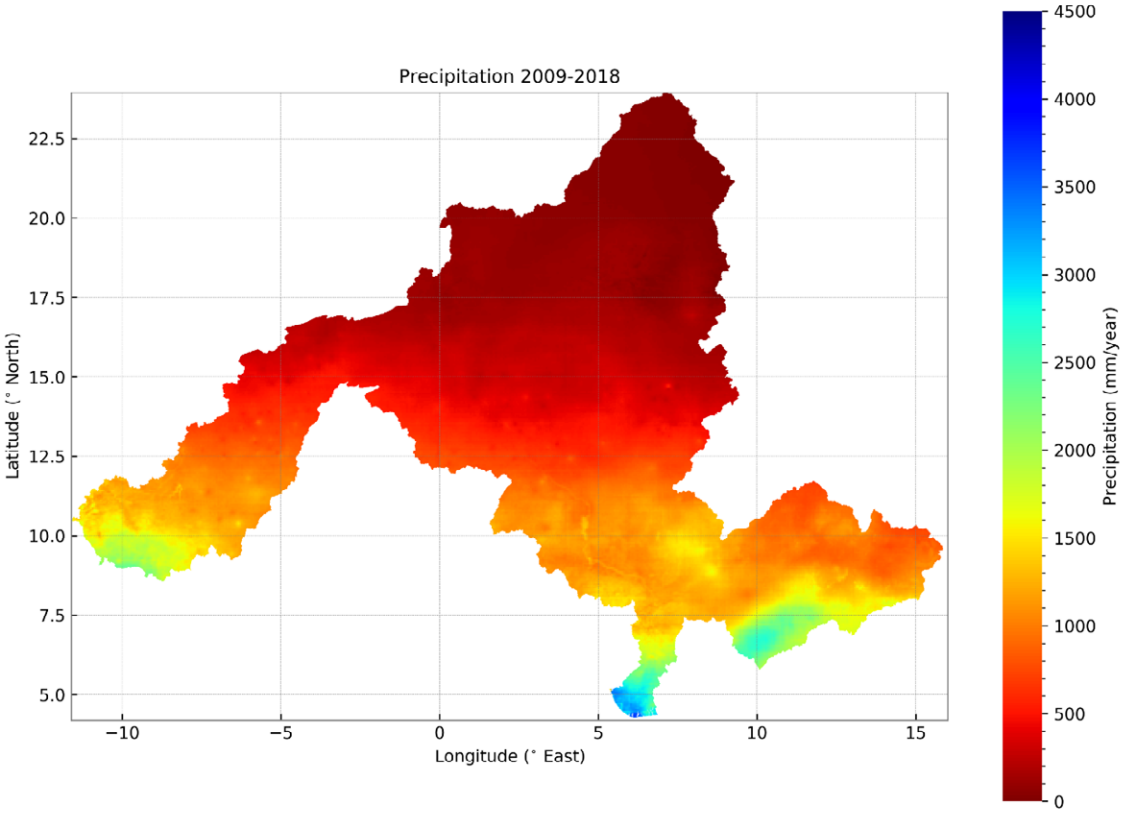

Figure 2-1: Spatial variation of WaPOR Precipitation (P) in the Niger River Basin based on the mean annual data from 2009 to 2018. Maps of the individual years are provided in Annex II.

WaPOR rainfall data is based on the CHIRPS database created by the United States Geological Survey (FAO, 2018a; Funk et al., 2015). Temporal variation of rainfall in WaPOR data can be seen in Figure 2-2. The monthly-average precipitation shows that hydrological year typically peaks in August, while December and January have very little rainfall. Therefore, for annual values aggregation, the hydrological year period was the same with the calendar year. The annual rainfall over the Niger River Basin varied between 630 to 760 mm/year during the period of 2009 - 2018. Figure 2-1 shows the spatial variability of the mean annual WaPOR precipitation (P) in the Niger River Basin for the years 2009-2018. It can be seen clearly in the precipitation map that most of the rainfall falls below the 150N latitude while the dryer part of the Niger River Basin receives less than 100 mm/year.

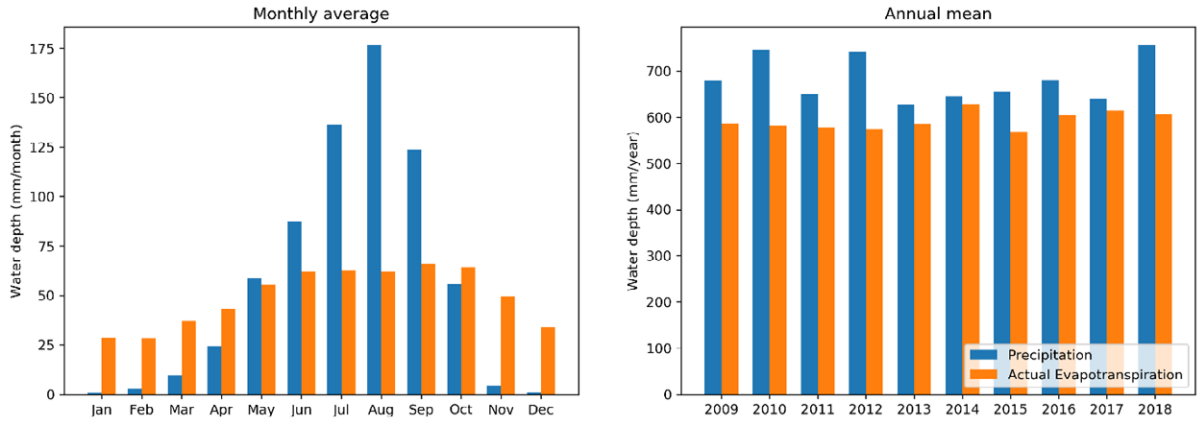

Figure 2-2: Monthly variation (left) and yearly variation (right) of precipitation and actual evapotranspiration in the Niger River Basin based on WaPOR data from 2009 to 2018.

2.1.2. Actual Evapotranspiration and Interception

The WaPOR evapotranspiration (ET_a) layer estimates the total evapotranspiration, including interception. Figure 2-3 shows the spatial variability of ET_a in the Niger River Basin. Similar to precipitation, ET_a in the inactive part of the basin is also less than 100mm/year. The highest ET_a value is observed in the Inner Niger Delta lakes and the forest near the border between Nigeria and Cameroon. It can be seen from this map that the Inner Niger Delta and Office du Niger have relatively high ET_a compared to the area at the same latitude. The mean annual ET_a of the whole basin ranges between 570 to 630 mm/year, which is lower than the mean annual rainfall of 630-760 mm/year. The basin therefore is a net water generator (Figure 2-2).The yearly variation of ET_a is different from that of rainfall, which causes the amount of water generated to vary between years. For example, the year 2014 shows highest annual ET_a, which is almost as high as annual precipitation of that year, resulting in almost zero available water. The monthly ET_a peaks one month later than precipitation and reaches as low as 28 mm/month in January and February, which is at the peak of the dry season. Therefore, the general pattern of monthly ET_a is similar to rainfall, which suggests that ET_a in the Niger River Basin is mostly limited by rainfall.

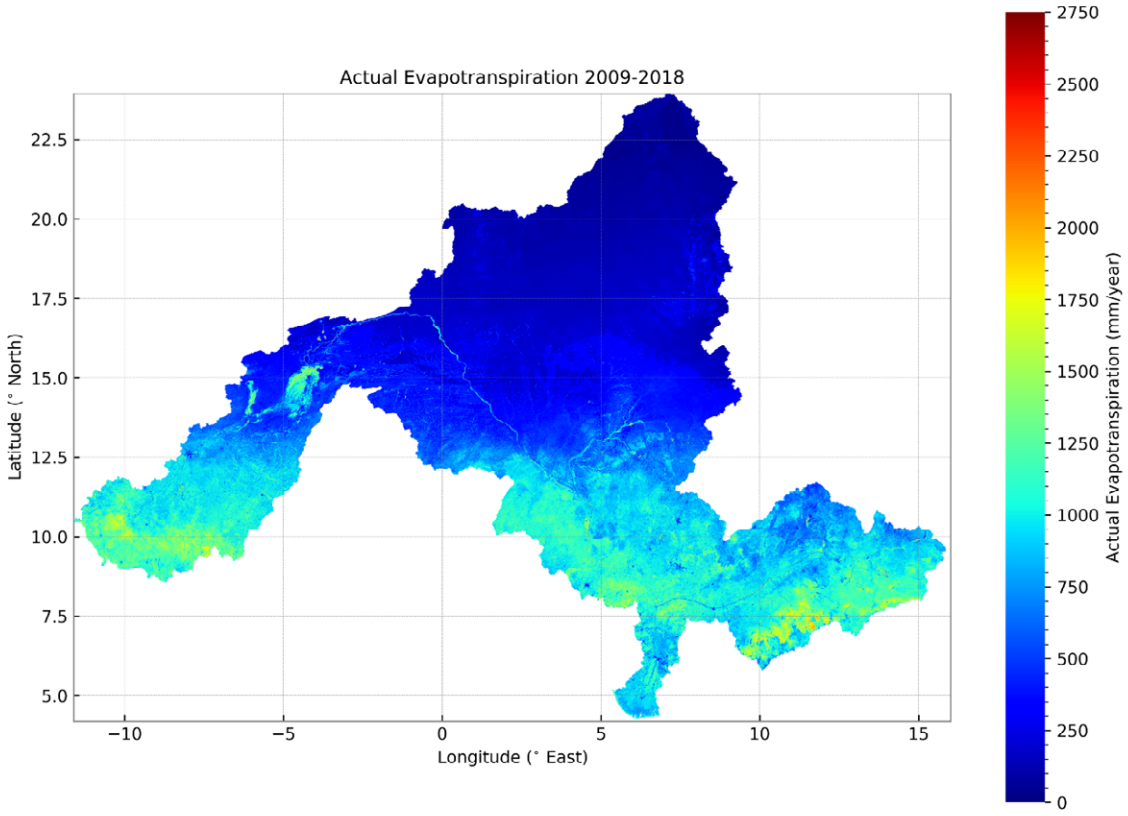

Figure 2-3: Spatial variation of WaPOR Actual evapotranspiration and Interception (ET_a) in the Niger River Basin based on the mean annual data from 2009 to 2018.maps of the individual years are provided in Annex III.

2.1.3. Land Cover Class

The WaPOR database provides a yearly land cover maps (LCC) for the Niger River Basin, which is based on the Copernicus land cover product (FAO, 2019). The land cover map of the year 2018 from the WaPOR database is presented in Figure 2-4. The land cover map provides 23 land use classes, with 11 different land cover classes for trees. This map shows that land cover varies mostly along latitudes with four main classes: bare/sparse vegetation at high latitude in Algeria, grassland in the Middle Basin, shrub land and rainfed crops in the lower basin, and finally forest (tree cover) in Guinea, Nigeria, and Cameroon at the lower latitudes. The largest area of irrigated cropland is in the Inner Delta and Office du Niger (Figure 2-4B). The largest water body is the Kainji reservoir in Nigeria (Figure 2-4C). Other large reservoirs can be also be distinguished from the land cover map: Selingue (Figure 2-4A) and Lagdo (Figure 2-4D). In these areas, there is a distinct boundary between the tree cover and the surrounding rainfed cropland suggesting large forest conversion to rainfed cropland with areas of protected forests remaining.

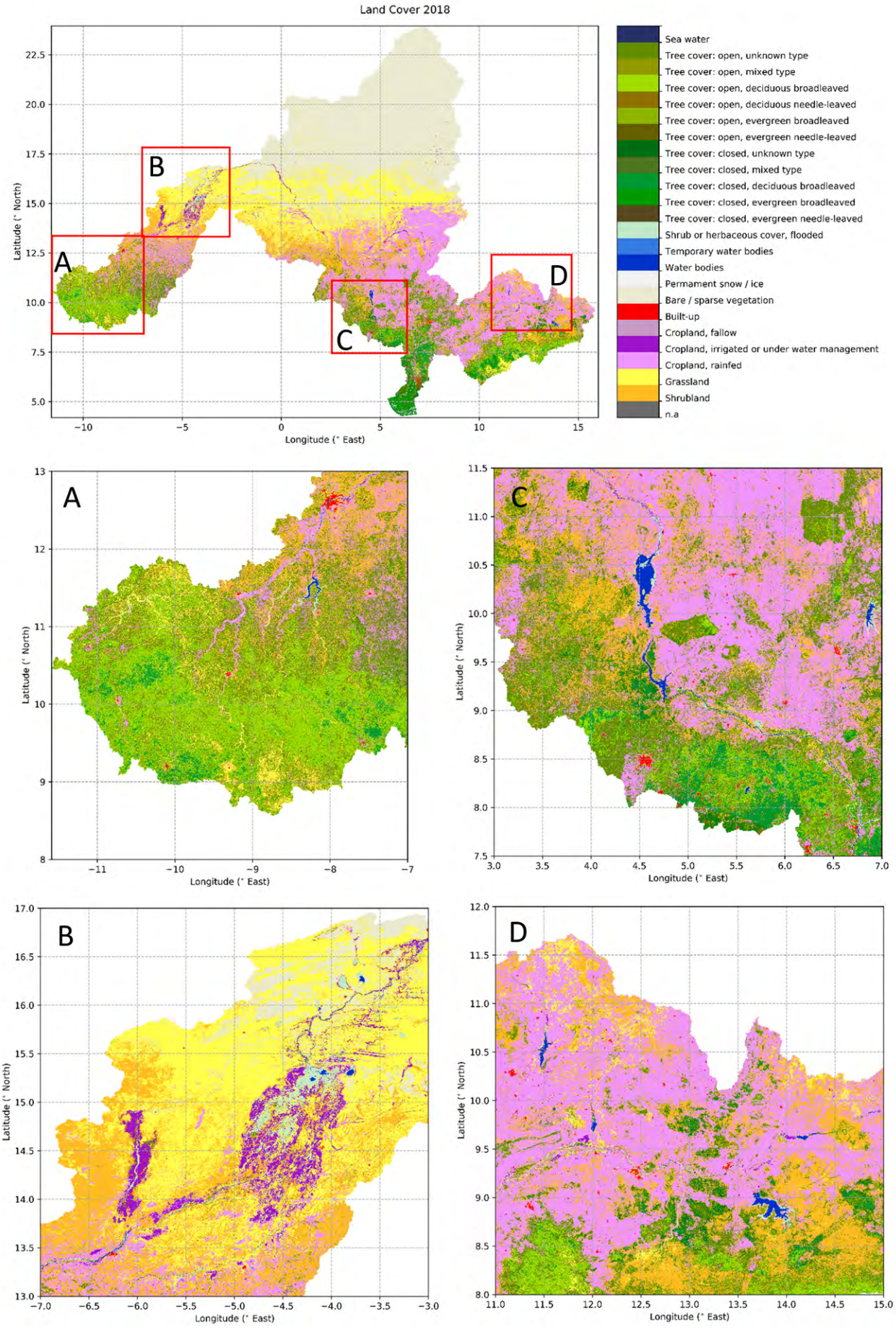

Figure 2-4: Spatial variation of the land cover area in the Niger River Basin in 2018 based on WaPOR L2_LCC_A layers. Maps of the individual years are provided in Annex IV.

Throughout the study period, there were no significant change in the area of natural land cover classes based on WAPOR data (Figure 2-5). There was only 0.2% (out of total basin area) increase in the area of irrigated area between 2009 and 2018 due to the expansion of irrigated scheme in the Inner Delta and Office du Niger. The total irrigated area estimated from WaPOR is 14,054 km2 in 2018, which shows an increase of 36% in 10 years from 10,333 km2 in 2009 and a 50% increase from 9,246 in 1997. The change in irrigated areas was significant in the years from 2011 to 2015. It should be noted that the irrigated cropland class in WaPOR's LCC layers is identified by applying a water deficit index that takes into consideration seasonal cumulated values of precipitation and actual evapotranspiration (FAO, 2019).

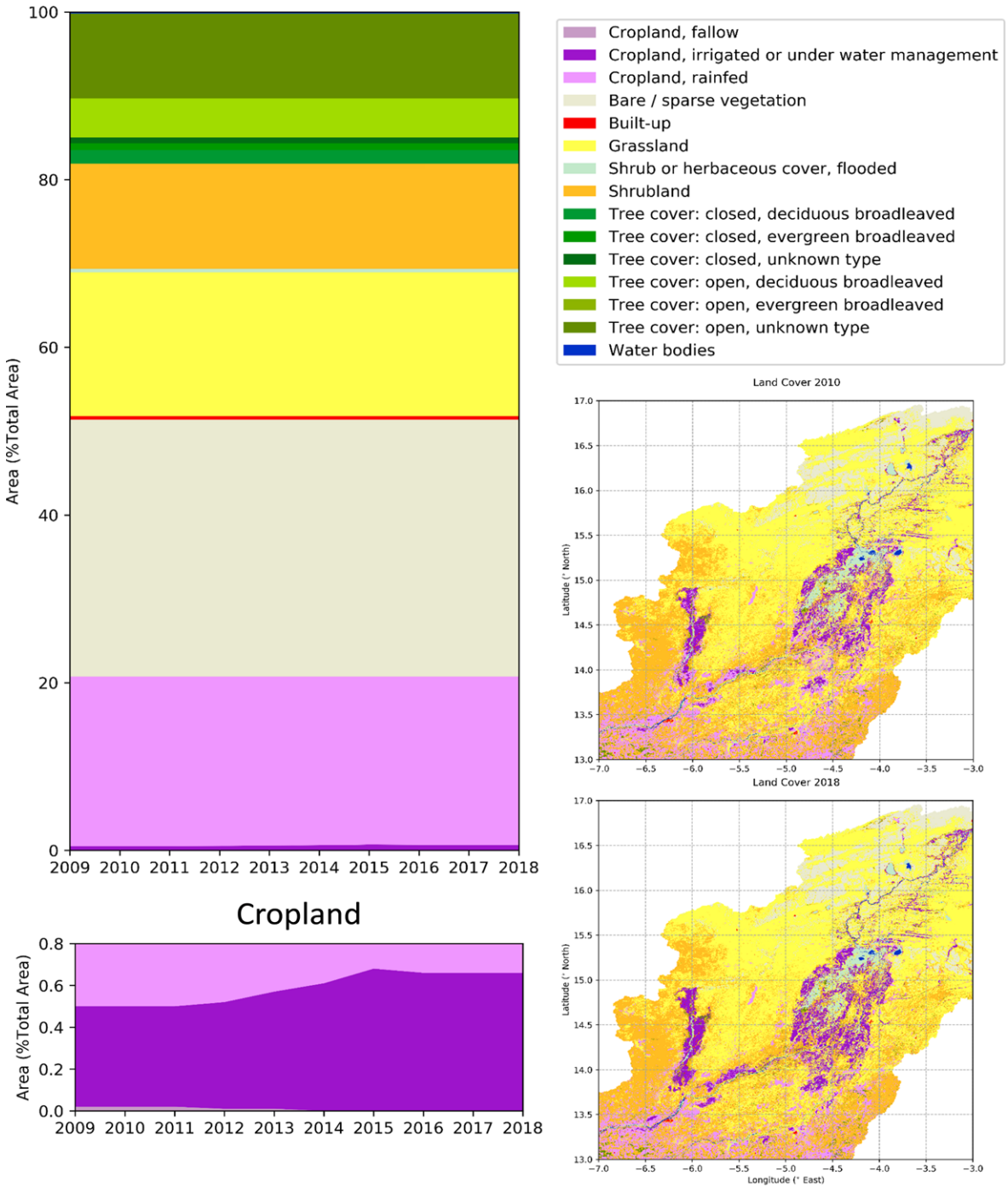

Figure 2-5: Land cover change in the Niger River Basin as detected from WaPOR L2_LCC_A layers

2.2. Preliminary assessments

Before using the data for the Water Accounting Plus, several checks were performed including [2.2.1] comparing WaPOR data with in situ observations, [2.2.2] mapping net water generation and consumption and identifying net consumer land cover class, and [2.2.3] assessing WaPOR-derived basin scale water balance using remotely sensed total water storage. The analyses presented here are based on annual values and do not incorporate the lag time of the river flow, which is significant in such a large river basin.

2.2.1. Comparison with in situ observations

The Niger River Basin is mostly ungauged: ground measurements of precipitation are discontinuous and usually dated before the 2000s, ground measurements of evaporation are monitored even less often. As studied by Prior (2016), remotely sensed precipitation data (including CHIRPS) shows poor correlation coefficient when comparing to the measurements at meteorological stations in the Niger River Basin collected from the National Oceanic and Atmospheric Administration (NOAA) database (average R2 < 0.6). However, the NOAA ground-based dataset was 54% missing data on daily basis, thus, the study also compared remotely sensed data with the NewLocClim estimates, which is based on nearest neighbour interpolation of available observations (Grieser et al., 2006 as cited in Prior, 2016). The results showed that CHIRPS data has the highest correlation with the NewLocClim estimates among other satellite products (CMORPH and TRMM) (Prior, 2016, p. 19). Since WaPOR Precipitation data is based on CHIRPS v2.0, it can be considered the best available precipitation product in the Niger River Basin. Nevertheless, it still remains a great challenge to validate and quantify uncertainty of remote sensing derived data such as WaPOR without reliable in situ measurements.

2.2.2. Water generation and consumption analysis

The WaPOR datasets for precipitation, actual evapotranspiration and interception, and land cover class were used to describe rainfall excess (water generation), and thus, lateral transport of water from water surplus to net water consumption per land cover class. Land cover classes that satisfy $P > ET_a$ are considered water generating areas while those fulfil $ET_a > P$ are net consumers of water (Bastiaanssen et al., 2014). The mean annual rainfall excess or deficit ($P - ET_a$) for the years from 2009 to 2018 is mapped in Figure 2-6. As can be seen in this map, the net water consumers are bare land/sparse vegetation in the dryer part of the basin, water bodies and irrigated cropland (mostly in the Inner Niger Delta and Office du Niger). Most of the Lower Basin are net water generating areas yielding less than 500 mm/year. The highest water yield is up to above 3000 mm/year in the Niger Delta, where the generated water cannot be stored and flows out to the ocean. The total $P - ET_a$ of the whole basin and each land cover class are reported in Table 2-1 and Table 2-2.

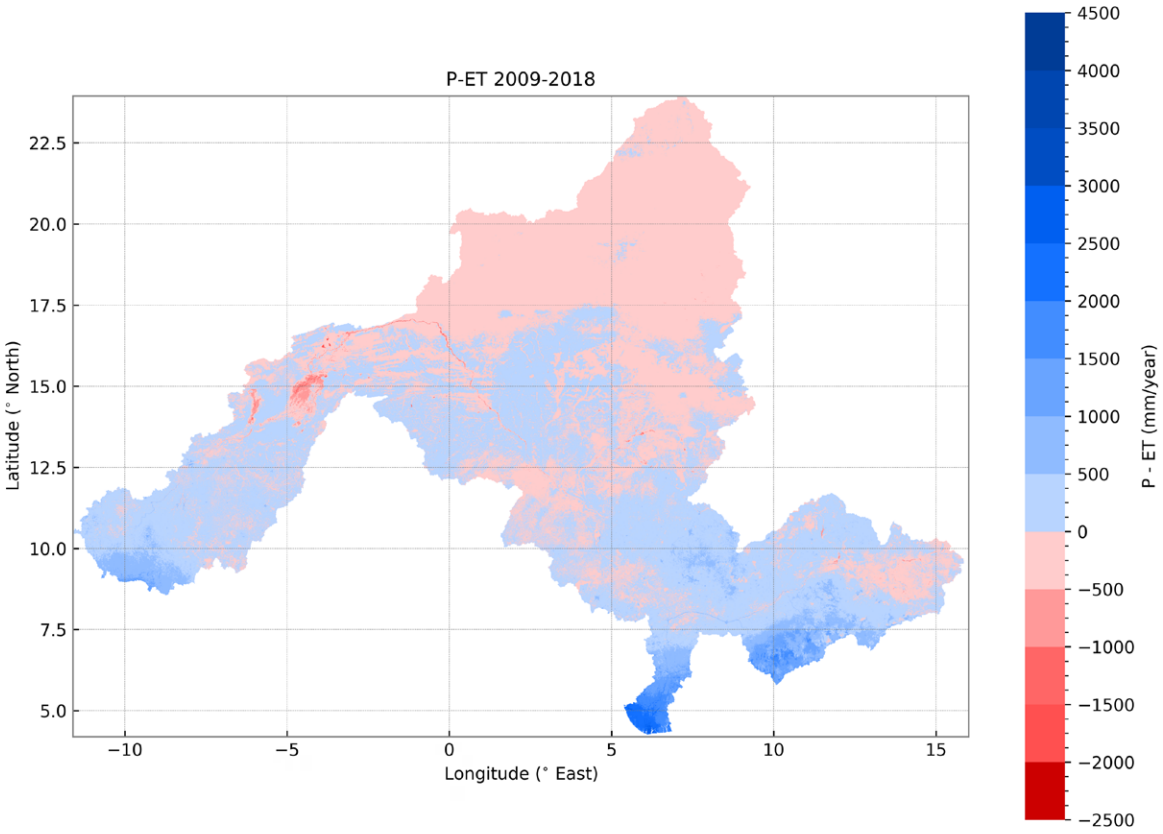

Figure 2-6: Mean annual difference between total Precipitation and total Actual Evapotranspiration and Interception ($P - ET_a$) from 2009 to 2018. Maps of individual years are provided in Annex V.

The basin wide long-term rainfall excess is 92 mm/year with positive value reported for all years between 2009 and 2018 (Table 2-1). Excess rainfall that is not consumed via evapotranspiration can generate surface runoff, interflow, drainage, groundwater recharge, seepage, and baseflow (Bastiaanssen et al., 2014). This is translated into about 196 km³/year of excess water generated from the basin, which is 13% of the total rainfall. This is also comparable to the mean outflow of 186 km³/year measured at Onitsha (250km downstream of Lokoja) from 1951 to 1980 (Mahé, 1993 as cited in Andersen et al., 2005, p. 91).

Based on the variation of $P - ET_a$ from WaPOR, 2010 and 2012 are the years with a lot of excess rainfall, while 2013, 2014, and 2017 are remarkably dry years. Though the damaging floods occurred in 2010 and 2012 at Niamey coincide with the high excess rainfall, the flood in 2013 cannot be explained with the same reason. This may be due to delayed flood from upstream in the previous year, but further validation is needed. Moreover, the significantly low excess rainfall derived from WaPOR in 2014 and 2017 does not seem to correspond with the drought observed from river flow measurements. For example, the flow monitored at all stations along the river in 2014 is higher than the quinquennial dry year (ABN, 2015). Therefore, a water balance assessment with consideration of water storage change is necessary to check if this low excess rainfall greatly reduce the outflow estimation in these supposed 'dry' years.

Table 2-1: The total annual precipitation (P) and actual evapotranspiration and interception (ET_a) from WaPOR data for the Niger River Basin from 2009 to 2018

Year	P (mm/year)	ET_a (mm/year)	$P - ET_a$ (mm/year)	P (km³/year)	ET_a (km³/year)	$P - ET_a$ (km³/year)	$P - ET_a$ (%P)
2009	688	594	95	1,471	1,269	202	14
2010	756	587	169	1,615	1,254	361	22
2011	658	584	74	1,406	1,248	159	11
2012	752	581	171	1,607	1,241	365	23
2013	635	591	44	1,357	1,263	94	7
2014	653	636	17	1,396	1,359	37	3
2015	664	575	89	1,419	1,228	190	13
2016	689	610	79	1,473	1,304	168	11
2017	648	621	28	1,385	1,326	59	4
2018	766	613	154	1,638	1,309	329	20
Average	**691**	**599**	**92**	**1,477**	**1,280**	**196**	**13**

The same calculation was done for each land cover class to identify net water generating and consuming land use class (Table 2-2). It can be seen here that about 30% of the Niger River Basin area is made up of the bare/sparse vegetation class, which is the biggest net water consumer (-20,268 Mm³/year). This class receives 15.7% of total precipitation, while contributing 16.8% of total ET_a (Figure 2-7). Irrigated cropland and water bodies are the second and third largest net water consumers, and consume -6,274 (23%) and -1,074 (4%) Mm³/year respectively, even though these two classes only accounts for less than 1% of the total area.

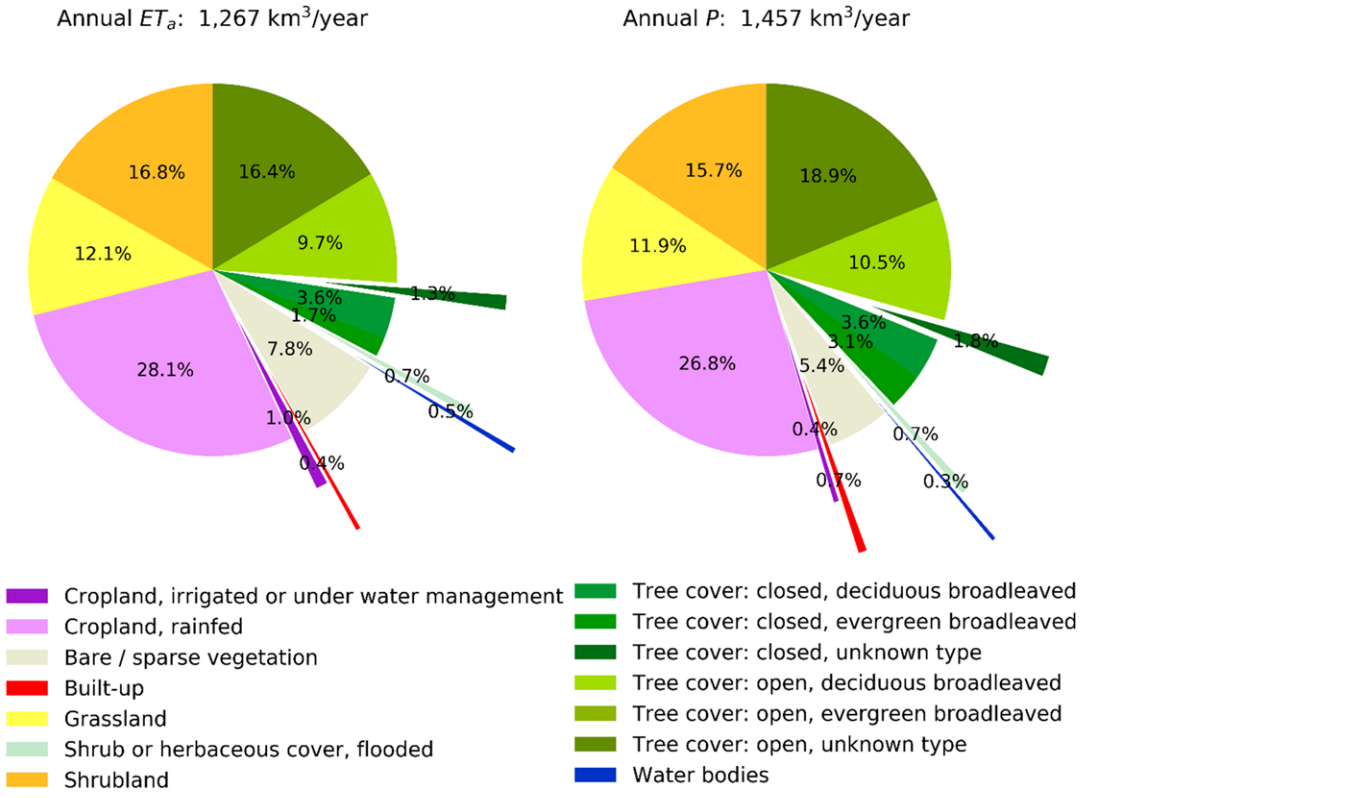

Figure 2-7: Contribution of the land cover classes to mean annual precipitation (P) and actual evapotranspiration (ET_a) of the Niger River Basin for the years from 2009 to 2018. The land cover classes that contribute less than 0.1% of the basin area are not presented in the graphs.

Table 2-2: The mean annual $P - ET_a$ for each land cover class from 2009 to 2018 in the Niger River Basin.

Land Cover Class Description	Area (km²)	Area (%)	P (mm/year)	P (Mm³/year)	ET_a (mm/year)	ET_a (Mm³/year)	$P - ET_a$ (mm/year)	$P - ET_a$ (Mm³/year)	$P - ET_a$ (%P)
Tree cover: open, unknown type	216,137	10.1%	1,286	277,925	970	209,677	316	68,238	25%
Cropland, rainfed	430,250	20.1%	918	394,913	835	359,276	83	35,636	9%
Tree cover: open, deciduous broadleaved	98,865	4.6%	1,562	154,383	1,257	124,279	304	30,104	19%
Tree cover: closed, evergreen broadleaved	17,772	0.8%	2,610	46,388	1,191	21,158	1,419	25,222	54%
Grassland	366,008	17.1%	480	175,595	424	155,350	55	20,245	12%
Shrubland	267,210	12.5%	868	231,953	804	214,798	64	17,153	7%
Tree cover: closed, unknown type	14,762	0.7%	1,768	26,094	1,115	16,462	652	9,627	37%
Tree cover: closed, deciduous broadleaved	34,543	1.6%	1,544	53,335	1,323	45,715	221	7,620	14%
Built-up	9,267	0.4%	1,155	10,704	537	4,972	618	5,731	54%
Shrub or herbaceous cover, flooded	9,563	0.4%	1,082	10,348	904	8,646	177	1,694	16%
Tree cover: open, evergreen broadleaved	335	<0.1%	2,188	733	1,364	457	824	276	38%
Sea water	103	<0.1%	2,713	281	909	94	1,799	186	66%
Cropland, fallow	156	<0.1%	260	41	172	27	27	4	10%
Water bodies	4,480	0.2%	1,108	4,963	1,346	6,032	-242	-1,085	-22%
Cropland, irrigated or under water management	12,612	0.6%	511	6,442	1,008	12,716	-497	-6,274	-97%
Bare / sparse vegetation	654,691	30.6%	122	79,702	153	99,970	-31	-20,268	-25%
Total	2,136,756	100%	-	1,473,799	-	1,279,629	-	194,109	13%

Figure 2-7 also shows that the relative contribution of all the land cover classes to total ET_a resembles the distribution of Precipitation, which means ET_a of each class is greatly limited by Precipitation. Net rainfall excess/deficit is also greatly dependant on available rainfall more than actual evaporative consumption. For example, the "Tree cover: Open, unknown type" class, which receives 1,286 mm/year of rainfall (Table 2-2), is the biggest net water generator (+68,238 Mm^3/year), though it has higher average ET_a (970 mm/year) than bare/sparse vegetation class (153 mm/year) – the biggest net water consumer, which receives only one-tenth of its rainfall (122 mm/year). Similarly, rainfed cropland, which is the second biggest net water generator (+35,636 Mm^3/year), also receives high rainfall (918 mm/year) while not consuming as much (835 mm/year). The "Tree cover: closed, evergreen broadleaved" class even has the same ratio of $(P - ET_a) / P$ with built-up class (54%) and consumes half as much ET_a. This might also suggests that ET_a values might be underestimated at some locations in the basin.

2.2.3. Basin and sub-basin scale water balance

Some components of the catchment water balance in the Niger River Basin, such as inter-basin transfer, groundwater and surface water outflow and change in storage cannot be directly derived from WaPOR datasets. Therefore, to check whether WaPOR data can close the water balance, additional data sources must be consulted: these include observed river discharge measurements and total water storage change estimate from satellite gravity measurement.

2.2.3.1. GRACE Total Water Storage Change

To assess how much of the difference between P and ET_a is due to change in total water storage, we used data from the Gravity Recovery and Climate Experiment (GRACE), a dual-satellite mission continuously monitoring and mapping Earth's changing gravity field to estimate the total water storage anomalies (TWSA). There are several GRACE solutions for TWSA estimation from gravity anomalies, which covers the whole globe from 2003 till end of 2015. The GSFC-v02.4-ICE6G solution (Luthcke et al., 2013) was used to validate the storage change in the water balance calculated using WaPOR data. Since GRACE solution provides mean monthly TWSA not the exact TWSA of the first and last day of the month, change of storage $(\Delta S / \Delta t)$ in a time period was approximated using a second order central difference as proposed by Biancamaria et al. (2019). After that, the residual $(P - ET_a - Q_{out})$ should be equal to the change of storage $(\Delta S / \Delta t)$ following the simplified water balance equation:

$$\frac{\Delta S}{\Delta t} = P - ET_a - Q_{out} \qquad \text{Eq.o}$$

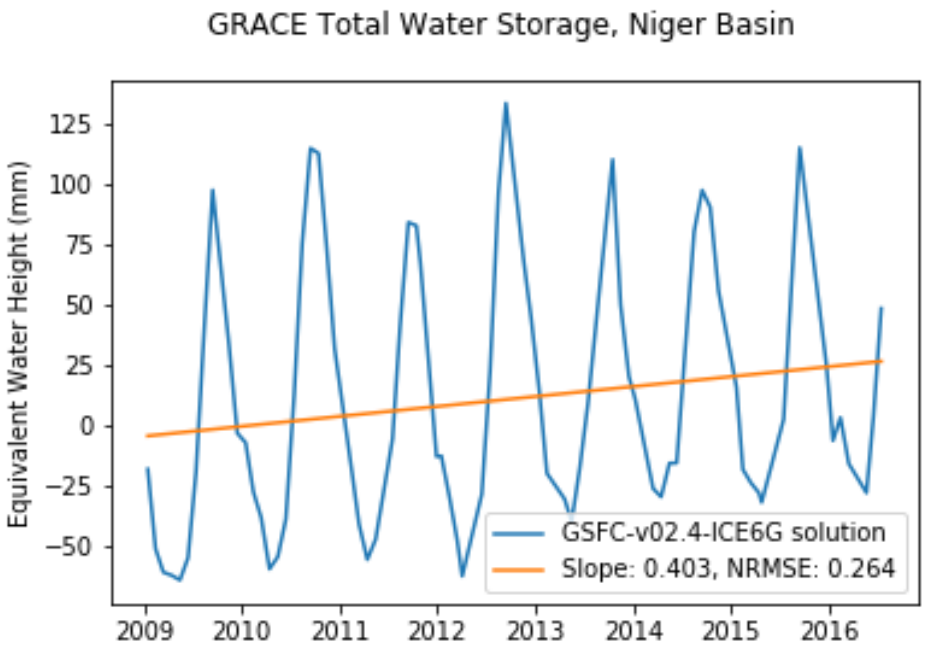

Figure 2-8: Monthly Total Water Storage solved from GRACE gravity anomaly measurements for the Niger River Basin in equivalent water height from 2009 to mid-2016.

The longer term trend in storage change (ΔS) as observed by GRACE is positive (Figure 2-8). The trend of total water storage in equivalent water height for a number of GRACE solution grids, or mass concentration (also called mascons), that cover the Niger River Basin from 2009 to 2016 is +0.4 mm/month, which is translated into about +10 km³/year increase. This amount accounts for 5% of the yearly excess rainfall of the whole basin (Table 2-1), which indicates that water storage change in the study period is not significant in the Niger basin water balance.

2.2.3.1. Observed river flows

The river flow hydrographs at several stations are available from the Niger River Authority's website (ABN, 2019). The monthly and annual flows at these locations were extracted from the hydrographs using Web Plot Digitizer (Ankit, 2019) during the study period when data is available. Since the total outflow from the Niger Delta to the Gulf of Guinea is not available, the water balance was also checked at sub-catchment scale. The delineation of upstream catchment for each station is based on HydroSHED data (Lehner and Grill, 2013). The location and catchment area of the selected monitoring stations is given in Figure 2-9.

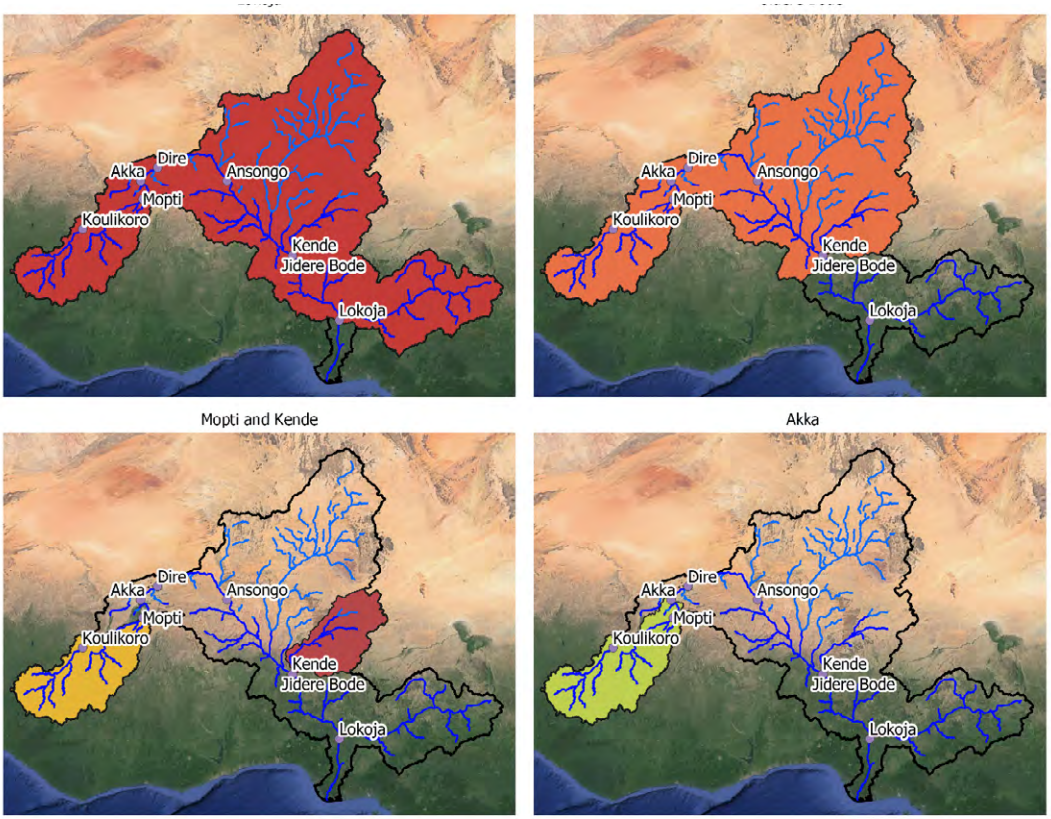

Figure 2-9: River flow stations and their corresponding watersheds: Akka, Mopti, Jidere Bode, Kende, and Lokoja. (Hydrographs at each station are provided in Annex VI)

2.2.3.1. Assessment of errors in water balance

The difference between residual $P - ET_a - Q_{out}$ and ΔS can be used as a proxy of error in water balance derived from available datasets. This error can be due to uncertainty in WaPOR P and ET_a, discharge measurement and/or from GRACE TWSA solution. For the water balance of the whole basin, the catchment upstream to Lokoja can be considered representative of the whole Niger River basin as it covers 97% of the total basin area (Figure 2-9). The result for Lokoja stations is provided in Figure 2-10.

Table 2-3: Estimation of Error in Water Balance of the Niger River Basin at Lokoja based on the difference between GRACE Total Water Storage changes from 2009 to 2015 and residual of $P - ET_a - Q$, where P and ET_a were aggregated from WaPOR data and Q was measured at Lokoja.

Year	ΔS from GRACE (km³/year)	Flow measurement at Lokoja			
		Q_{Lok} (km³/year)	$P - ET_a - Q_{lok}$ (km³/year)	Error of ΔS (km³/year)	Error of ΔS (%P)
2009	5	241	-39	-44	-3
2010	75	228	133	58	4
2011	-73	181	-22	51	4
2012	89	244	122	33	2
2013	-47	181	-87	-40	-3
2014	16	207	-170	-186	-13
2015	-6	186	4	10	1
Mean	8	210	-9	-118	-1

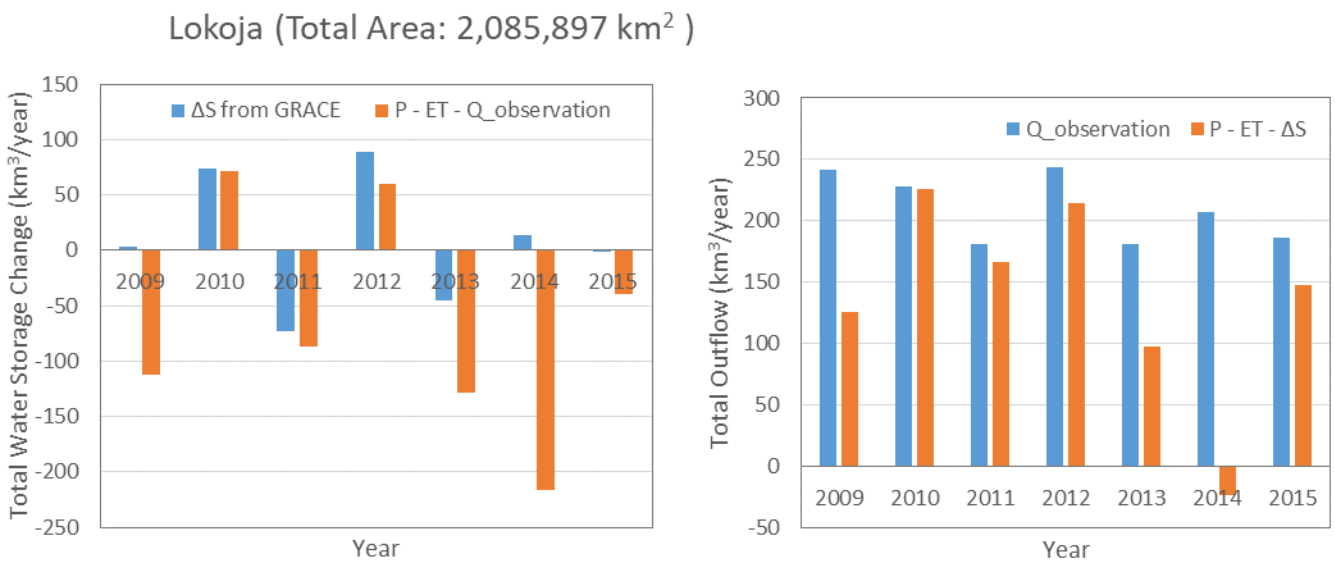

Figure 2-10: Comparison of discharge at Lokoja station with WaPOR water balance. The results of other sub-catchments are given in Annex VII.

The comparison between different total water storage change estimations from 2009 to 2015, as can be seen in Figure 2-10 (left), shows that the residual of $P - ET_a - Q$ calculated from WaPOR data and measurement at Lokoja has similar trend with to total water storage change estimation from GRACE-GS-FC solution except for 2014 and 2015. The alternative approach is to estimate total outflow from remotely sensed data, as can be seen in Figure 2-10 (right). Similarly, the largest difference between observed and estimated outflows based on $P - ET_a - \Delta S$ from WaPOR and GRACE is in the year 2014. On average, the mean difference between GRACE TWSA change and WaPOR-based ΔS is -1% of total precipitation using flow measurement at Lokoja as total outflow (Table 2-3). The comparison between the observed discharge and the discharge estimated based on WaPOR $P - ET_a - \Delta S$ as well as the comparison between GRACE change in storage and WaPOR derived change in storage for each station is provided in Annex VII.

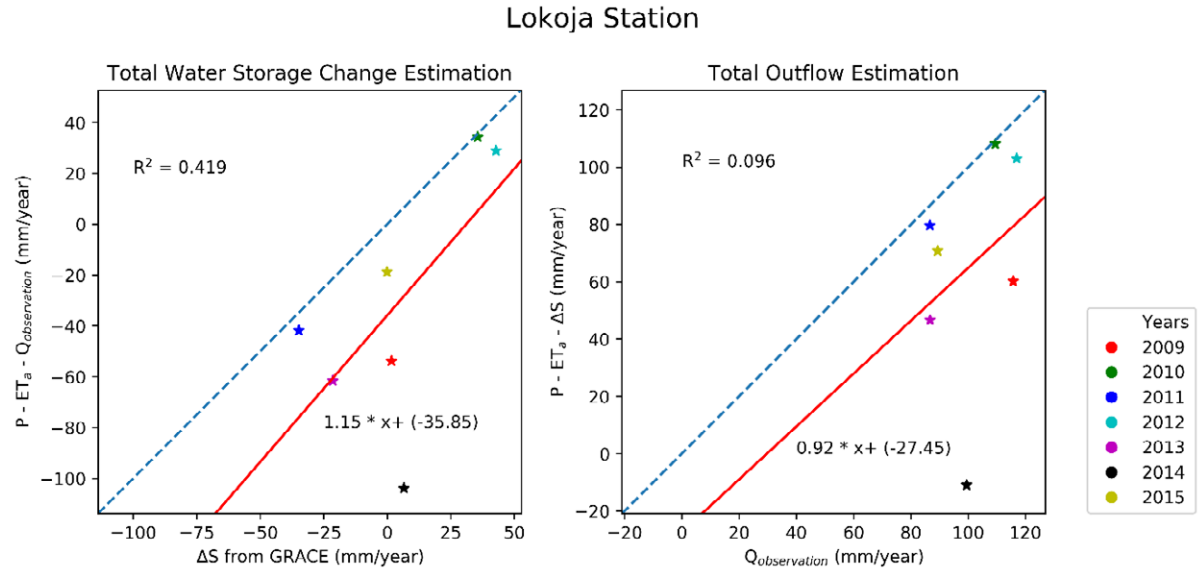

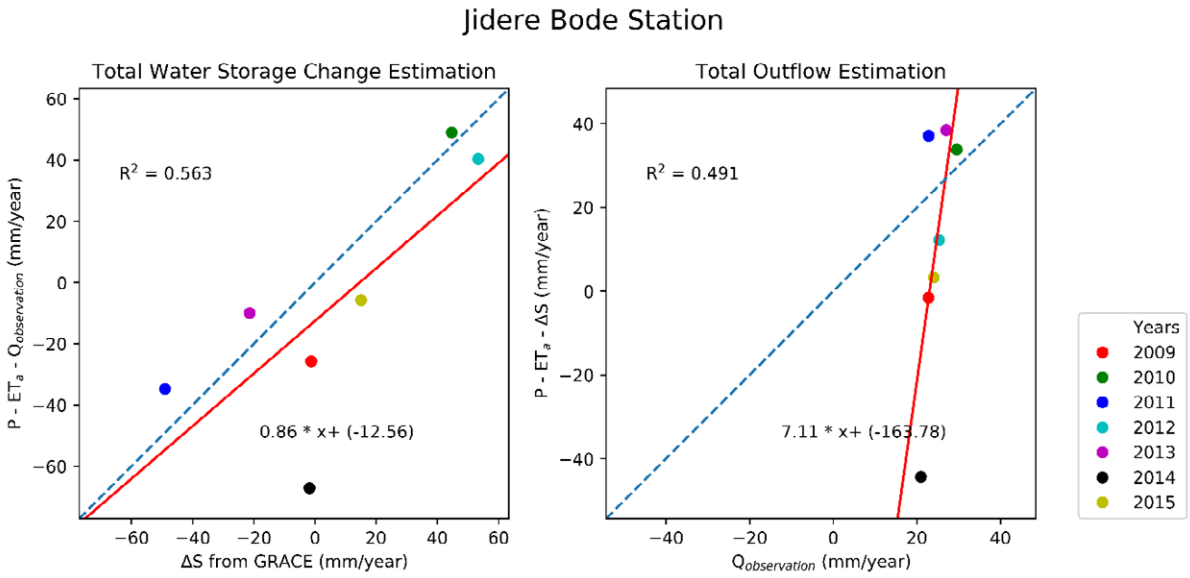

Figure 2-11: Correlation between total water storage change estimation from $P-ET_a-Q_{observation}$ and GRACE TWSA (left), and between total outflows estimation from $P-ET_a-\Delta S$ and observations (right) at several sub-catchments in the Niger River Basin from 2009 to 2015. Comparison at individual stations is provided in Annex VII.

For the other stations (Figure 2-9), the overall correlation coefficient between WaPOR-based water balance and observed data is between 0.1 and .67 for total outflow, and between 0.22 and 0.97 for total water storage change (Figure 2-11). For all sub-catchments, both total water storage change and total outflow derived from WaPOR-based water balance is consistently under-estimated in 2014. In addition, the error in the water balance estimation for the more downstream stations (Lokoja and Jidere Bode) is lower error than for the upstream stations (Kende and Mopti). The sub-catchments with lowest correlation are Mopti and Akka (0.22 and 0.35) (Figure 2-11 and Annex VIII). These stations are affected by abstractions for the Office du Niger from the Markala dam (see Figure 1-2 for location), for which we do not have data. The unaccounted diverted water makes up a large part of the gap in estimated water balance at these two stations, which mainly causes the over-estimation of the discharge based on WaPOR. Overall, the mean of total water storage derived from water balance can be an adequate estimate for the average of a long-term period but not for individual years due to very low correlation of coefficient (0.13) with GRACE measurements. Meanwhile, the total outflow estimations, despite having higher coefficient of correlation (0.58), still has large errors for individual stations and years.

2.2.4. Conclusion

The preliminary data quality assessments shows that WaPOR 2.0 Level 2 data can be useful to map the spatial patterns and identify hot spots of net water generation and water consumption in the basin. In general, spatial variation of P and ET_a are consistent with the characteristics of the basin. However, when using these values as absolute in water balance, the excess rainfall $P-ET_a$ is often over-estimated, both at local and basin scales. Moreover, in 2014, there is a large discrepancy between WaPOR derived discharge and observed discharge, this was also observed in the Awash basin (FAO and IHE Delft, 2020).

In summary, the following aspects of the WaPOR datasets are highlighted:

- Precipitation (P): Though there is insufficient in situ rainfall measurements in the study period for direct comparison, previous studies have shown that most remotely sensed precipitation products have very low pixel-to-point accuracy. Among the studied products, CHIRPS v.2 product, on which WaPOR Precipitation layer is based, provides better estimate of rainfall in the Niger River Basin (Prior, 2008). Therefore, WaPOR precipitation maps were used without modification.

- Actual Evapotranspiration and Interception (ET_a): The annual P and ET_a per land cover class shows that ET_a seems to be underestimated for some natural vegetation classes. It also shows that ET_a is mainly limited by P in the Niger River Basin, in terms of monthly values and per land cover class except for irrigated agriculture and water bodies. Bareland and sparse vegetation estimates and unrealistic water consumption value, which in mm/year is low, but due to the large area covered by this land use class (>30%) this accounts for a large part of the total water consumed (73%). However, the yearly ET_a follows different trend from P. ET_a is very high for some years from 2014, which results in very low excess rainfall and high gap in water balance when comparing with total outflow observations.

- Land cover maps from WaPOR include some essential Land cover classes (rainfed and irrigated croplands). The total irrigated crop area is close to historical records, if considering expansion of irrigation schemes in recent years.

- Error in Water balance: For the WaPOR-based Water Accounts of 2009-2018, the total storage change estimated from water balance will be used as GRACE data is not available for the whole period. However, the error estimated for years 2009-2015 should be kept in consideration when interpreting the rapid WA+ outputs. The total error as percentage of precipitation is 1% at Lokoja station using observed data. For periods and locations without GRACE data and/or observed flow data the error may be larger.

2.3. WA+ methodology

The longer term planning process of water and environmental resources in river basins requires that a measurement – reporting – monitoring system is in place. The Water Accounting Plus (WA+) framework is based on the early WA work of Molden (1997) focussing on agriculture and irrigation systems. WA+ was further developed by Karimi (2014) and Karimi and Bastiaanssen (2015) for river basin analyses to incorporate all water use sectors. Further developments include more hydrological and water management processes and focus on specific land uses.

A key element of WA+ is that it separates ET into rainfall (ET_{rain}) and incremental ET (ET_{incr}), thereby clearly identifying managed water flows. WA+ includes the hydrology of natural watersheds that provide the mains generation of water in streams and aquifers, as well as quantifying water consumption (Bastiaanssen, 2014). The current study utilises the WaPOR v2.0 Level 2 data (100 m resolution) for the analyses. As such, it provides a rapid WaPOR-based water accounting plus framework.

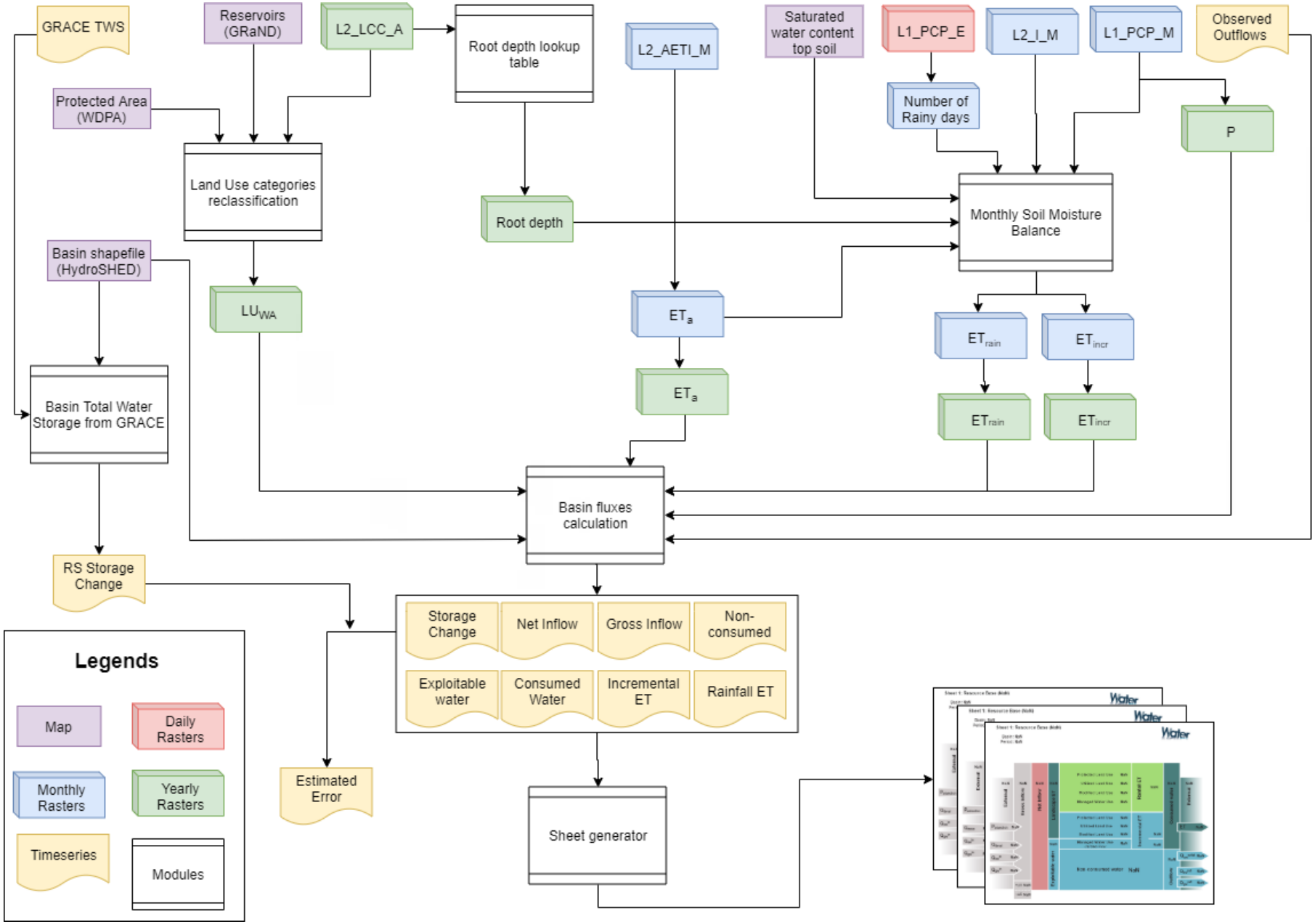

Figure 2-12: Flowchart of steps in WaPOR-based WA+ process, where ET is Evapotranspiration, P is Precipitation, I is Interception, TWS is Total Water Storage, LUWA is WA+ Land Use maps, ET_{incr} is ET incremental, ET_{rain} is ET from rainfall. L1_P_M, L2_I_M and L2_AET. 'Land Use categories reclassification' module is described in Section 2.3.1. Section 2.3.2 describes the modules for 'FAO effective rainfall formula', 'ET Rainfall estimation', and 'ET incremental estimation'. Section 2.3.3 describes the modules for 'Basin fluxes calculation' and 'Sheet generator'.

The output of WA+ is presented a number of sheets and supporting spatial maps. Remote sensing, GIS and spatial models form the core methodology, so all data has a spatial context. The accounts are reported on an annual basis, as WA+ is meant for longer term planning. Software tools have been developed that automatically collect and download data from WaPOR database as well as for the calculations. The models and scripts for the creation of the water accounts and the elaboration of the reports are available on GitHub under the Water Accounting account . The WA+ framework is public and open for all users.

Figure 2-12 shows the flow chart of the rapid WA+ process and the data used. The rapid WA+ mainly uses WaPOR data such as the level 1 monthly precipitation and level 2 annual time series of land cover classification, interception and actual evapotranspiration and interception. External data sources used include GRACE satellite data for estimating the change in storage in the basin, Global Reservoir and Dam Database (GRanD) to identify dam locations and extents, the World Database on Protected Areas to identify the protected land uses, and the map of top soil saturated water content (de Boer, 2016).

2.3.1. WA+ Land Use categorization

The WaPOR land cover map forms the basis for dividing the basin landscape into the four main categories (PLU, ULU, MLU, and MWU). Four main categories of land and water uses are distinguished:

- **Protected Land Use** (PLU); areas that have a special nature status and are protected by National Governments or Internationals NGO's
- **Utilized Land Use** (**ULU**); areas that have a light utilization with a minimum anthropogenic influence. The water flow is essentially natural
- **Modified Land Use** (**MLU**); areas where the land use has been modified. Water is not diverted but land use affects all unsaturated zone physical process such as infiltration, storage, percolation and water uptake by roots; this affects the vertical soil water balance
- **Managed Water Use** (**MWU**); areas where water flows are regulated by humans via irrigation canals, pumps, hydraulic structures, utilities, drainage systems, ponds etc.

The underlying reason for framing these four land use categories is that their management options widely differ from keeping them pristine to planning hourly water flows.

The land use categories map (Figure 2-13) is based on the land cover layer (LCC) from WaPOR database, but needed to be reclassified into the Water Accounting classes. Protected Land Use (PLU) class was updated using the protected area profile from the World Database on Protected Areas (UNEP-WCMC, 2019). The areas which are designated as IUCN categories Ia (strict nature reserve), Ib (wilderness area) and II (national park) are reclassified as PLU. The Managed Water Use class was reclassified from the 'Cropland, irrigated or under water management' and 'Built-up' classes in WaPOR LCC layer and updated with the area of constructed reservoirs from the Global Reservoir and Dam Database (GRanD) (Lehner et

al., 2011). WaPOR 'water bodies' class except for natural lakes were also reclassified as Managed Water Use class. The Modified Land Use was reclassified from the class 'Cropland, fallow' and 'Cropland, rainfed' in the WaPOR LCC layer. Thereafter, the rest of the area was reclassified as Utilized Land Use class. Figure 1-9 shows the reclassified land use map of the Niger River Basin in 2018.

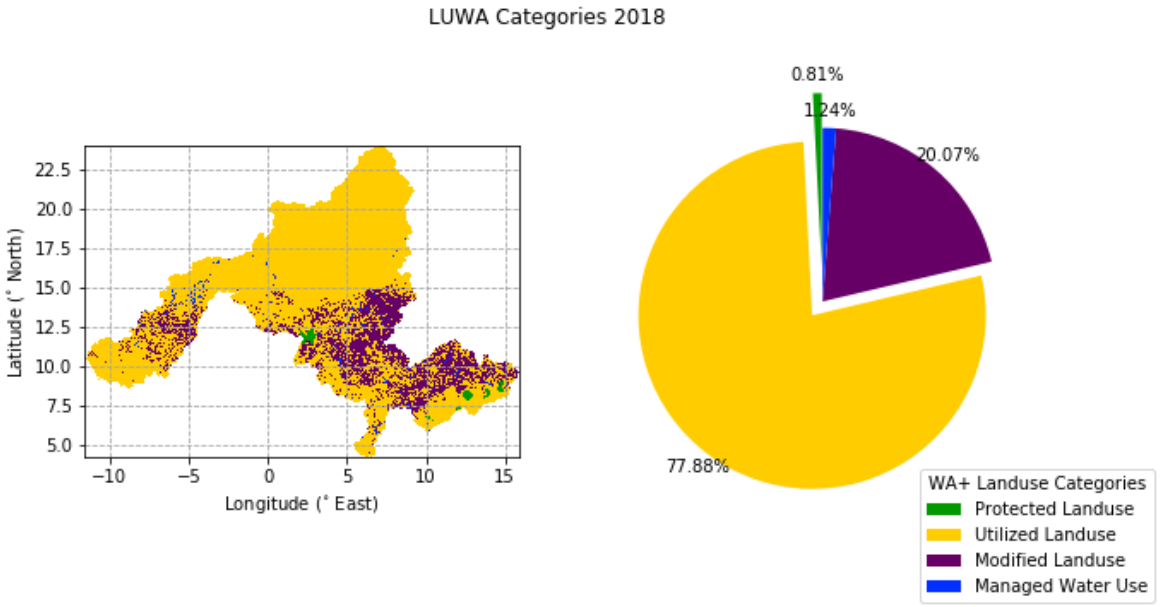

Figure 2-13: WA+ Land Use category map of the Niger River Basin in 2018 based on WaPOR Level 2 Land cover (LCC) layers and global datasets of protected area, reservoirs. Maps of the individual years are provided in Annex IX.

2.3.2. Pixel scale analysis

2.3.2.1. Method

The water accounting framework distinguishes between a vertical and horizontal water balance. A vertical water balance is made for the unsaturated root zone of every pixel and describes the exchanges between land and atmosphere (i.e. rainfall and evapotranspiration) as well as the partitioning into infiltration and surface runoff. Percolation and water supply are also computed for every pixel, to facilitate attributing water supply and consumption to each land use class.

The WaterPix model calculates for each pixel the vertical soil water balance (See Figure 2-14 and described below). Rainfall ET (ET_{rain}) and incremental ET (ET_{incr}) are separated by keeping track of the soil moisture balance and determining if ET_a is satisfied only from rainfall or stored in the soil moisture or additional source (supply) is required. The main inputs into WaterPix are provided in Table 2-4 and the outputs are provided in Table 2-5. Each parameter is calculated at the model resolution of 100m and available for monthly and annual time steps.

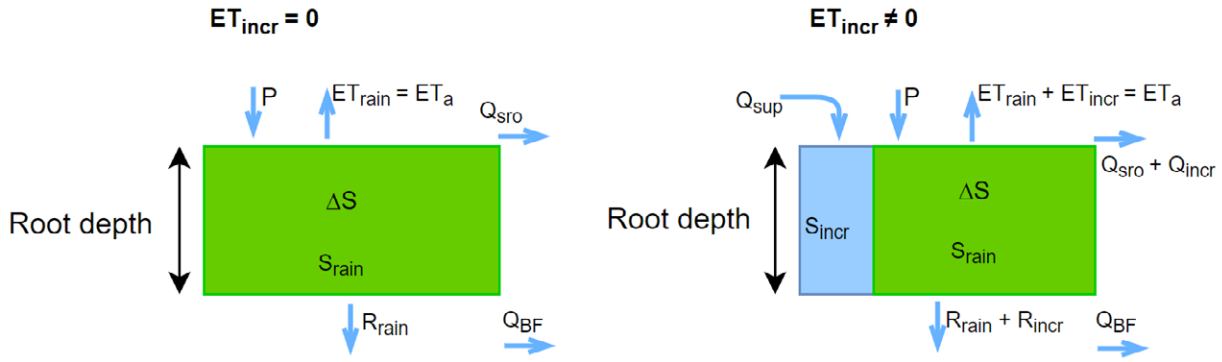

Figure 2-14: Main schematization of the flows and fluxes in the WaterPix model

Table 2-4: Inputs of WaterPix

Variable	Parameter	Source	Spatial Resolution	Temporal resolution
Precipitation	P	WaPOR	5,000 m	Daily
Actual Evapotranspiration	ET_a	WaPOR	100 m	Monthly
Interception	I	WaPOR	100m	Monthly
Land cover map	LULC	WaPOR	100 m	Yearly
Saturated Water Content	θ_SAT	HiHydroSoil	0.008333 degree (about 900m at the equator)	Static

Table 2-5: Outputs of WaterPix

Variable	Calculation step	Definition
S	1	Soil Moisture
Q_{sro}	1,4	Surface Runoff
R	1,4	Recharge
ET_{rain}, ET_{incr}	2	Rainfall ET and incremental ET
Q_{sup}	3	Supply

Step 1 Compute soil moisture

The soil moisture (Srain,t) is computed as the soil moisture storage at the end of the previous timestep ($S_{rain,t-1}$) plus the effective rainfall ($P-I$) minus recharge (R_{rain}) and surface runoff (Q_s):

$$S_{rain,t} = S_{rain,t-1} + P - I - R_{rain} - Q_{sro,rain} \quad \text{Eq.1}$$

Where the surface runoff ($Q_{sro,rain}$) is calculated using an adjusted version of the Soil Conservation Service runoff method. The adjusted version replaces the classical Curve Numbers by a dynamic soil moisture deficit term that better reflects the dry and wet season infiltration versus runoff behaviour (see Schaake et al., 1996; Choudhury & DiGirolamo, 1998). As the Curve Number method is developed for event based runoff, we calculated $Q_{sro,rain}$ on daily basis, dividing the effective rainfall by the number of

rainy days (n) and a calibration parameter f to account for the soil moisture variation due to drying up and filling with in a month. The total surface runoff for a month is then multiplied by n:

$$Q_{sro,rain} = \begin{cases} 0 \text{ if } P = 0 \\ \dfrac{\left(\dfrac{P-I}{n}\right)^2}{\dfrac{P-I}{n} + f\left(S_{sat} - S_{rain,t-1}\right)} * n \text{ if } P > 0 \end{cases}$$

Eq.2

Where the saturated soil moisture (S_{sat}) is calculated by multiplying the Saturated Water Content (θ_SAT) by the effective root depth (RD) for each land cover class estimated based on the effective root depth by Yang et al. (2016) (Table 2-6).

Table 2-6: Root depth look-up table. The values of root depth for each land cover class is based on study by Yang et al. (2016)

WaPOR Land cover class	Root depth (mm)
Shrubland	370
Grassland	510
Cropland, rainfed	550
Cropland, irrigated or under water management	550
Fallow cropland	550
Built-up	370
Bare/sparse vegetation	370
Permanent snow/ice	0
Water bodies	0
Temporary water bodies	0
Shrub or herbaceous cover, flooded	0
Tree cover: closed, evergreen needle-leaved	1,800
Tree cover: closed, evergreen broad-leaved	3,140
Tree cover: closed, deciduous broad-leaved	1,070
Tree cover: closed, mixed type	2,000
Tree cover: closed, unknown type	2,000
Tree cover: open, evergreen needle-leaved	1,800
Tree cover: open, evergreen broad-leaved	3,140
Tree cover: open, deciduous needle-leaved	1,070
Tree cover: open, deciduous broad-leaved	1,070
Tree cover: open, mixed type	2,000
Tree cover: open, unknown type	2,000
Seawater	0

Step 2 Separate ET_a into ET_{rain} and ET_{incr} and update S

To compute the rainfall and incremental component of ET_a, ET_a is subtracted from $S_{rain,t}$. When $S_{rain,t}$ is insufficient for ET_a, the difference will be supplied by surface or groundwater uptake. ET_{rain} becomes the amount which can be supplied by the soil moisture, whereas the difference will become ET_{incr}:

$$ET_{rain} = if(S_{rain,av} > ET_a, ET_a, S_{rain,av}) \quad \text{Eq.3}$$

$$ET_{incr} = ET_a - ET_{rain} \quad \text{Eq.4}$$

The new soil moisture storage then becomes:

$$S_{rain,t} = S_{rain,av} - ET_{rain} \quad \text{Eq.5}$$

Step 3 Estimation of Water Supply

The amount of water supplied to each pixel is a function of ET_{incr} and the so called consumed fraction (f_c).

$$Q_{sup} = f(ET_{incr}, LU) = \frac{ET_{incr}}{f_c} \quad \text{Eq.6}$$

f_c is dependent on the land use class and was suggested to replace the classical irrigation efficiencies (Molden, 1997; Simons et al., 2016).

The consumed fractions applied in this study are specified in Table 2-7.

Table 2-7: Consumed fraction per land use class

Land use class	Consumed fraction (fc)
Natural land use classes	1.00
Rainfed crops	1.00
Irrigated crops	0.80

Step 4 Estimating incremental soil moisture

A separate soil moisture storage (blue area in Figure 2-14) is added to store Q_{sup} and calculate incremental recharge and runoff as follows:

$$S_{incr,t} = S_{incr,t-1} + Q_{supply} - ET_{incr} - R_{incr} - Q_{sro,incr} \quad \text{Eq.7}$$

And total soil moisture storage (S_t) becomes:

$$S_t = S_{rain,t} + S_{incr,t} \quad \text{Eq.8}$$

Then total recharge (R_t) is calculated as exponential function of the soil moisture. If the soil moisture is above a certain percentage (calibration parameter) of the saturated content, the percolation will be computed using the following simple exponential function:

$$R_t = S_t * \exp\left(\frac{-1}{S_t}\right) \quad \text{Eq.9}$$

And the incremental recharge (R_{incr}) and the recharge from rainfall (R_{rain}) are computed as proportions of the incremental and rain soil moisture values.

The surface runoff is updated to account the increase due to incremental surface runoff from the supply:

$$Q_{sro,tot} = \begin{cases} 0 \text{ if } P = 0 \\ \dfrac{\left(\dfrac{P + Q_{sup} - I}{n}\right)^2}{\dfrac{P + Q_{sup} - I}{n} + f\left(S_{sat} - \left(S_{rain,t} + S_{incr}\right)\right)} * n \text{ if } P \neq 0 \text{ or } Q_{sup} \neq 0 \end{cases} \quad \text{Eq.10}$$

The incremental surface runoff ($Q_{sro,incr}$)is then computed as:

$$Q_{sro,incr} = Q_{sro,tot} - Q_{sro,rain} \quad \text{Eq.11}$$

2.3.2.1. Results

The maps of estimated annual ET_{rain} and ET_{incr} averaged over the study period are shown in Figure 2-15 and Figure 2-16. It can be seen in these maps that the hot spots of ET_{incr} are open water bodies, flooded shrub cover, and irrigated crops. The small lakes and flooded shrub cover in the Inner Delta system can have up to above 2000 mm/year of ET_{incr}. Meanwhile, most part of the basin at latitude lower than 120N has significantly higher ET_{rain}. In the Lower Basin, tree cover patches or forest can also be distinguished for having high ET_{rain} and built-up area for having low ET_{rain} (Figure 2-16).

Figure 2-17 describes the partition of ET_{rain} and ET_{incr} of each land cover class and the ratio of each component relative to total rainfall. ET_{incr} over open water bodies is about 7 times its total rainfall. ET_{incr} of irrigated cropland is 98% of its total rainfall, which shows that blue water supply is important source for these crop area. ET_{rain} of all tree cover classes is about 50% of the received rainfall. The ratio of ET_{rain}/ET_{incr} depends greatly on the parameterised maximum root depth. For example, the 'Evergreen' tree cover classes have ET_{rain}/ET_{incr} of between 5 to 8 and parameterised root depth of 3,140 mm (Table 2-6), while the 'Deciduous' ones have ET_{rain}/ET_{incr} of about 2 times and root depth of one-third as much. In the Niger River Basin, all tree cover classes account for about 18% of total basin area (Table 2-2). Therefore, it is important to calibrate root depth parameters when tree covers are significant land cover classes, given that suitable data is available.

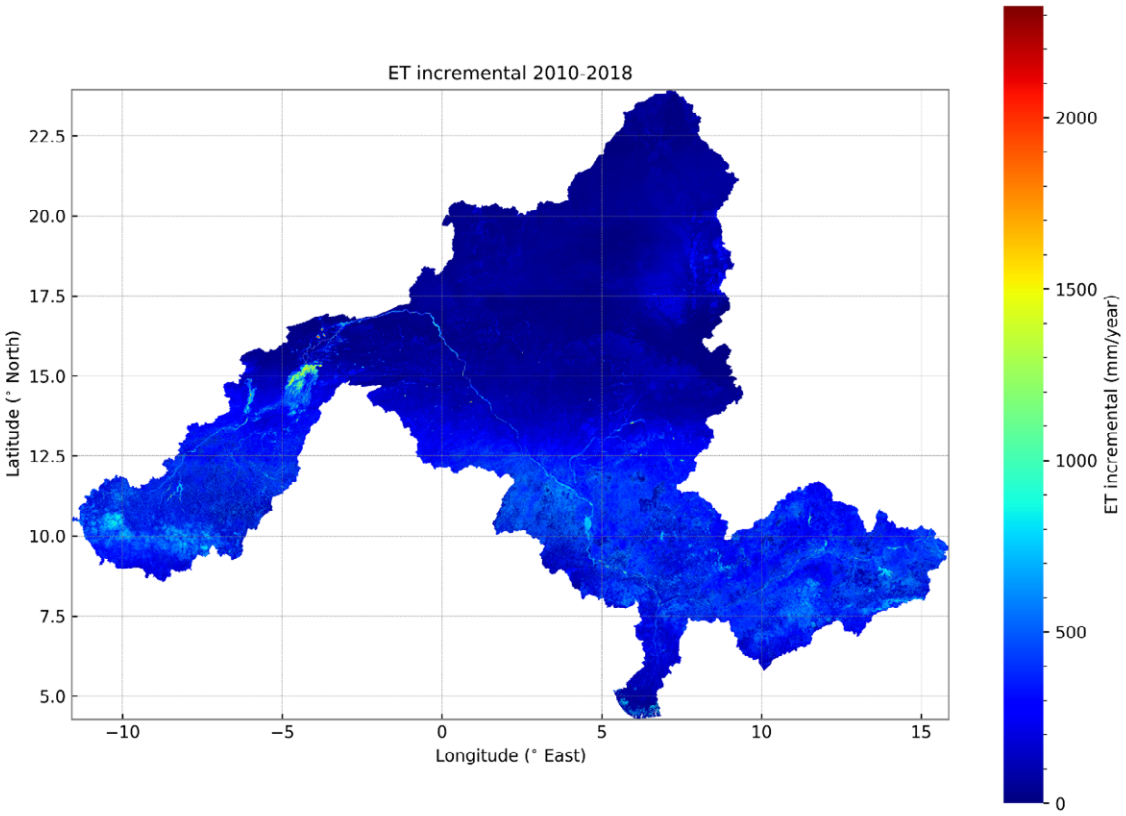

Figure 2-15: The yearly average map of ET_{incr} estimated from WaPOR data in the Niger River Basin from 2010 to2018. Maps of the individual years are provided in Annex X.

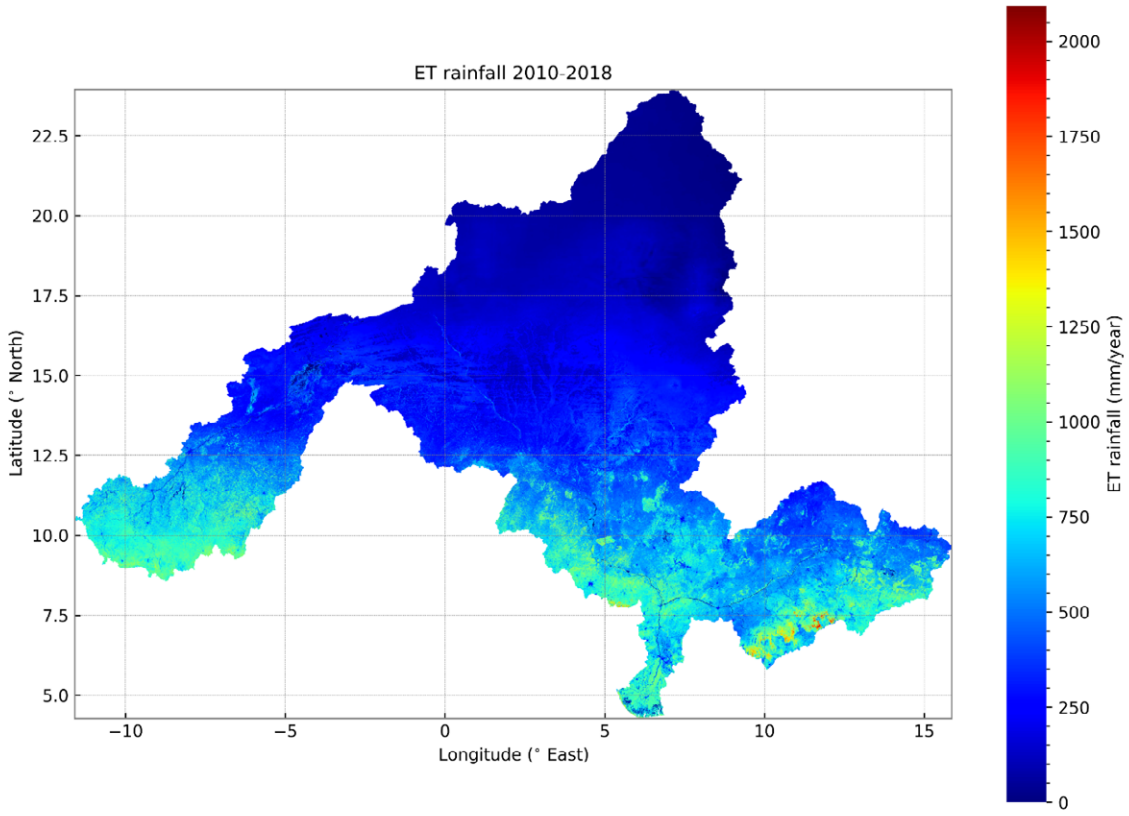

Figure 2-16: The yearly average map of ET_{rain} estimated from WaPOR data in the Niger River Basin from 2010 to2018. Maps of the individual years are provided in Annex XI.

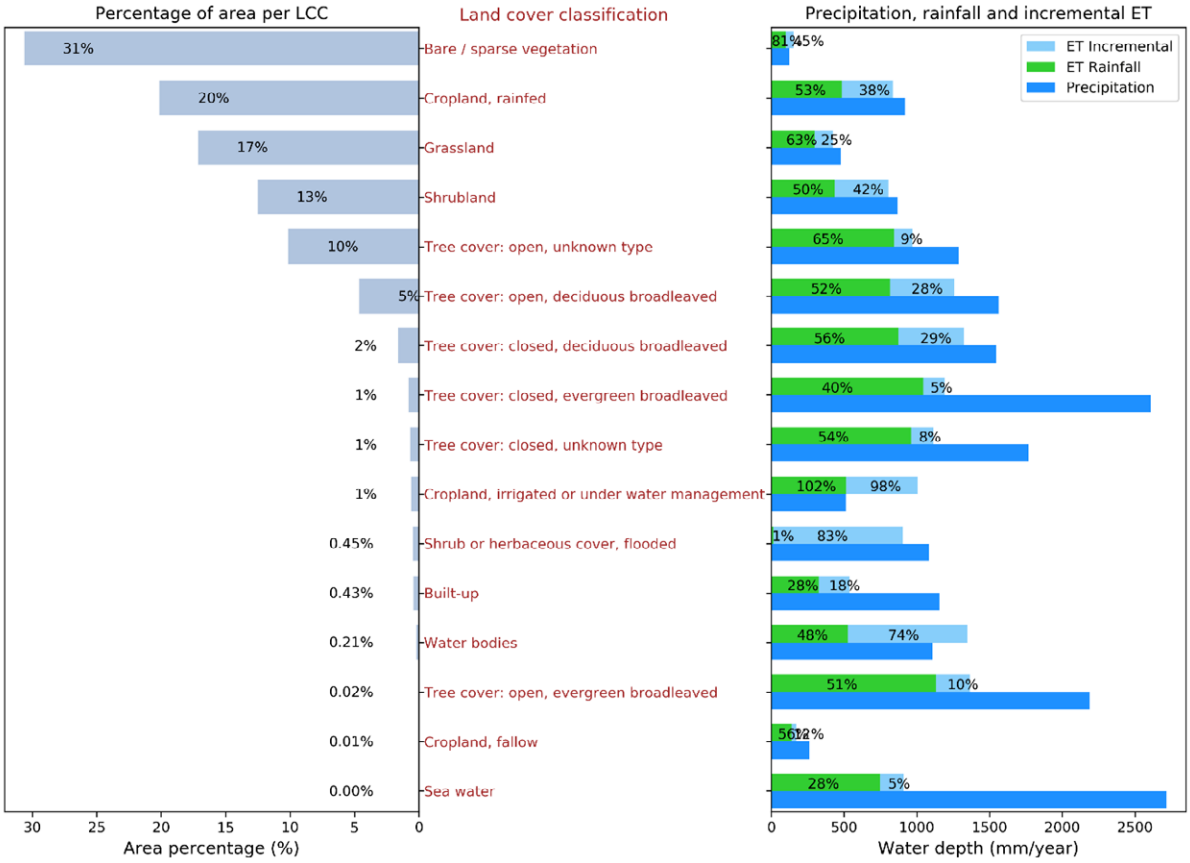

Figure 2-17: The area percentage (left) and yearly average Precipitation, ET_{rain} and ET_{incr} (right) of each land cover class for the years 2010-2018. The percentage in the right indicate the proportion of ET_{rain} and ET_{incr} to Precipitation.

2.3.3. WaPOR-based WA+ Sheet 1: Resource Base

The WA+ sheet 1 Resource Base provides an overview of the water resources and its current utilisation per different land use categories. The rapid WaPOR-based WA+ approach estimates gross inflow, rainfall and incremental evapotranspiration for each of the WA+ land use categories. Therefore, it provides and overview of the current utilisation of rainfall for each land use for the study period. Details of how each flux in the WA+ Sheet 1 was estimated is given in Table 2-8.

The WaPOR-based WA+ Sheet 1 is developed for the entire Niger River Basin, with the most downstream location of observed discharge at Lokoja, the outflow at the Delta was estimated by adding run-off from downstream of Lokoja, derived from WaPOR $P - ET_a - \Delta S$, to the discharge measured at Lokoja.

Based on the WA+ sheet 1, a number of key performance indicators, which were developed by Dost et al. (2013) in consultation with the Land and Water Division of FAO, can be calculated to describe the entire system. These indicators help the basin planners to understand the key information on water management in the basin (Karimi, 2014).

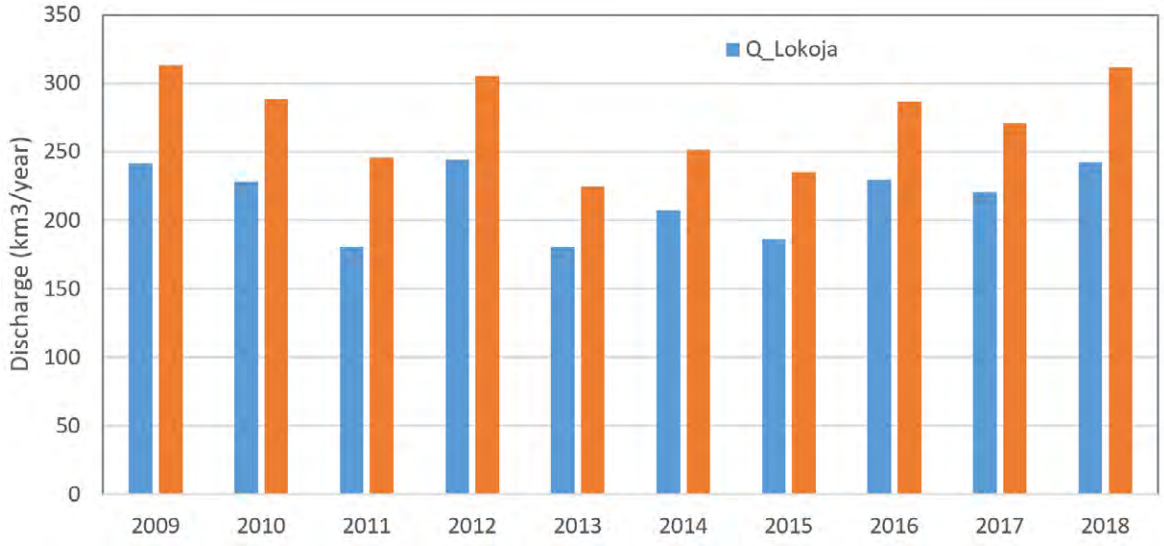

Figure 2-18: The Niger River Basin outflow from 2009-2018 based on observed discharge at Lokoja and estimated runoff from Niger Delta using WaPOR $P\text{-}ET_a\text{-}\Delta S$.

The first set of indicators can be related to the Resource Base Sheet:

1. ET Fraction $= \dfrac{ET_{tot}}{(P + Q_{in})}$ (%)

ET fraction indicates which portion of the total inflow of water is consumed and which part is converted into renewable resources. A value higher than 100% indicates over- exploitation or a dependency on external resources.

2. Stationarity Index = $\frac{\Delta S}{ET_{tot}}$ (%)

Stationarity Index is an indication of the depletion of water resources. Positive values indicate that water is added to the groundwater and/or surface water storage. Negative values indicate a depletion of the storage.

3. Basin Closure = $\frac{1 - Q_{out}}{(P + Q_{in})}$ (%)

Basin Closure defines the percentage of total available water resources (Precipitation + basin inflow) that is consumed and/or stored within the basin. A value of 100% indicates that all available water is consumed and/or stored in the basin.

The second set of indicators focuses on the actual amount of water that is currently managed, or is available to be managed:

4. Available Water (AW) = Gross Inflow – Landscape *ET* – Reserved flow (km^3/year)

Total amount of water that is available to be managed.

5. Managed Water (MW) = Incremental *ET* of Managed Water Use (km^3/year)

Total amount of water that is abstracted for Managed Water Use.

6. Managed Fraction = $\frac{\text{Managed Water}}{\text{Available Water}}$ (%)

Percentage of water that is actually managed from the total amount of water that is available.

2.4. Assessing the impacts of irrigation in the Office du Niger on the Inner Niger Delta using WaPOR data and WA+

This section describes the methodologies used to analyse the current trend of irrigation water consumption in the Office du Niger [2.4.1] and the maximum flooding extent in Inner Niger Delta [2.4.2] over the period from 2009 to 2018. Since seasonal flooding is a crucial ecological function of the Inner Niger Delta, the relationship between the two variables will then be used to assess the hydro-ecological impact of irrigation scheme in the Office du Niger on the Inner Niger Delta.

Table 2-8: Data and calculation approach used for fluxes in WA+ Sheet 1. N/A stands for Not Available

WA+ Sheet 1 Flux	Description	Data used	Calculation approach
$P_{advection}$	Precipitation	WaPOR's L1_PCP_M	Aggregate by hydrological year
Q_{desal}	The inflow from desalinated water	N/A	-
Q_{sw}^{in}	The inflow from surface water (i.e. interbasin surface water inflow)	N/A	-
Q_{gw}^{in}	The inflow from groundwater (i.e. interbasin groundwater inflow)	N/A	-
Gross Inflow	Total inflow from all sources	-	$P_{advection} + Q_{desal} + Q_{sw}^{in} + Q_{gw}^{in}$
Net Inflow	The gross inflow and the storage change	-	Consumed water + Outflow
ΔS	Change in total water storage	-	Net Inflow – Gross Inflow
Rainfall ET (PLU, ULU, MLU, MWU)	ET that occurs from effective rainfall and canopy interception. Effective rainfall is the part of the rain water that does not percolate below the root zone, flows away over the soil surface as run-off, or evaporates from canopy interception, thus, available in the root zone and can be used by the plants.	WaPOR-derived ET rainfall; WA+ Landuse maps	Aggregate by hydrological year and LU classes
Incremental ET (PLU, ULU, MLU, MWU)	ET that occurs from other sources except effective rainfall and interception. For example, evaporation of irrigation water, evaporation of groundwater through deep rooted vegetation, water evaporation from a lake or other water surface that exceeds the rainfall on the water body itself.	WaPOR-derived ET incremental; WA+ Landuse maps	Aggregate by hydrological year and LU classes
Landscape ET	ET that occurs naturally, not due to water management (i.e. evaporation on managed reservoirs, or ET from irrigation water).	-	Rainfall ET + Total Incremental ET of PLU, ULU, MLU
Consumed water/ ET	ET occurs as interception, evaporation, soil evaporation, water evaporation, canopy transpiration/ The total Evapotranspiration is evapotranspiration from non-manageable, manageable and managed land uses.	WaPOR's L2_AETI_M	Aggregate by hydrological year
Utilized flow	ET from managed water use (i.e. irrigated crops, managed reservoirs)	-	MWU Incremental ET
Exploitable water	The net inflow minus Landscape ET	-	Utilized flow + Outflow
Q_{sw}^{outlet}	The river outflow at the outlet of the basin	Measurements at Lokoja	Aggregate by hydrological year
Q_{sw}^{out}	The outflow as surface water (i.e. interbasin surface water outflow)	N/A	-
Q_{gw}^{out}	The outflow as groundwater (i.e. interbasin groundwater outflow)	N/A	-
Non-consumed water /Outflow	Total outflow	-	$Q_{sw}^{outlet} + Q_{sw}^{out} + Q_{gw}^{out}$

2.4.1. Estimation of irrigation water consumption in the Office du Niger

In the WA+ framework, the irrigation water consumption is considered as the depth of ET_{incr} over an area times the total area of the irrigated crop cover. Therefore, two datasets needed are the land cover classification maps that have irrigated cropland class and the ET_{incr} maps. The WaPOR land cover maps are used to classify irrigated cropland area and the ET_{incr} maps are resulted from the WA+ pixel scale analysis (2.3.2). Since the official boundary of the Office du Niger were not acquired in digital format, all calculations which are mentioned as 'Office du Niger' in this report are meant to be the aggregation of the pixels inside the manually digitized boundary shown in Figure 1-4.

The WaPOR database provides a yearly land cover maps (LCC) for the Niger River Basin, which is based on the Copernicus land cover product for 2015 (FAO, 2020), with further classification of the "cropland" class to distinguish between rainfed, fallow and irrigated cropland by applying a water deficit index (FAO, 2020). Therefore, the total cropland area does not change in WaPOR LCC yearly maps. Based on WaPOR LCC yearly maps, the surface area of irrigated cropland in the Office du Niger was increasing (Figure 2-19), probably as a result of change in yearly water deficit index. However, the official records of irrigated area in the Office du Niger show a lower total irrigated area of 1,173.82 km2 in 2018 (see Annex I). Since currently we do not have access to high resolution irrigated maps with higher accuracy available for the Office du Niger, the WaPOR LCC maps were used with this quality remark.

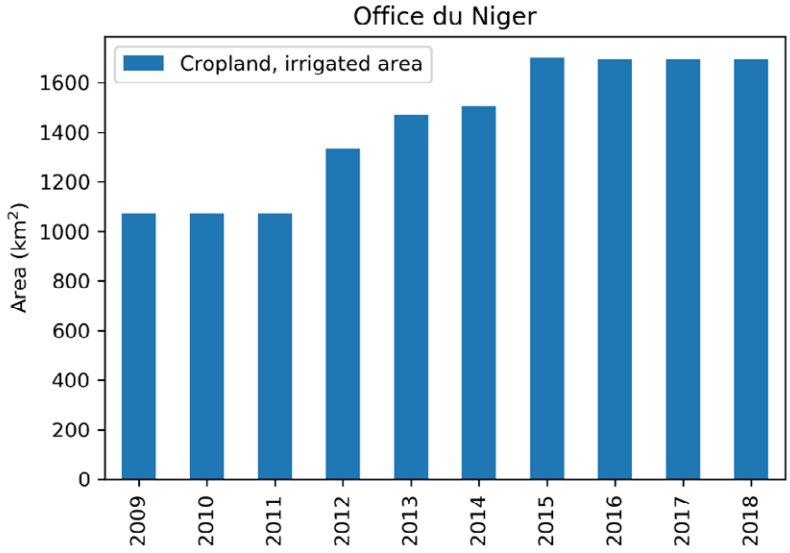

Figure 2-19: The total surface area of the "cropland, irrigated or under water management" class in Office du Niger production zones (as delineated in Figure 1-4) from yearly WAPOR LCC maps.

2.4.2. Delineation of flood extent in the Inner Niger Delta

In the past, there have been several attempts to use satellite data (both optical and radar imagery) to delineate flooded extent and derive relationship between the maximum flooded extent in the Inner Niger Delta and the water level measured at gauges in the delta (the stations most often used are Mopti and Akka) (Davids et al., 2018; Mahe et al., 2011; Ogilvie et al., 2015; Zwarts et al., 2005). All of these

methods require collecting a large amount of data from several satellite products, hand-picking the images corresponding to flooding occasions, pre-processing raw data, and classifying inundation by thresholding spectral reflectance indices. The studies often use Near Infrared or Shortwave Infrared band. In this report, we tested using the available WaPOR Actual Evapotranspiration (ET_a) data and the resulted WA+ Incremental ET (ET_{incr}) data to delineate flooded extent since these data are readily available without additional data collection and pre-processing steps. The WaPOR ET_a data was essentially computed using MODIS and PROBA-V (from 2014) Normalized Difference Vegetation Index (NDVI) products, which are also based on Near Infrared band (FAO, 2018b). Moreover, as the flood peaks in the Inner Niger Delta when the local rainfall is low (September-December), it is expected that relatively high ET_a during this period most likely takes place from inundated areas, including those areas where vegetation is obscuring the flooding. Although, wetland evaporation do not always behave similarly to open surface water evaporation (Mohamed et al., 2012), both will be significantly higher than the surrounding areas where ET_a is constraint by limited water availability.

In order to check the potential of using ET_a and ET_{incr}, the mean and standard deviation of ET_a and ET_{incr} for WaPOR water bodies in the Inner Niger Delta and the rest of the delta were compared (Figure 2-20). The extent of the Inner Niger Delta vary in the literature due to different considered time periods and discordant recognition of the northern and southern parts of the Inner Niger Delta by all authors (Liersch et al., 2013). Therefore in this report, we abide by the contour of the Inner Niger Delta provided on the interactive flood viewer OPIDIN developed by Wetlands International and Altenburg & Wymenga consultants (2017), which is shown in Figure 1-4. Thereby, when mentioning physical values of the Inner Niger Delta, it is meant to be the area in this boundary. It can be seen in Figure 2-20 that the standard deviation of ET_a was smaller from 2014 onwards probably due to the switch of WaPOR input data from MODIS (resampled 250m product) to PROBA-V (100m) products. The water bodies' pixels have highest mean monthly ET_a in April, at the beginning of the rainy season, while for the rest of the Inner Niger Delta ET_a peaks in November, during the flood period. This might be because ET_a of water bodies is only energy-constraint, while ET_a of the vegetation in the delta is also water-constraint when there is no flooding. Therefore, the signature of water bodies is used as a baseline to delineate inundated vegetation by separating the ET_a constrained by water supply from flood and the non-water-constraint ET_a. Four threshold selection methods were used and compared:

- **Method 1:** Pixels with ET_a above the monthly mean minus standard deviation value of water bodies' pixels were classified as inundated at a monthly time-step.
- **Method 2:** Pixels with ET_a above the monthly mean minus standard deviation value of water bodies' pixels averaged for all the years from 2009 until 2014 were classified as inundated at a monthly time-step
- **Method 3:** Pixels with ET_{incr} above the monthly mean minus standard deviation value of water bodies' pixels were classified as inundated at a monthly time-step.
- **Method 4:** Pixels with ET_{incr} above a fixed threshold (50mm) were classified as inundated at a monthly time-step.

Furthermore, to improve the delineation of the flooded extent, we constrain the ET_a and ET_{incr} maps within the Inner Niger Delta boundary.

After computing the maximum flooded area based on these thresholds, this was compared with the maximum flooded area computed using an empirical formula published on OPIDIN (2019). This formula is the result of the study by Zwarts et al. (2005), in which water maps derived from the Near Infrared and Mid-Infrared bands of satellite images (Landsat TM), were combined to construct a digital flooding model showing the water coverage in steps of 10 cm water level in Akka. The maximum flooded area was related to peak water level in Akka through a polynomial equation (Annex XIII-2). Since the water coverage products were not accessible, we used the water level in Akka to calculate the maximum flooded area for comparison. The yearly water level in Akka used, which was obtained from Niger River Authority's website (ABN, 2019), is provided in Annex XII.

In addition, the estimated inundation map using WaPOR data was also compared with the flood map estimated by change detection method using Sentinel-1 Synthetic Aperture Radar (SAR) data. This method is based on the backscatter signal change in SAR imagery between the before-flood and after-flood mosaics, which is caused by change in surface backscattering properties due to inundation (Figure 2-21). The Sentinel-1 SAR datasets are readily available and can be easily accessed and analyzed on Google Earth Engine, following the flood mapping practice recommended by UN-SPIDER (2020). The yearly maximum flooded area, however, was not compared with this method because the Sentinel-1 data was only available for 3 years from 2016 to 2018 and maximum flooded area derived from Sentinel-1 flood maps is highly sensitive to tuning parameters and before-flood window selection. The details of the data used, processing codes are provided in Annex XIII-3, which also includes the parameters sensitivity analysis.

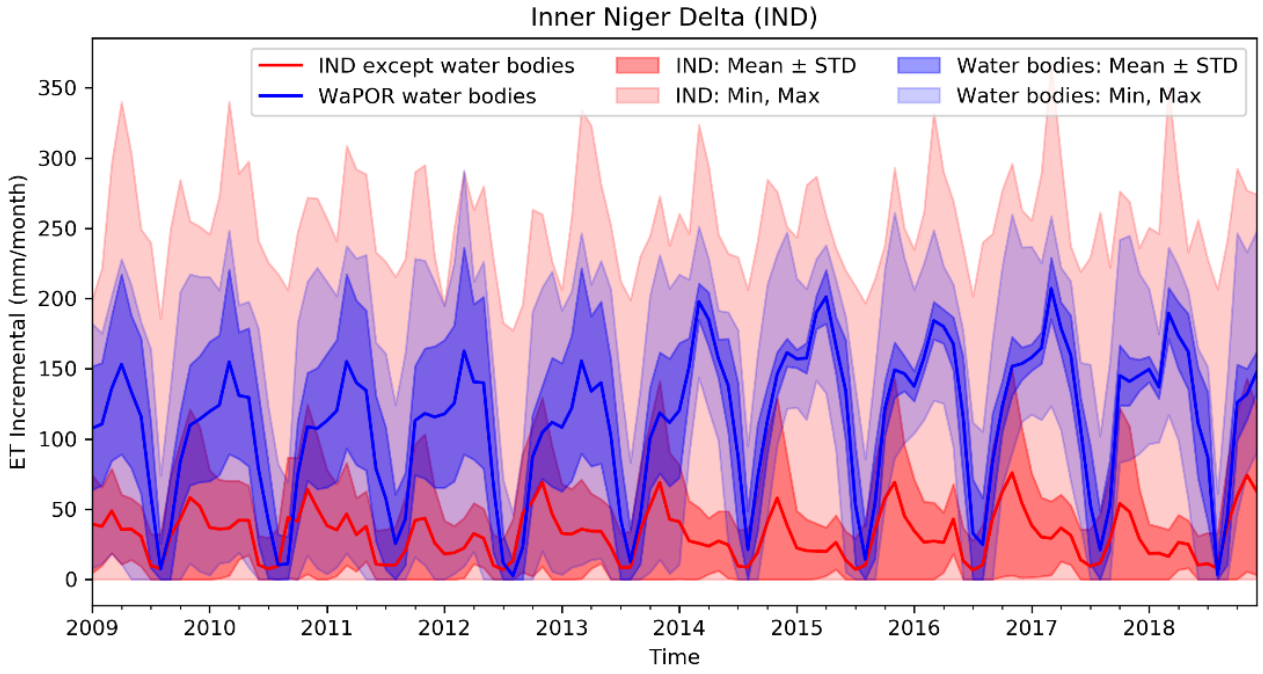

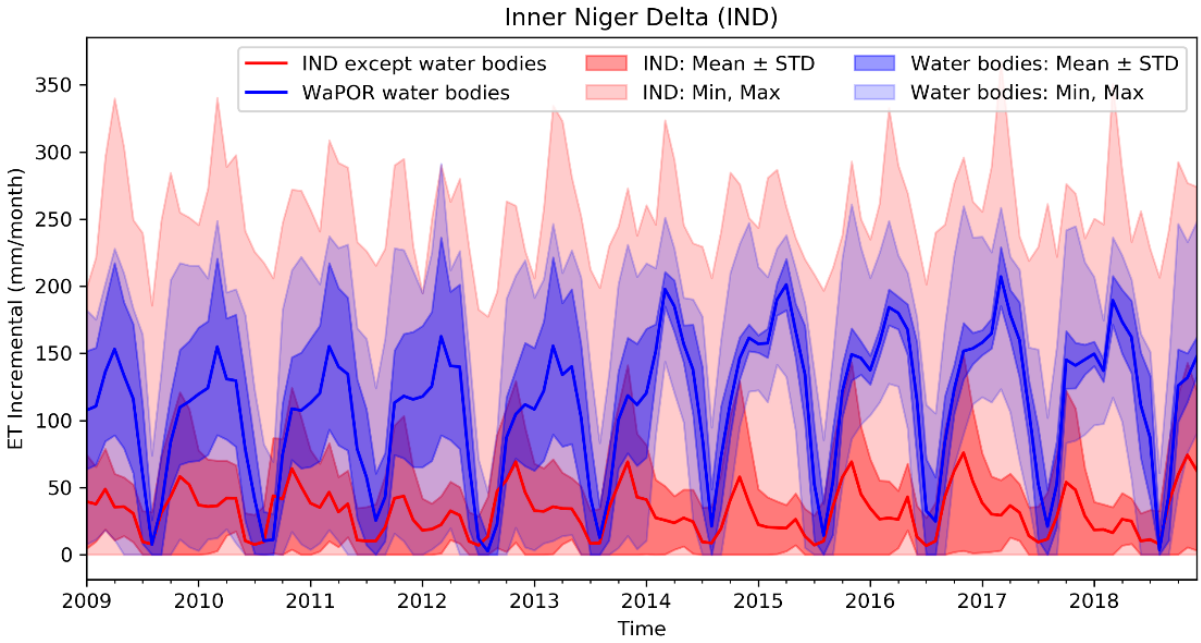

Figure 2-20: The monthly ET_a and ET_{incr} of permanent water pixels, and other pixels in the area bounded by Inner Niger Delta contour (Figure 1). The dark blue and red lines represent mean values, the blue and red bands represent range of mean ℗ standard deviation, and the light blue and red bands represent the range between minimum and maximum values.

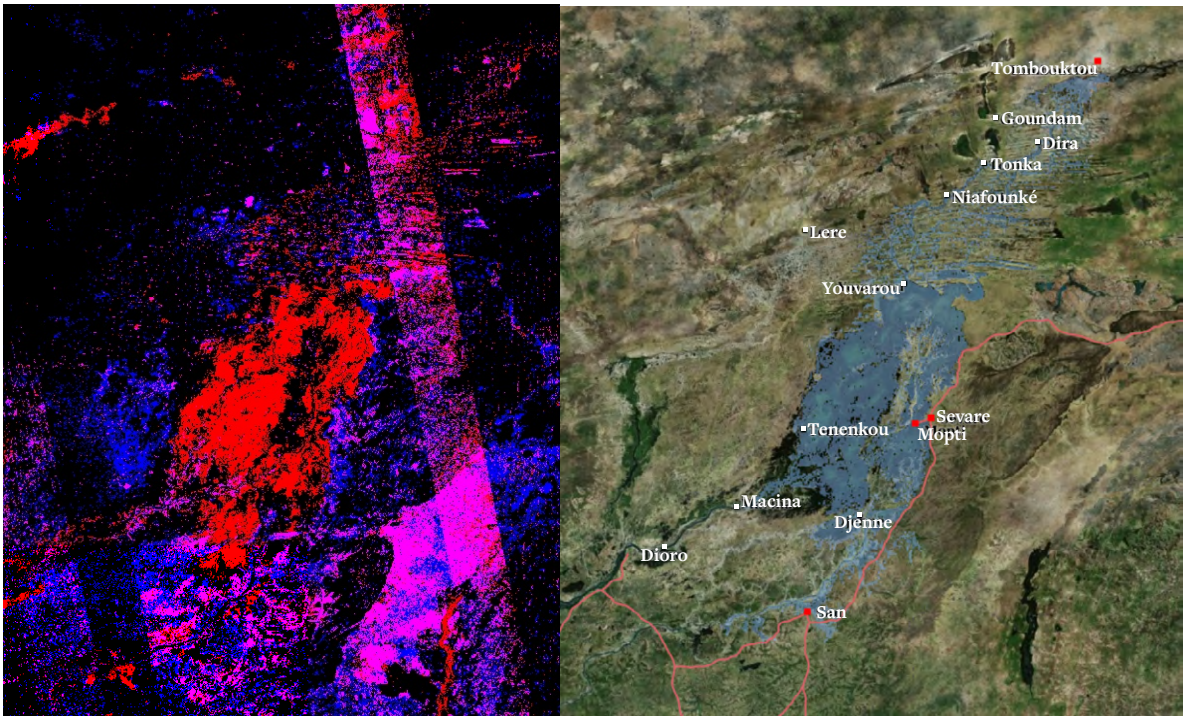

Figure 2-21: Change of backscatter signal in SAR imagery of the 2016 peak flood period (left) compared with OPIDIN flood-viewer (right). The light blue colour in the right graph is the modelled flooded area corresponding to the peak flood in Akka. The left graph is generated using Google Earth Engine combining the backscatter coefficient difference of the two SAR polarisation bands (VV and VH) between before and after the peak flood level in Akka that exceeds a threshold of -2. The colour show significant reduction of signal for only VV (Red), only VH (Blue), both (Pink), and none (Black) of the bands.

3. Water Accounting + Results

3.1. WA+ Sheet 1: Resource Base

Figure 3-1 shows the summary of water resources in the Niger River Basin of the WA+ framework for Sheet 1 only and depicts average values for the 2010-2018 years (Annex XIV shows the WA+ Sheet 1 for the individual years). The sheet depicts the results for the entire Niger River Basin, using the estimated outflow at the Delta as Qsw out. The year 2009 is considered 'warm-up' year for pixel-based soil moisture balance model and therefore not included in the analyses. The gross inflow is 1,477 km³/year and the total outflow and consumed water is 1,552 km³/year, which results in -75 km³/year decrease in total water storage change. This surface water outflow accounts for 271 km³/year. The Utilized Land Use has the highest water consumption (607 km³/year from ET_{rain} and 273 km³/year from ET_{incr}). The Protected Land Use consumes the least water (19 km³/year). Almost half of Managed Water Use consumption is ET_{incr} (49 %). The Modified Land Use category consumes about 360 km³/year with about 58% from ET_{rain}.

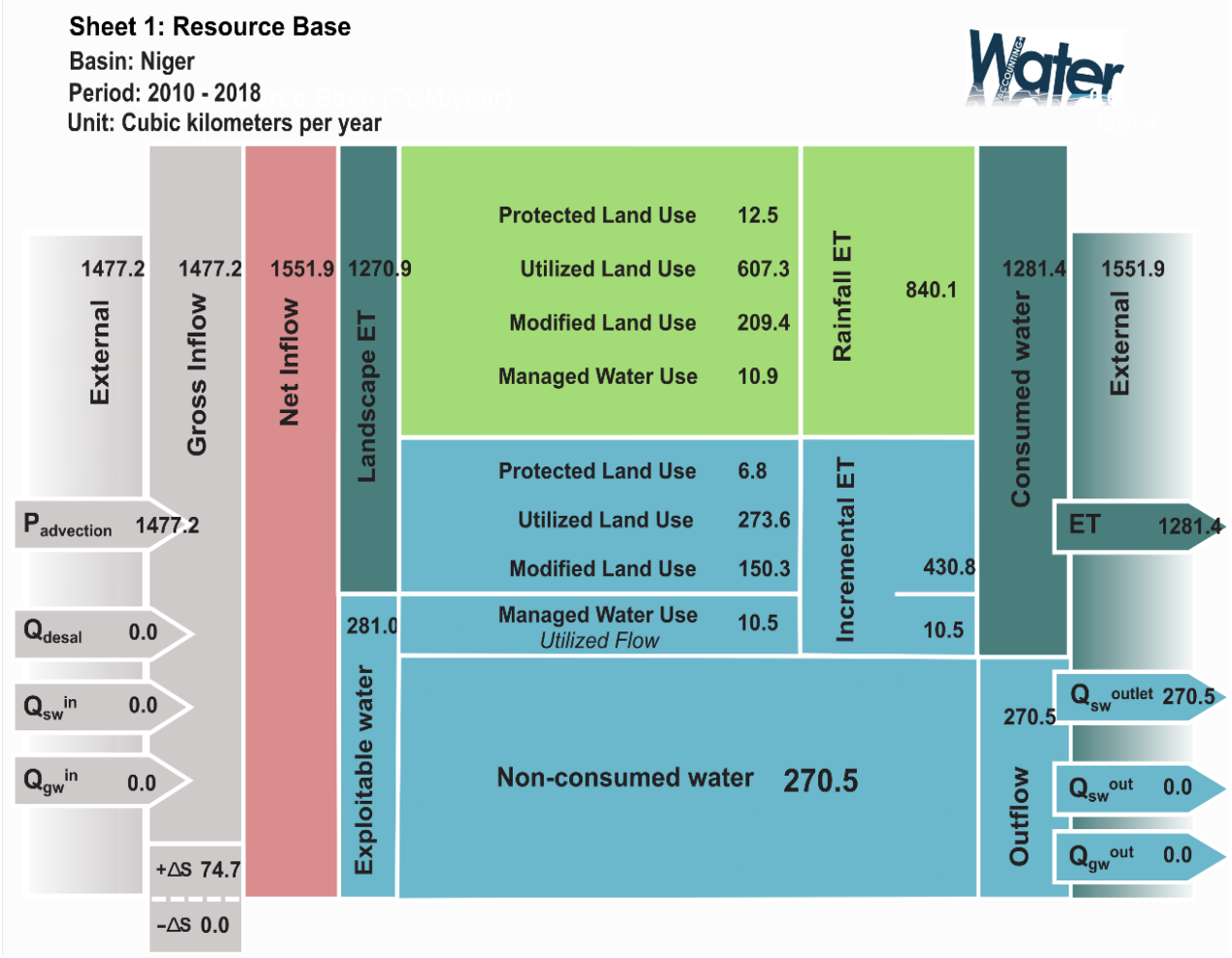

Figure 3-1: The WA+ Sheets 1: Resource Base of the Niger River Basin with average values of the years 2010-2018.

The variation of the main fluxes in these sheets is shown in Figure 3-2 and Figure 3-3. Overall, the proportion of each component relative to gross inflow is stable over the study period, except for total water storage change. In this case, total water storage change is estimated based on the available data on Precipitation, Evapotranspiration and discharge, and not correlated to other remotely sensed measurement such as GRACE gravity anomalies. Landscape ET, which is the sum of ET_{rain} and ET_{incr} of non-managed water use, is the largest component. The utilized flow, which is incremental consumption of the Managed Water Use, is the largest component. The surface water flow at outlet Q_{sw}^{out} is comparatively high in the recent three years and the highest in 2012.

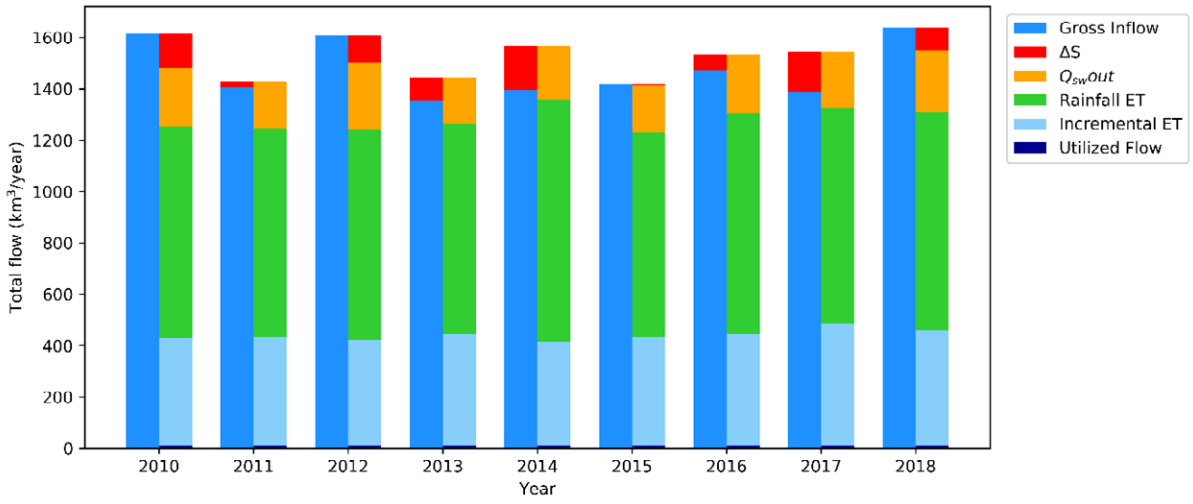

Figure 3-2: Yearly variability of Sheet 1 fluxes. Total storage change (ΔS) was estimated as the difference $P - ET_a - Q_{swout}$ to close the water balance.

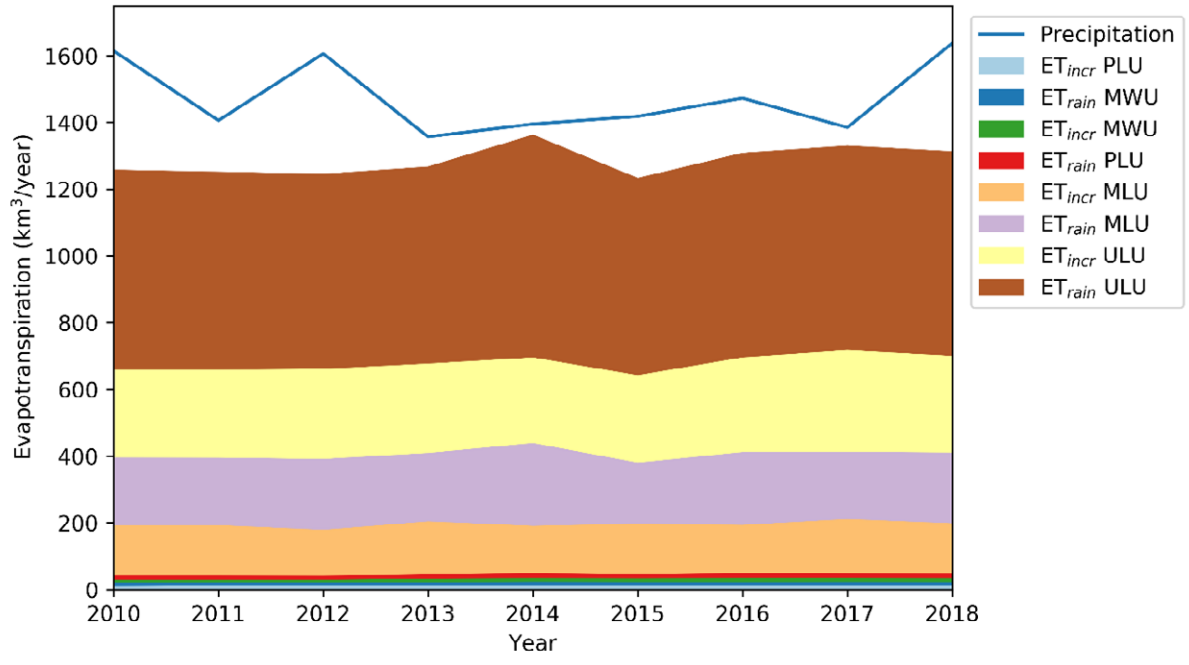

Figure 3-3: Variability of ET_{rain} and ET_{incr} in the Niger River Basin from 2010 to 2018. PLU: Protected Land Use. MWU: Managed Water Use. MLU: Modified Land Use, ULU: Utilized Land Use.

The trend of total annual ET is different from Precipitation (Figure 3-3), which causes the amount of excess rainfall fluctuated greatly during the period, from less than 50 to 200 km³/year. Among the four categories, Managed Water Use and Protected Land Use have very low consumptive use because of their very small share of total area. The ET of Utilized Land Use is the biggest consumptive use. Since Utilized Land Use in the Niger River Basin is mostly bare/sparse vegetation cover, which contribute to non-beneficial consumptive use (FAO, 2017, p. 76), it suggests that by mitigating desertification and improving the landscape, total water consumptive use can be decreased and/or more beneficial. The Modified Land Use, which is mostly Rainfed crops, is the second largest consumptive category.

3.2. WA+ Key indicators

The key performance indicators are presented in Table 3-1. From 2010 to 2018, the average ET fraction of the Niger River Basin is ranging from 77.3 to 97.4 %, which indicates from 2.6 to 22.7% of rainfall is not consumed. The excess rainfall either contributes to increase storage and/or generate outflow from the basin. In case of the Niger River Basin, the outflow from 2010-2018 is higher than excess rainfall, thus, total water storage is decreasing. Therefore, the estimated average stationarity index is -5.7% whereas GRACE total storage change estimates an increase in storage. Therefore, the state of total water storage change from 2010-2018 cannot be definitely concluded from the estimated values. Fortunately, the trend in water storage change was not of significant magnitude compared to other processes.

Table 3-1: WA+ Sheet 1 key indicators of the Niger River Basin for the years from 2010 to 2018 based on water balance derived from WaPOR datasets

Year (%)	ET fraction (%)	Stationarity Index	Basin Closure (%)	Available water (km³/year)	Managed water (km³/year)	Managed fraction (%)
2010	77.7	5.80	82.2	370.5	9.7	2.6
2011	88.7	-6.97	82.5	168.1	9.4	5.6
2012	77.3	3.63	80.1	374.8	9.4	2.5
2013	93.1	-10.33	83.5	104.7	10.8	10.3
2014	97.4	-15.78	82.0	47.7	10.9	22.8
2015	86.6	-3.66	83.4	200.9	10.6	5.3
2016	88.6	-9.09	80.5	180.0	11.7	6.5
2017	95.7	-15.97	80.4	70.6	11.4	16.2
2018	79.9	1.29	81.0	339.4	10.8	3.2
Average	**87.2**	**-5.7**	**81.7**	**206.3**	**10.5**	**8.3**

The average basin closure index of the study period is 81.7%, which indicates that about 82% of all water resources is consumed and/or stored in the basin. The remaining percentage, about 18% of gross inflow, is the total outflow at the Niger Delta. The average available water is 206.3 km³/year, out of which only 8.3% is currently managed. The Managed water, (ETinc of Managed Water Use category), is on aver-

age 10.5 km³/year, which is only 3.7% of total exploitable water and 5% of Available water. Manage Water Use includes irrigated crops, dammed water bodies, and built-up area evaporation. Among these, irrigated crops consumed 59% of total managed water, which shows irrigation is of importance in managed water in terms of consumptive use (Table 3-2).

Table 3-2: Contribution of irrigated crop's ETinc to Managed Water

Year	ET_{incr} of irrigated crops (km³/year)	Managed water (km³/year)	ET_{incr} of irrigated crops/ Managed water (%)
2010	5.4	9.7	55
2011	5.0	9.4	53
2012	5.1	9.4	54
2013	6.4	10.8	59
2014	6.6	10.9	61
2015	6.6	10.6	62
2016	7.6	11.7	65
2017	6.9	11.4	60
2018	6.6	10.8	61
Average	6.2	10.5	59

3.2.1. Non-recoverable water

A significant problem for the Niger River is the degradation of water quality due to the lack of wastewater collection and treatment plants for industrial and domestic uses in most of the riparian cities (UNEP, 2010, p. 61). In addition, fertilizer use in agriculture were also found to have impact on water quality (Andersen et al., 2005, p. 56). In the studies on the Global Grey Water Footprint and Water Pollution Levels (WPL) related to anthropogenic Nitrogen and Phosphorus loads to fresh water, it was estimated that the WPL in the Niger River Basin is 0.15 and 2.6 for Nitrogen and Phosphorus respectively (Mekonnen and Hoekstra, 2018, 2015). These values indicate that it would take 2.6 times of the actual mean annual runoff of the basin to dilute the pollution related to anthropogenic Nitrogen and Phosphorus loads in combination to reach the acceptable standard. Though the uncertainty range of the global GWF is of -33% to +60% must be taken into account, the WPL implies that the estimated available water might not be suitable for some uses (irrigation, drinking water...) unless adequate treatment is applied.

4. The impacts of irrigation water consumption in Office du Niger on the Inner Niger Delta

The comparison of discharge at Mopti and WaPOR water balance estimations showed a significant overestimation using WaPOR data (Table 4-1 and Annex VI). On average, the discrepancy between WaPOR water balance and observed discharge at Mopti is 29 km³/year. It was suspected that the gap in water balance of the Mopti catchment was due to the amount of water being transferred from the Markala dam to the irrigation zones in Office du Niger.

Table 4-1: Estimation of Error in Water Balance of the Mopti catchment based on the difference between observed discharge at Mopti (QMopti) from 2009 to 2015 and residual of $P - ET_a - \Delta S$, where P and ET_a were aggregated from WaPOR data and ΔS is GRACE Total Water Storage changes

Year	QMopti (km³/year)	Water Balance of Mopti catchment			
		ΔS (km³/year)	$P - ET_a - \Delta S$ (km³/year)	Error of Q_{Mopti} (km³/year)	Error of Q_{Mopti} (%P)
2010	36	17	93	56	15
2011	22	-15	46	25	8
2012	33	17	57	24	7
2013	27	-15	85	58	17
2014	24	0	7	-17	-5
2015	27	-4	57	30	9
Mean	**28**	**0**	**58**	**29**	**9**

4.1. Irrigation water consumption in the Office du Niger

The mean annual total ET_{incr} of the area of the Office du Niger is 2,160 Mm³/year (Figure 4-1), which is about the estimation magnitude of 2.7 km³/year (Zwarts et al., 2005). However, the total ET_{incr} of irrigated crop land cover is only 40% of total ET_{incr}, which means the constant water intake into Office du Niger is not only made available for crop production, but is consumed by different land use classes. This is consistent with the reported ratio of crop water requirements over the supply in the Office du Niger (Hertzog et al., 2012; Vandersypen et al. 2006). However, neither the value estimated using ET_{incr} or in the literature can match the gap in water balance of the Mopti catchment as both accounts for only less than 10% of the error in water balance (Table 4-1). Therefore, other sources of error, such as biases in remote sensing derived data, are more likely the culprit.

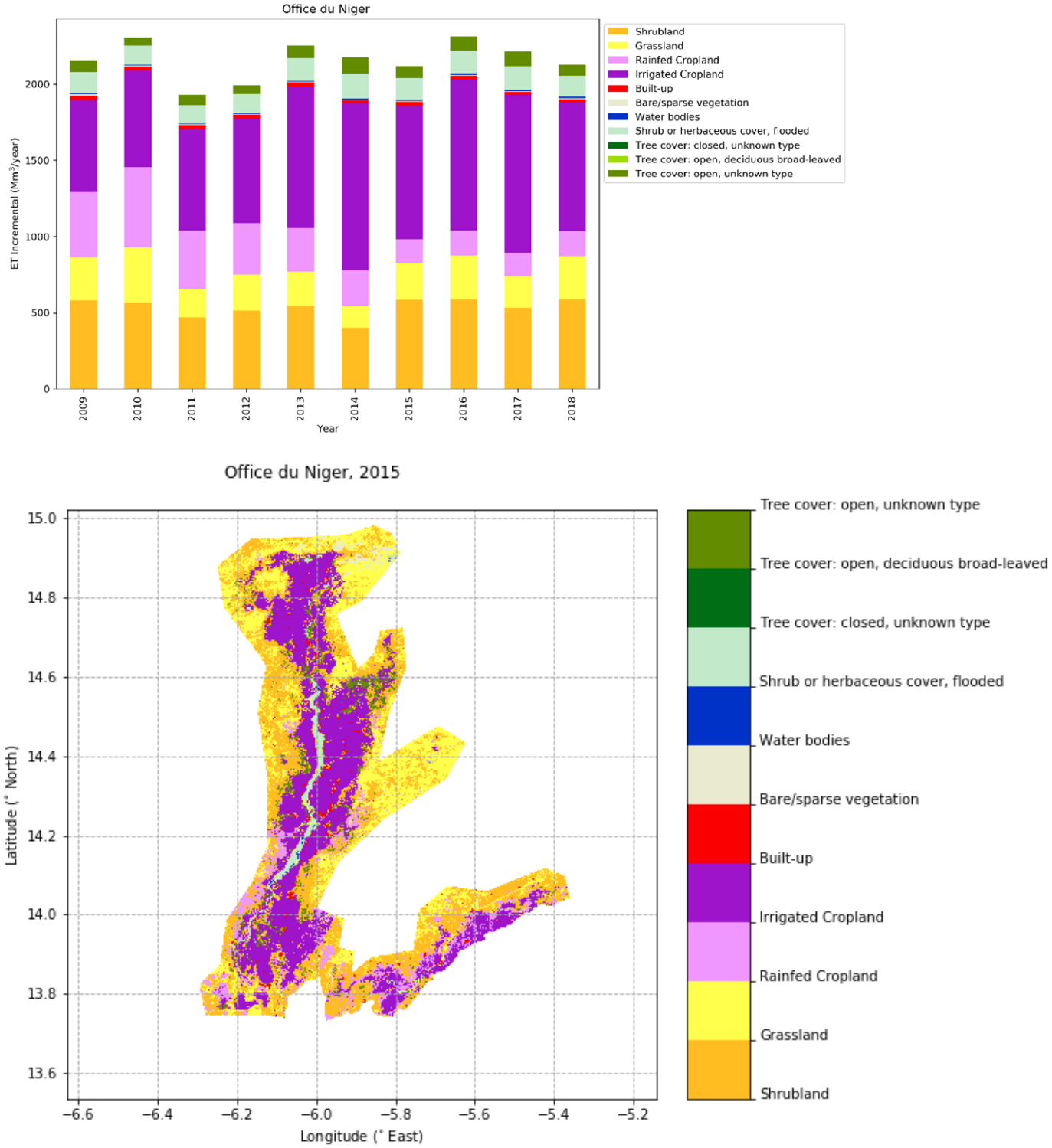

Figure 4-1: Yearly total ET_{incr} of each land cover class (upper) and the spatial distribution of land cover of the year 2015 in the Office du Niger zone, based on WaPOR LCC.

Figure 4-2 compares the water consumption per area of the land cover classes in the Office du Niger by showing mean annual ET_a and ET_{incr} of all classes in mm/year. It can be seen that ET_a and ET_{incr} for water bodies and closed tree cover classes, is significantly higher after 2014 (when source of WaPOR L2 data was switched from MODIS to PROBA-V). Other classes such as cropland, built-up, and grassland do not show such shifts during the study period. ET_a and ET_{incr} of these classes fluctuated between dry and wet years.

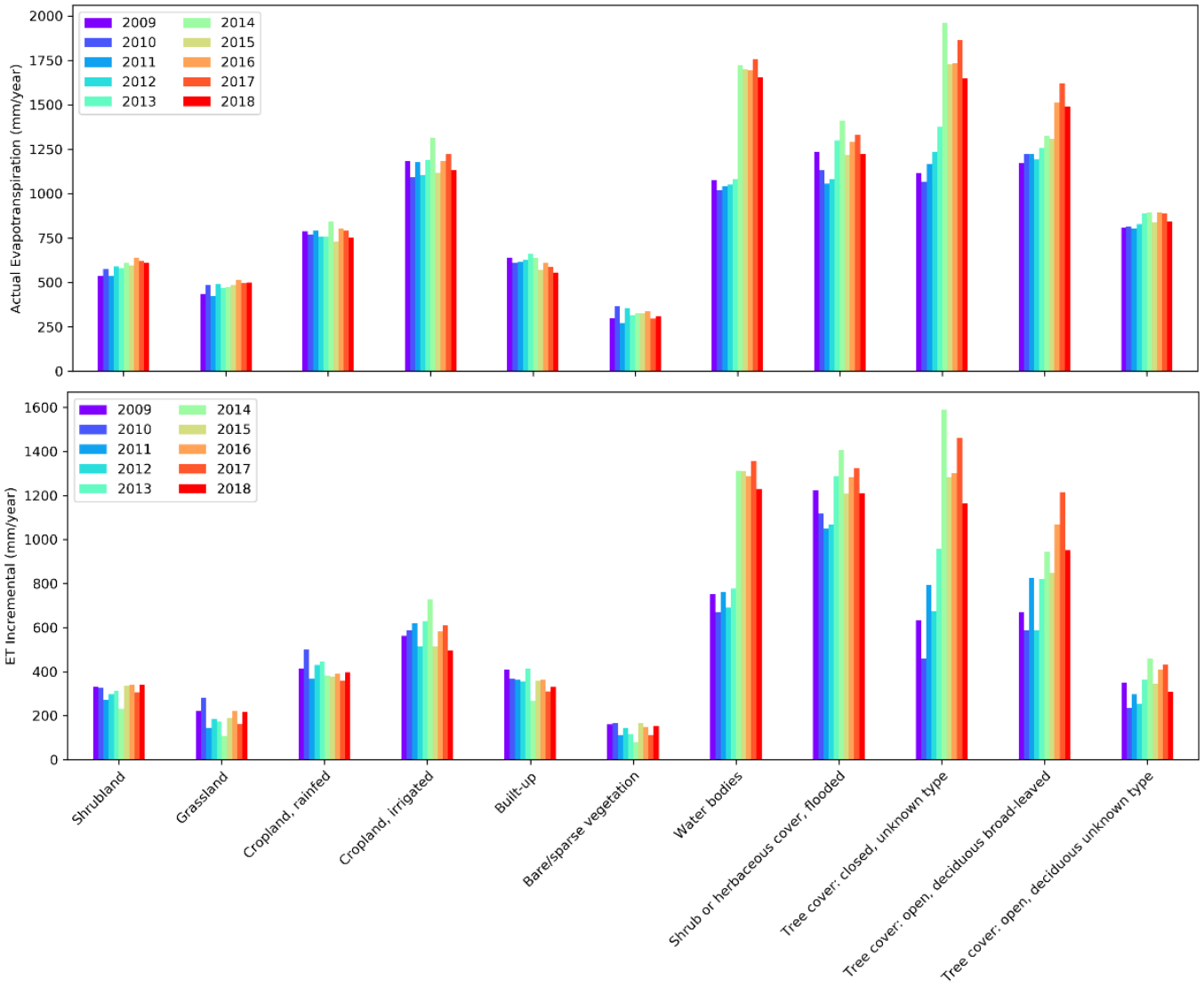

Figure 4-2: Mean annual ET_a and ET_{incr} of each land cover class in the Office du Niger zone.

4.2. Change in flood extent in the Inner Niger Delta

4.2.1. Comparison between different threshold selection methods

Using ET_a and ET_{incr} maps to estimate flooded extent can show variation of flooded area between months. For example, Figure 4-3 shows the flooded extent in the 2009 flood season, in which the vegetation cover in the southern part of the Inner Niger Delta during the flood season months, and in the northern part water bodies can be seen. For the same month, for example November 2009, the four methods differ in terms location of flooded area (Figure 4-4). Method 1 and method 3, which both use monthly value of Mean – STD of water bodies, do not classify some small lakes in the northern part of the delta as flooded even though November 2009 is the month with peak water level in Akka. Meanwhile, method 3 and 4 show more flooded water bodies in the northern part of the delta.

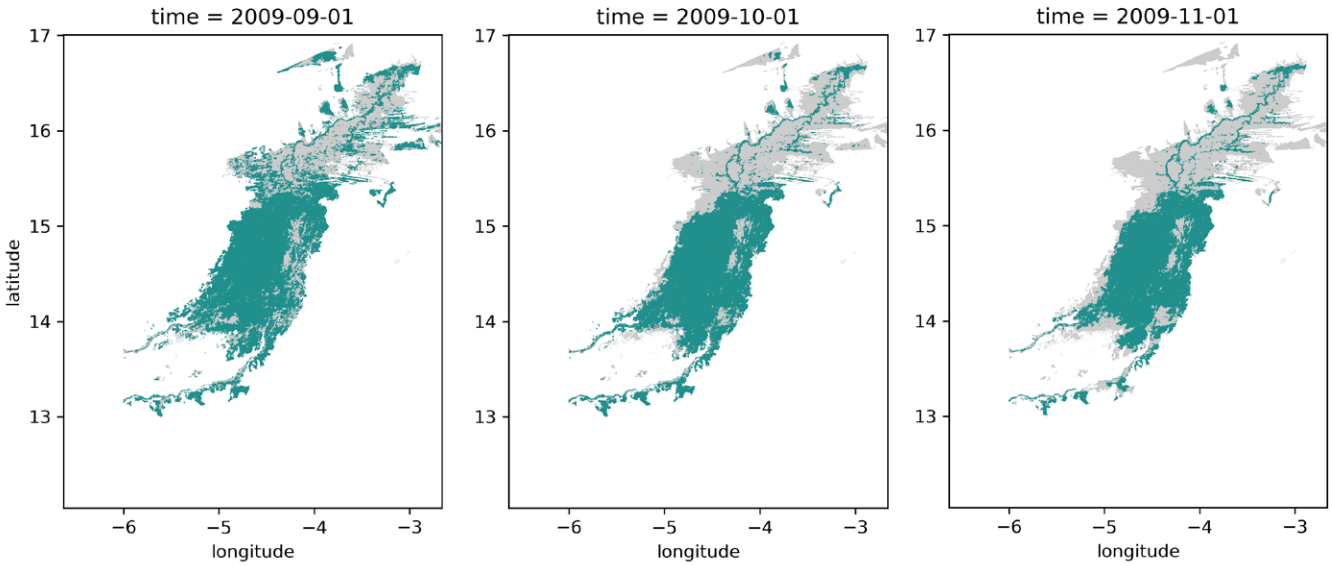

Figure 4-3: Flooded maps estimated for flood peak months in 2009 using Method 1. Turquoise colour indicates flooded pixels and grey colour indicates the Inner Niger Delta boundary.

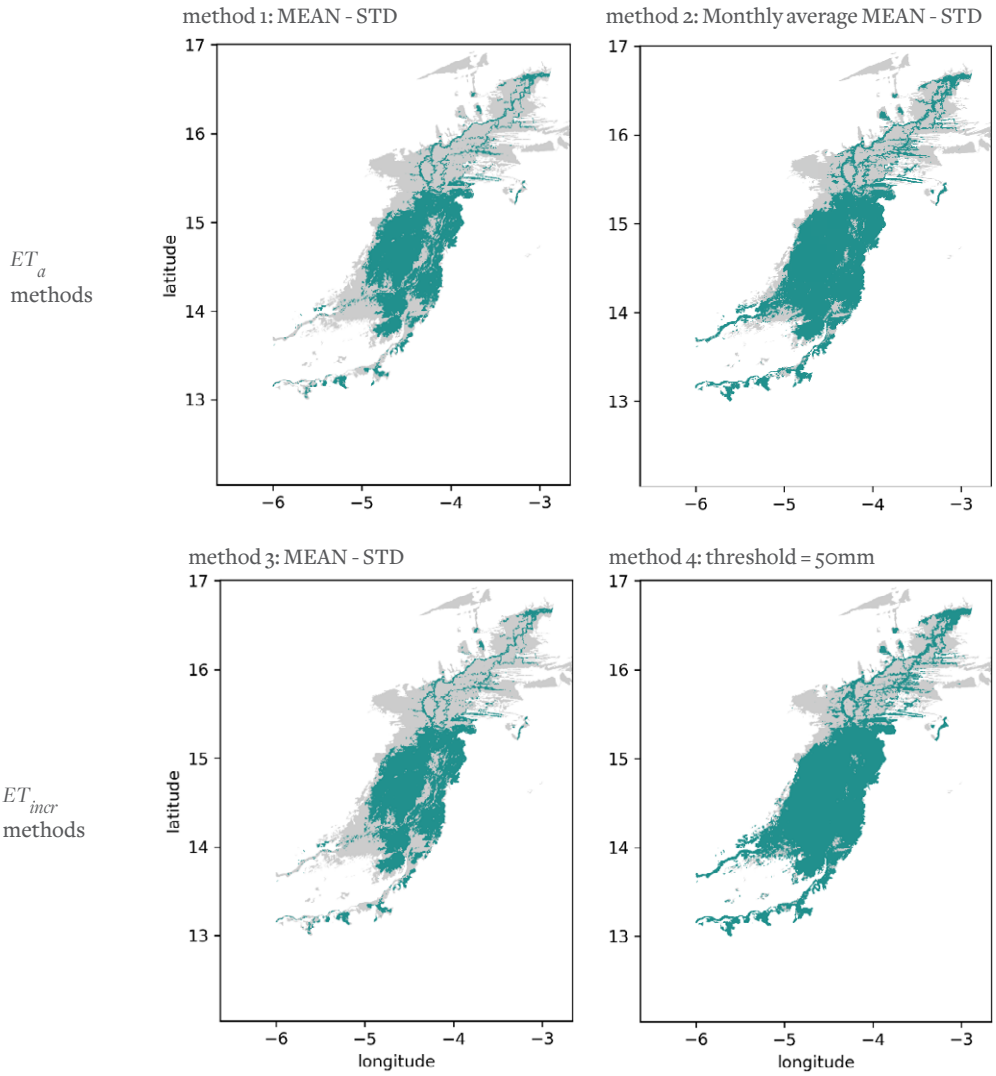

Figure 4-4: Flood extent in November 2016 as estimated by ET_a and ET_{incr} threshold methods

Comparing the monthly average flooded area of the methods, it can be seen that all methods except method 4 show peak flooded area in September, which is quite too early during the flood season. On the other hand, method 4 shows the peak flooded area in November, which coincides with the maximum water level in Akka (Annex XII). Therefore, in terms of monthly variation to flooded area, using a fixed threshold for all the months produces the most realistic pattern.

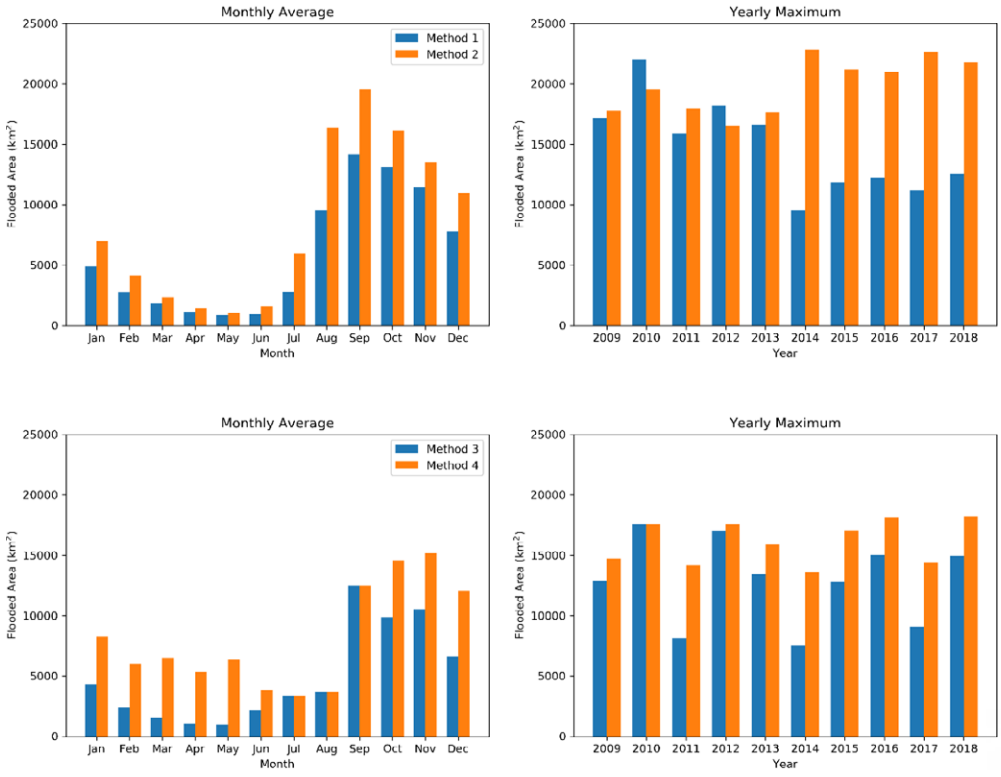

Figure 4-5: Estimated monthly and yearly maximum flooded area in the Inner Niger Delta by thresholding WaPOR ET_a and ET_{incr}.

When comparing the yearly maximum flooded area of the four methods, it should be kept in mind that for different method, maximum flooded area occurs in different month (Figure 4-5). The yearly maximum flooded area using ET_a data shows a significant difference between the years before and after 2014, which might be due to reduction of standard deviation of ET_a in the water bodies from 2014 (Figure 2-20). Therefore, using ET_a data to calculate maximum flooded extent, compared to ET_{incr} might not be useful for detecting yearly trend, if there is any.

4.2.2. Comparison with other methods not using WaPOR data

4.2.2.1. Maximum flooded area

Zwarts et al. (2005) derived the relationship between the water level measured at Akka gauging station and the maximum flooded area in the Inner Niger Delta (Annex XIII-2). Based on this relationship and the maximum water level records published by the Niger Basin Authority (ABN) (Annex XII), we calculated the maximum flooded area for the period 2009-2018, and use this as a 'Reference' method:

Table 4-2: Maximum flooded area calculated from peak water level in Akka using the formula by Zwarts & Grigoras (2005)

Year	Peak water level (cm)	Maximum Flooded area (km2)
2009	496	15,451
2010	504	15,958
2011	403	10,486
2012	501	15,775
2013	476	14,230
2014	438	12,146
2015	471	13,936
2016	497	15,521
2017	427	11,619
2018	539	18,322

The maximum flooded area comparison of 'Reference' method with the four methods is shown in Figure 4-6. Since the peak water level in Akka occurs in November for all the years from 2009 to 2018, the flooded area in November was used for this comparison instead of the peak flooded area, which occurs in September for 3 out of 4 methods (Figure 4-5). Before 2014, all the methods show very close value of flooded area compared to the reference. From 2014, method 1 and 3 show significantly lower flooded area. Method 2 and 4 shows the high agreement with the Reference method in terms of flooded area in November. However, the maximum flooded area by method 2 was actually in September (Figure 4-5). Therefore, method 4 was considered the best considering both the timing and area of the maximum flood extent

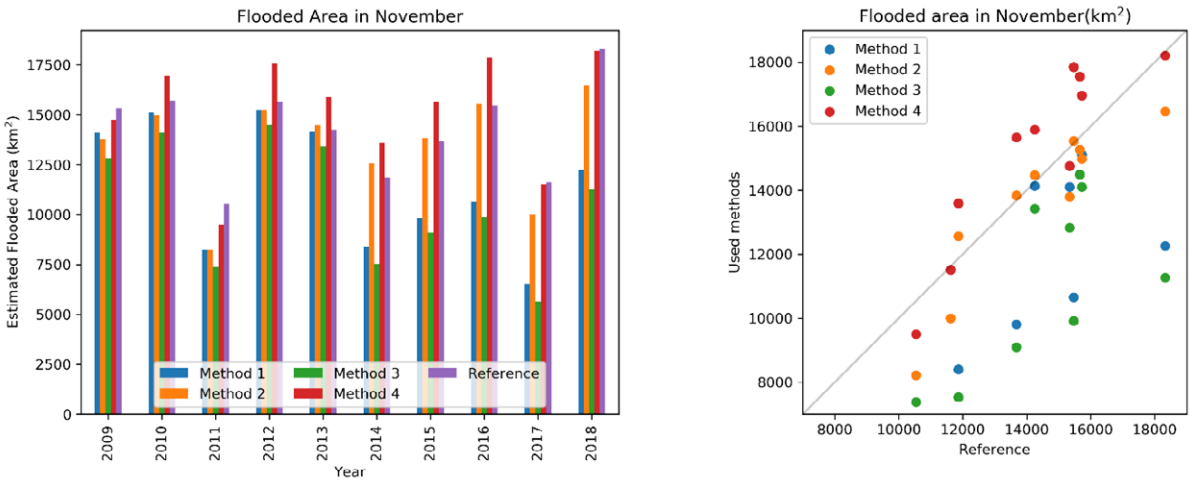

Figure 4-6: Flooded area in November by the 4 different ET threshold methods compared to Zwarts & Grigoras formula. *Reference: Maximum flooded area derived from the peak water level in Akka using equation by Zwarts et al. (2005).

4.2.2.2. Flooded area maps

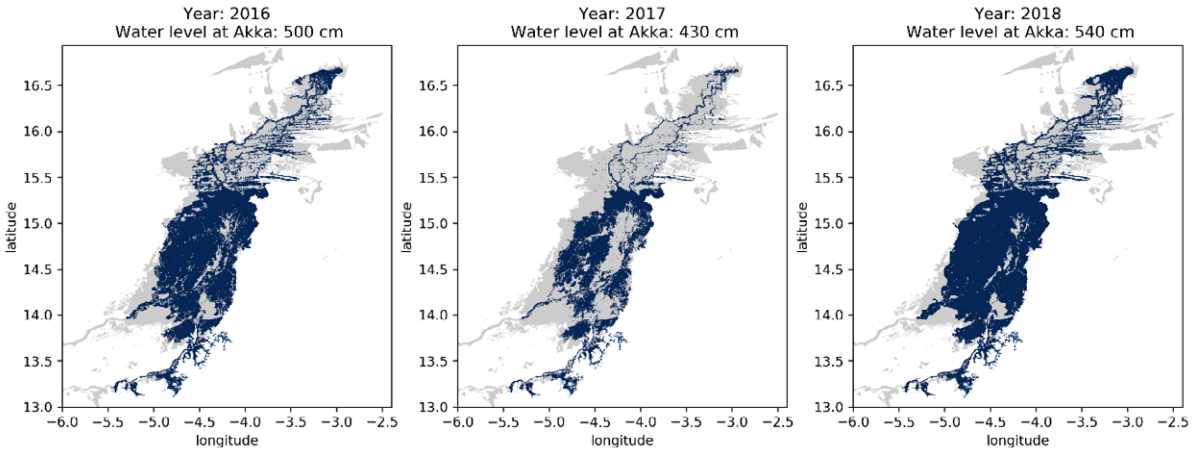

Figure 4-7: The flooded maps from digital flood model by Zwarts et al. (2005), which can also be viewed on OPIDIN flood-viewer, corresponding to the peak water level in Akka during the 2016, 2017, and 2018 flood seasons (which peaked in November)

The digital flood model developed by Zwarts et al. (2005) and improved by Davids et al. (2018) also produce flood map corresponding to every 10 cm of peak water level in Akka. For example, Figure 4-7 shows the flood maps corresponding to the peak water level in Akka in 2016, 2017, and 2018. Pixel-by-pixel comparison of these reference maps with the flood maps of the same month generated by the 4 methods used above are shown in Figure 4-8 and Figure 4-9. All of the methods underestimated most of the flooded area in the northern part of the delta. Method 1 and 3 greatly underestimated the flooded area in the middle of the delta. Meanwhile, method 4 shows the largest overestimation of flooded area in the inlet of the delta at Macina, and the area between Youvarou and Mopti (See locations in Figure 2-21). The greatest difference in flood maps was in the year 2017, which was relatively drier than 2016 and 2018. It should be noted that the flooded maps from digital flood model are based on composites of all selected satellite images during a flood season to capture the maximum flooded area of the season corresponding to the peak water level, and not a flood map at a particular time (Zwarts et al., 2005).

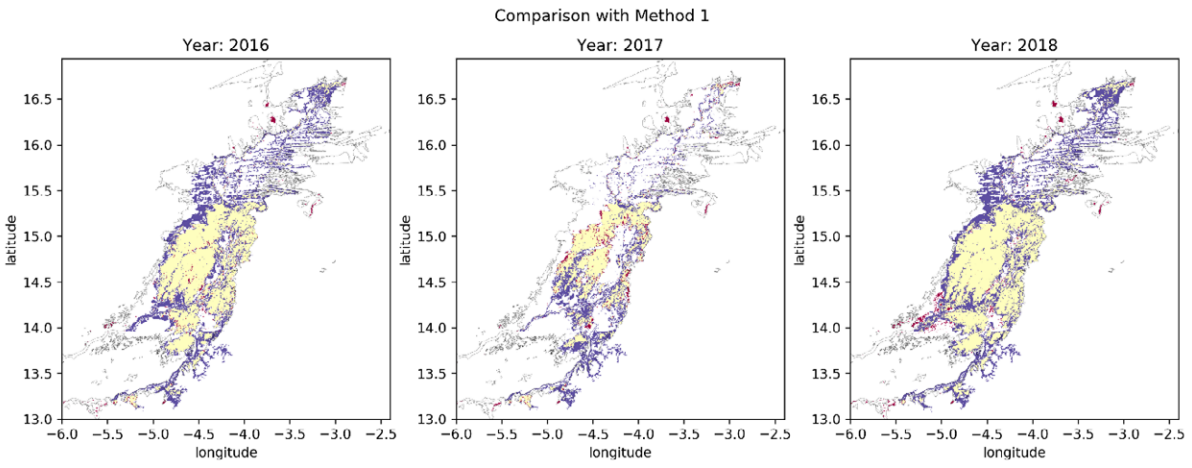

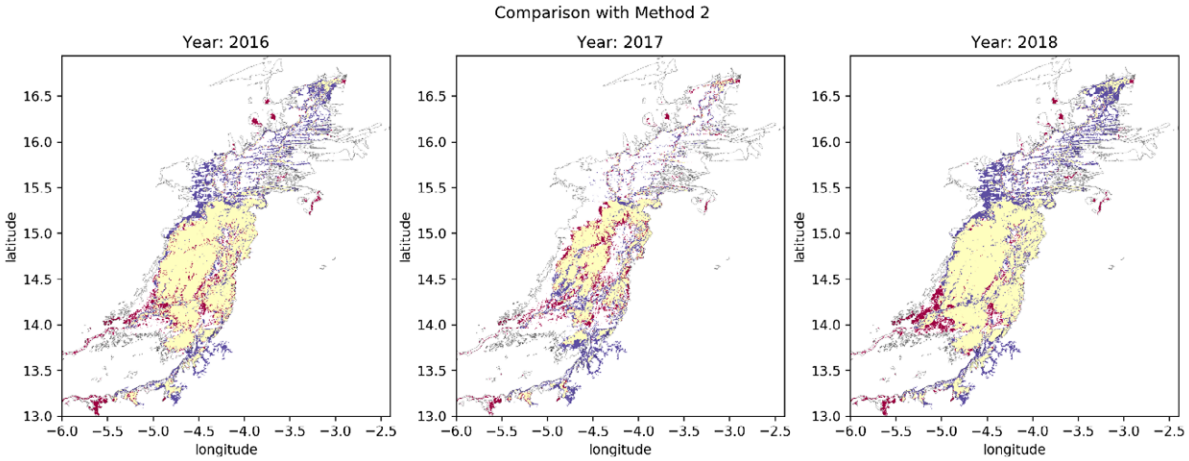

Figure 4-8: The difference between flooded maps using method 1 and 2 compared to the flooded maps from digital flood model by Zwarts et al.(2005). Yellow color indicates flooding in both maps. Red color indicates flooding in the maps of method 1 and 2. Blue color indicates flooding in the reference maps.

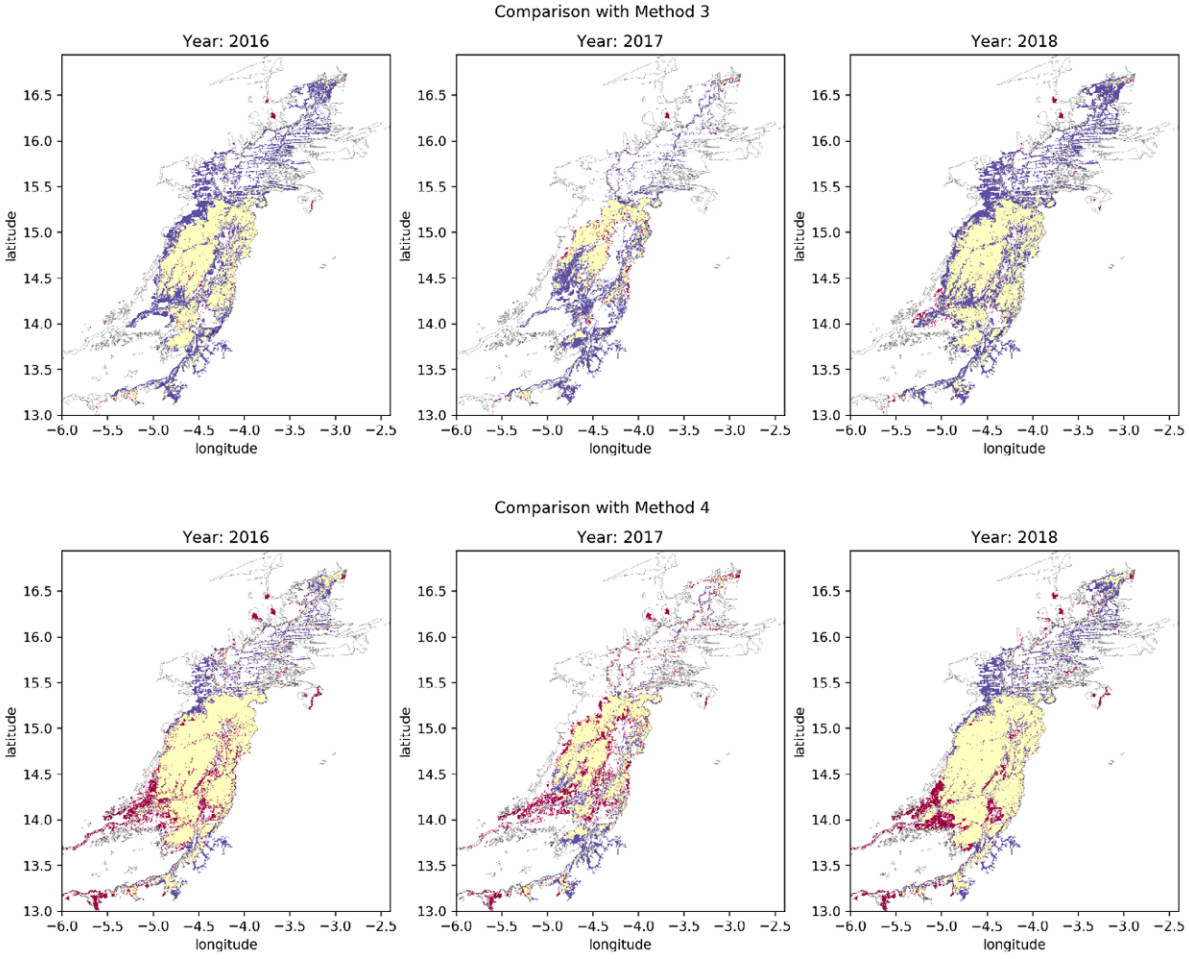

Figure 4-9: The difference between flooded maps using method 3 and 4 compared to the flooded maps from digital flood model by Zwarts et al.(2005). Yellow color indicates flooding in both maps. Red color indicates flooding in the maps of method 3 and 4. Blue color indicates flooding in the reference maps.

Figure 4-10 further compares the flood area resulted from Method 1 and 4 to the method using Sentinel-1 SAR imagery change detection (the details of the procedure given in Annex XIII-3). It can be seen that using SAR data, there are more flooded pixels in the Northern part and less flooded pixels in

the Southern part of the delta compared to Method 1 and 4. The selection of the period to create mosaics of SAR scenes before the flood might have also influenced the results. If the area was already flooded the before flood period, the change detection method would have misclassified the flooded area because the change of backscatter signals was not significant. Moreover, the southern part is not flooded at the same time with the northern part of the inner delta, the change detection method might not be able to capture flooded area in both area since it only considers the change before and after the day of peak flood level.

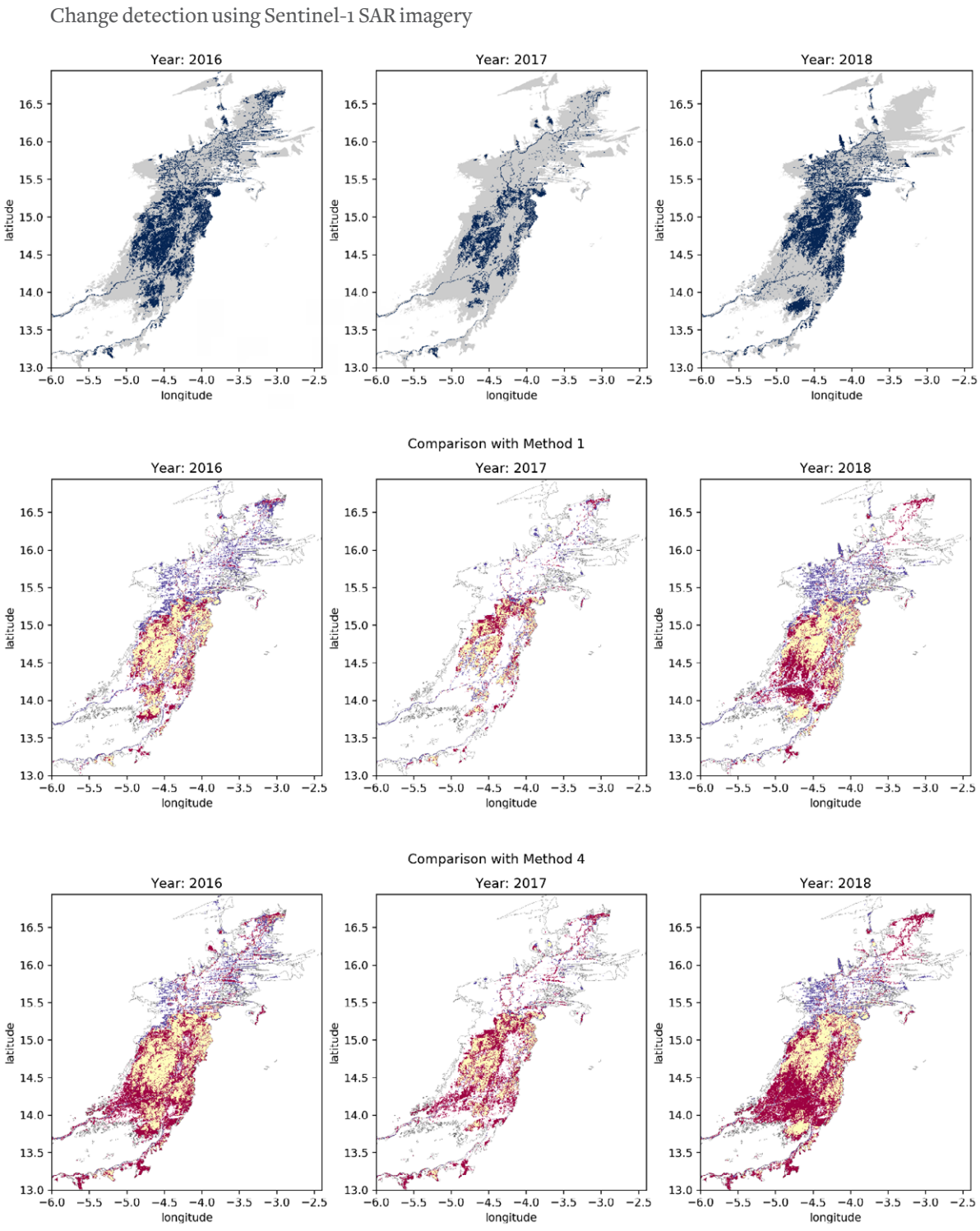

Figure 4-10: Comparison of flood maps in peak flood month (November) derived from Sentinel-1 SAR data using change detection method with Method 1 and 4 for the years from 2016-2018. Yellow color indicates flooding in both maps. Red color indicates flooding in the maps of method 1 and 4. Blue color indicates flooding in the SAR-derived flood maps.

4.2.3. Correlation of irrigation water consumption and flood extent

The relationship between ET_{incr} of the whole Office du Niger area, as an estimate for total supply, and the maximum flooded area in the Inner Niger Delta was given in Figure 4-11. Pearson correlation was calculated using percentage of mean for pairs of variables with different units. The correlation coefficients of the 2 maximum flooded area estimates in the Inner Niger Delta with ET_{incr} of irrigated crop in the Office du Niger (-0.06 and -0.28) are close to no correlation, while the correlation coefficients with ET_{incr} of the whole area (0.4 and 0.28) are also lower than moderate. In both cases, we cannot confirm a significant correlation between irrigation consumption in Office du Niger and the maximum flooded area in the Inner Niger Delta.

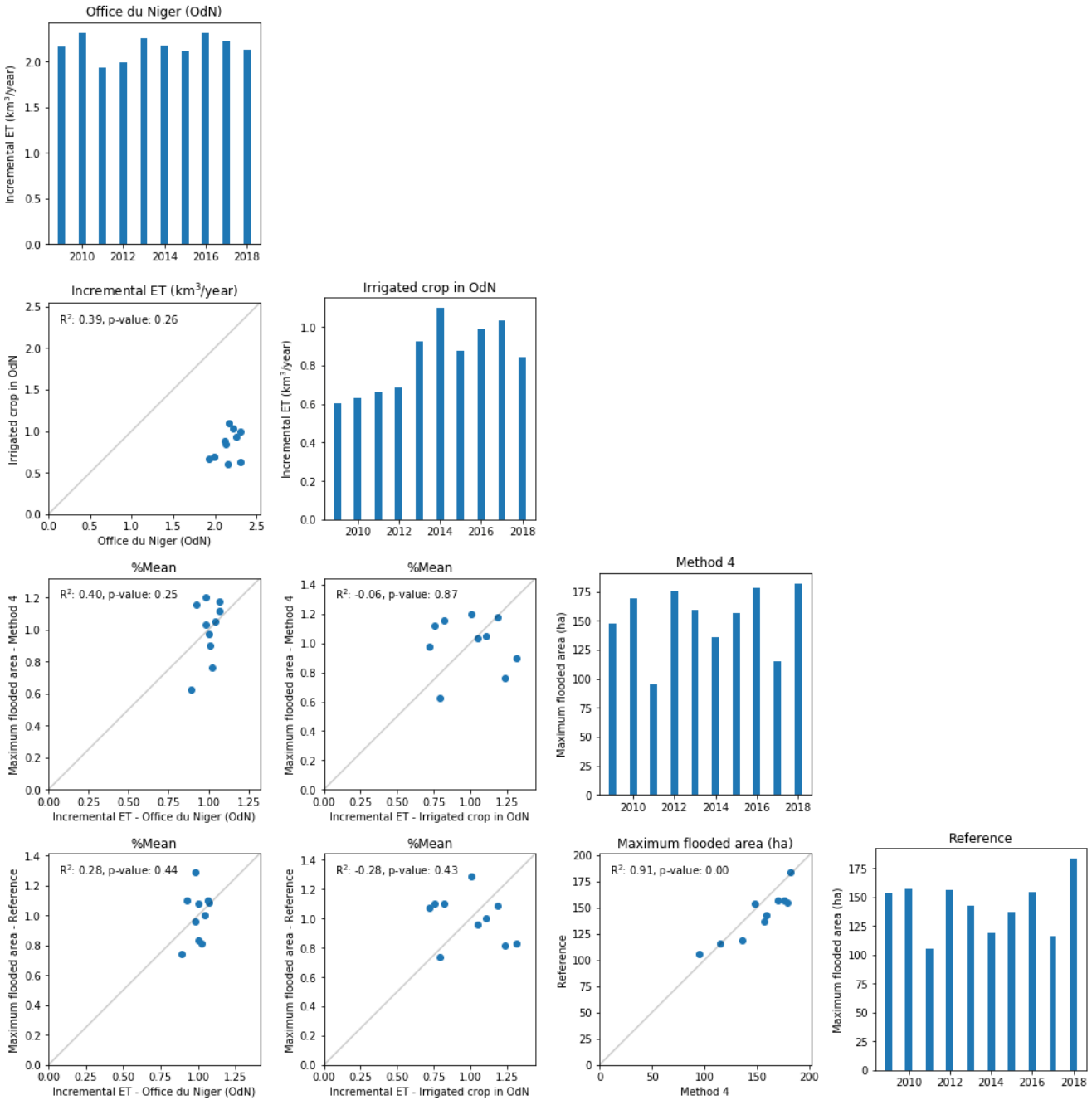

Figure 4-11: Correlations between the total ET_{incr} of the whole Office du Niger area and ET_{incr} of irrigated crop with the estimates of maximum flooded area in the Inner Niger Delta using Method 4 and the reference method (Zwarts et al., 2005). The yearly variation of these quantities are shown in the diagonal plots.

4.2.4. Synthesis

The total annual Incremental ET of irrigated area in the Office du Niger was found to be increasing in the 10-year period from 2009-2018. This is mostly due to the increase of irrigated area based on WaPOR LCC, since the Incremental ET per area unit did not actually increase. This study shows that the total water consumption (ET_{incr}) of the irrigated area in the Office du Niger (assuming the irrigated area as in WaPOR LCC) is 40% of that of the whole Office du Niger area, from which we can estimate an irrigation efficiency of 40%. This ratio reported by Vandersypen et al. (2006) was about 50% based on official records. Therefore, we evaluated that the irrigation efficiency of the Office du Niger did not change much in the recent years compared to the past, if not decreased. Moreover, as the Markala dam's diversion is continuous regardless of irrigation demand (Vandersypen et al., 2006), there is a lot of space for improvement to make better use of the supply from this diversion. The discrepancy between observed discharge and WaPOR water balance estimation of the Mopti catchment, however, cannot be explained by the water diversion.

WaPOR data can somehow capture flooded vegetation due to relatively high ET_a and ET_{incr} compared to surrounding pixels. However, the month of peak flooding and flooded area varies considerably for different threshold methods. Two of the four tested methods resulted in maximum flooded area close to the one derived from the empirical formula by Zwarts et al. (2005), though the maps showing the spatial variability of the floods differ. Either using these two methods or the formula, the maximum flooded extent in the Inner Niger Delta did not show significant trend of increasing or decreasing over the study period, except for variation in dry and wet years. This might be because the influence of precipitation during this period is more dominant than that of withdrawals from the river, which is less than 5% of peak flow at Mopti. It is also probable that the study period was not very long to capture the long-term trend.

5. Conclusions

The Niger River is a complex water system that covers an extremely large area, on which million human lives and wildlife are dependant. As a result, this 'simple and rapid' water accounts analysis could only aim to look at the state of the water resources in the basin from a satellite view. It is valuable in terms of demonstrating the suitability of the WaPOR datasets for applying the WA+ framework and closing the water balance. The WaPOR $P - ET_a$ analysis showed that, on average, the runoff generated in the entire Niger River Basin is 18.6% of total rainfall. In general, by averaging over a period of (2009-2010), the uncertainty in water balance can be reduced. However, when looking at individual years, this uncertainty increases depending on the anomaly of P and ET_a data. For this water accounts, the discrepancy in water balance from available data is kept in total water storage change, which is of a magnitude less than 1% of annual rainfall. As this storage change is small and the groundwater storage was reported to be abundant and not over-exploited, it is potential to use groundwater storage during low rainfall period.

With consideration of data uncertainty and errors in water balance, it is still safe to say that the available water in the Niger River Basin is currently not over-exploited and managed extensively. Therefore, there is still potential for agriculture expansion in the basin. Since the managed water is only 8.3% of available water and 3.7% of exploitable water, out of which 59% is incremental consumption of irrigated crops, agricultural water withdrawals can be augmented in the future. However, it is recommended that implementation of agricultural expansion should take into account the impacts of climate variability on seasonal and periodic availability of water resources, in particular the locally important Inner Niger Delta in Mali is highly dependent on the natural flow regime. Where water is withdrawn might have great impacts on the downstream ecosystem and waterway navigation. Thus, integrated water resources management is important if development of water use takes place. This study also provide a spatial overview of where in the basin water is generated and consumed via ET_a. The largest net water consumption is in bare/sparse vegetation cover. While irrigated crops, and water bodies have net water consumptive use, their contribution to total ET_a is low and often beneficial. Therefore, agricultural development if combined with improvement of landscape strategies, such as mitigating desertification, is recommended to reduce non-beneficial water consumptive use.

Moreover, in the analysis on the impacts of irrigation water consumption in Office du Niger on the Inner Niger Delta using WaPOR data and derived Incremental ET, we evaluated that the irrigation efficiency of Office du Niger did not change much from the study in 2006 (Vandersypen et al., 2006). Therefore, it is recommended that improvement on water productivity in this irrigation scheme is possible and should be prioritized in the context of increasing water demand and uncertain climate condition. The maximum flooded area, as an indicator of ecosystem health in the Inner Niger Delta, was estimated using WaPOR ET and other recommended practices (UN-SPIDER, 2020; Zwarts et al., 2005). No significant trend of maximum flooded area estimate was found to be correlated with irrigation water consumption in Office du Niger on a yearly basis during the study period 2009-2018. However, we recommend that this relationship should be monitored continuously in the long-term while accounting for the seasonality, in order to assess the impacts of irrigation extension in both dry and wet season cropping.

References

Abam, T.K.S. 1999. Impact of dams on the hydrology of the Niger Delta. *Bulletin of Engineering Geology and the Environment*. 57, 239–251. https://doi.org/10.1007/s100640050041

ABN (**Niger Basin Authority**). 2019. Direct data access, http://nigerhycos.abn.ne/user-anon/htm/(accessed 11.10.19).

ABN (**Niger Basin Authority**). 2015. *Bilan hydrologique du bassin du Niger 2014/2015*. Niger Basin Authority. http://nigerhycos.abn.ne/portal/IMG/pdf/bilan_hydrologique_2014-2015_r24062015.pdf

Aich, V., Liersch, S., Vetter, T., Fournet, S., Andersson, J.C.M., Calmanti, S., van Weert, F.H.A., Hattermann, F.F., Paton, E.N. 2016. Flood projections within the Niger River Basin under future land use and climate change. *Science of the Total Environment*. 562, 666–677. https://doi.org/10.1016/j.scitotenv.2016.04.021

Akujieze, C.N., Coker, S., Oteze, G. 2003. Groundwater in Nigeria – a millennium experience – distribution, practice, problems and solutions. *Hydrogeology Journal*. 11, 259–274. https://doi.org/10.1007/s10040-002-0227-3

Amogu, O., Descroix, L., Yéro, K.S., Le Breton, E., Mamadou, I., Ali, A., Vischel, T., Bader, J.-C., Moussa, I.B., Gautier, E., Boubkraoui, S., Belleudy, P. 2010. Increasing River Flows in the Sahel? *Water*, 2, 170–199. https://doi.org/10.3390/w2020170

Andersen, I., Dione, O., Jarosewich-Holder, M., Olivry, J.-C. 2005. The Niger River Basin. A vision for sustainable management. *Directions in development*. The World Bank, Washington, DC.

Ankit, R. 2019. *WebPlotDigitizer: HTML5 based online tool to extract numerical data from plot images*. Version 4.2. https://automeris.io/WebPlotDigitizer.

Aw, D., Dejou, C. 1996. *Office du Niger : Ensuring Food Security for Mali*. World Bank Africa Region.

Bastiaanssen, W.G.M., Karimi, P., Rebelo, L.-M., Duan, Z., Senay, G., Muthuwatte, L., Smakhtin, V. 2014. Earth observation based assessment of the water production and water consumption of Nile Basin agro-ecosystems. *Remote Sensing*. 6, 1030610334. https://doi.org/10.3390/rs61110306

Biancamaria, S., Mballo, M., Le Moigne, P., Sánchez Pérez, J.M., Espitalier-Noël, G., Grusson, Y., Cakir, R., Häfliger, V., Barathieu, F., Trasmonte, M., Boone, A., Martin, E., Sauvage, S. 2019. Total water storage variability from GRACE mission and hydrological models for a 50,000 km2 temperate watershed: the Garonne River basin (France). *Journal of Hydrology: Regional Studies*. 24, 100609. https://doi.org/10.1016/j.ejrh.2019.100609

Casse, C., Gosset, M., Peugeot, C., Pedinotti, V., Boone, A., Tanimoun, B.A., Decharme, B. 2015. Potential of satellite rainfall products to predict Niger River flood events in Niamey. *Atmospheric Research*, 6th Workshop of the International Precipitation Working Group 163, 162–176. https://doi.org/10.1016/j.atmosres.2015.01.010

Davids, L., Bekkema, M., Zwarts, L., Grigoras, I. 2018. *An improved spatial flooding model of the Inner Niger Delta*. (No. 2529), A&W-report. Altenburg & Wymenga ecologisch onderzoek, Feanwâlden.

Davies, S. 1996. Livelihood Safety Nets: The Inner Niger Delta in the Sahel, in: Davies, S. (Ed.), Adaptable Livelihoods: Coping with Food Insecurity in the Malian Sahel. Palgrave Macmillan UK, London, pp. 109–136. https://doi.org/10.1007/978-1-349-24409-6_6

de Boer, F. 2016. *HiHydroSoil: A High Resolution Soil Map of Hydraulic Properties* (Version 1.2), Report FutureWater: 134.

Descroix, L., Mahé, G., Lebel, T., Favreau, G., Galle, S., Gautier, E., Olivry, J.-C., Albergel, J., Amogu, O., Cappelaere, B., Dessouassi, R., Diedhiou, A., Le Breton, E., Mamadou, I., Sighomnou, D. 2009. Spatio-temporal variability of hydrological regimes around the boundaries between Sahelian and Sudanian areas of West Africa: A synthesis. *Journal of Hydrology. Surface processes and water cycle in West Africa, studied from the AMMA-CATCH observing system.* 375, 90–102. https://doi.org/10.1016/j.jhydrol.2008.12.012

Dost, R., Obando, E.B., Bastiaanssen, W., Hoogeveen, J. 2013. *Water Accounting Plus (WA+) in the Awash River Basin. Coping with Water Scarcity – Developing National Water Audits Africa.* https://www.wateraccounting.org/files/projects/awash_basin.pdf (accessed 1.8.19).

FAO. 2019. *FAO Water Productivity - Catalog - Land Cover Classification*. https://wapor.apps.fao.org/catalog/2/L2_LCC_A (accessed 9.20.19).

FAO. 2018a. *WaPOR Database Methodology: Level 1. Remote Sensing for Water Productivity (Technical Report)*. Food and Agriculture Organization of the United Nations, Rome.

FAO. 2018b. *WaPOR Database Methodology: Level 2, Remote Sensing for Water Productivity Technical Report: Methodology Series.* Rome.

FAO. 2017. *Water accounting and auditing , a sourcebook*. 238.

FAO, IHE Delft. 2020. *Water accounting in the Awash River Basin*. FAO WaPOR water accounting reports. Rome.

Favreau, G., Cappelaere, B., Massuel, S., Leblanc, M., Boucher, M., Boulain, N., Leduc, C. 2009. Land clearing, climate variability, and water resources increase in semiarid southwest Niger: A review. *Water Resources Research.* 45. https://doi.org/10.1029/2007WR006785

Funk, C., Peterson, P., Landsfeld, M., Pedreros, D., Verdin, J., Shukla, S., Husak, G., Rowland, J., Harrison, L., Hoell, A., Michaelsen, J. 2015. The climate hazards infrared precipitation with stations—a new environmental record for monitoring extremes. *Scientific Data*. 2, 1–21. https://doi.org/10.1038/sdata.2015.66

Goulden, M., Few, R. 2011. *Climate Change, Water and Conflict in the Niger River Basin.* U.S. Agency for International Development (USAID), Washington, DC.

Hertzog, T., Adamczewski, A., Molle, F., Jean-Christophe, P., Jean-Yves, J. 2012. Ostrich-like strategies in Sahelian Sands? Land and water grabbing in the Office du Niger, Mali. *Water Alternatives.* 5, 304–321.

Karimi, P. 2014. *Water Accounting Plus for Water Resources Reporting and River Basin Planning*. TU Delft, Delft, The Netherlands (PhD dissertation).

Karimi, P., Bastiaanssen, W.G.M. 2015. Spatial evapotranspiration, rainfall and land use data in water accounting – Part 1: Review of the accuracy of the remote sensing data. *Hydrology and Earth System Sciences*. 19, 507–532. https://doi.org/10.5194/hess-19-507-2015

Kassambara, B., Ganji, H., Kajisa, T. 2018. Impact of agricultural water allocation on the ecosystems in the Inner Niger River Delta. *International Journal of GEOMATE*. 14, 164–170.

Leblanc, M.J., Favreau, G., Massuel, S., Tweed, S.O., Loireau, M., Cappelaere, B. 2008. Land clearance and hydrological change in the Sahel: SW Niger. *Global and Planetary Change.* 61, 135–150. https://doi.org/10.1016/j.gloplacha.2007.08.011

Lehner, B., Grill, G. 2013. Global river hydrography and network routing: baseline data and new approaches to study the world's large river systems. *Hydrological Processes*. 27, 2171–2186.

Lehner, B., Liermann, C.R., Revenga, C., Vörösmarty, C., Fekete, B., Crouzet, P., Döll, P., Endejan, M., Frenken, K., Magome, J., Nilsson, C., Robertson, J.C., Rödel, R., Sindorf, N., Wisser, D. 2011. High-resolution map-

ping of the world's reservoirs and dams for sustainable river-flow management. *Frontiers in Ecology and the Environment*. 9, 494–502. https://doi.org/10.1890/100125

Liénou, G., Mahé, G., Dieulin, C., Paturel, J.-E., Bamba, F., Sighomnou, D., Dessouassi, R. 2010. *The river Niger water availability : facing future needs and climate change.* 12.

Liersch, S., Cools, J., Kone, B., Koch, H., Diallo, M., Reinhardt, J., Fournet, S., Aich, V., Hattermann, F.F. 2013. Vulnerability of rice production in the Inner Niger Delta to water resources management under climate variability and change. *Environmental Science & Policy*: *Management of wetlands in river basins: the WETwin project*, 34, 18–33. https://doi.org/10.1016/j.envsci.2012.10.014

Liersch, S., Fournet, S., Koch, H., Djibo, A.G., Reinhardt, J., Kortlandt, J., Van Weert, F., Seidou, O., Klop, E., Baker, C., Hattermann, F.F. 2019. Water resources planning in the Upper Niger River basin: Are there gaps between water demand and supply? *Journal of Hydrology: Regional Studies*. 21, 176–194. https://doi.org/10.1016/j.ejrh.2018.12.006

Luthcke, S.B., Sabaka, T.J., Loomis, B.D., Arendt, A.A., McCarthy, J.J., Camp, J. 2013. Antarctica, Greenland and Gulf of Alaska land-ice evolution from an iterated GRACE global mascon solution. *Journal of Glaciology*. 59, 613–631. https://doi.org/10.3189/2013JoG12J147

Mahe, G., Orange, D., Mariko, A., Bricquet, J.P. 2011. *Estimation of the flooded area of the Inner Delta of the River Niger in Mali by hydrological balance and satellite data.* 6.

Mahé, G., Paturel, J.-E. 2009. 1896–2006 Sahelian annual rainfall variability and runoff increase of Sahelian Rivers. *Comptes rendus Geoscience*. 341, 538–546. https://doi.org/10.1016/j.crte.2009.05.002

Mekonnen, M.M., Hoekstra, A.Y. 2018. Global Anthropogenic Phosphorus Loads to Freshwater and Associated Grey Water Footprints and Water Pollution Levels: A High-Resolution Global Study. *Water Resources Research.* 54, 345–358. https://doi.org/10.1002/2017WR020448

Mekonnen, M.M., Hoekstra, A.Y. 2015. Global Gray Water Footprint and Water Pollution Levels Related to Anthropogenic Nitrogen Loads to Fresh Water. *Environmental Science & Technology*. 49, 12860–12868. https://doi.org/10.1021/acs.est.5b03191

Mohamed, Y.A., Bastiaanssen, W.G.M., Savenije, H.H.G., van den Hurk, B.J.J.M., Finlayson, C.M. 2012. Wetland versus open water evaporation: An analysis and literature review. *Physics and Chemistry of the Earth*. Parts ABC 47–48, 114–121. https://doi.org/10.1016/j.pce.2011.08.005

Molden, D. 1997. *Accounting for water use and productivity. SWIM (System-Wide Initiative for Water Management).* International Water Management Institute, Colombo, Sri Lanka.

NBA. 2019. *The history of Niger Basin Authority.* http://www.abn.ne/index.php?option=com_content&view=frontpage&Itemid=1&lang=en (accessed 10.28.19).

Ogilvie, A., Belaud, G., Delenne, C., Bailly, J.-S., Bader, J.-C., Oleksiak, A., Ferry, L., Martin, D. 2015. Decadal monitoring of the Niger Inner Delta flood dynamics using MODIS optical data. *Journal of Hydrology*. 523, 368–383. https://doi.org/10.1016/j.jhydrol.2015.01.036

OPIDIN. 2019. Floodviewer. *Forecast tool to predict the inundations in the Inner Niger Delta. OPIDIN.* https://www.opidin.org/en/floodviewer/floodviewer (accessed 10.15.19).

Prior, A.D. 2016. *WA+ as a technical tool for transboundary water governance: the potential of satellite data for water accounting in ungauged basins.* Vrije Universiteit Brussel, Katholieke Universiteit Leuven, Belgium.

Ramsar. 2020. *The List of Wetlands of International Importance*. https://www.ramsar.org/sites/default/files/documents/library/sitelist.pdf

Ramsar. 2004. *Fact sheet - Inner Niger Delta (Mali)*.

UNEP. 2010. *Africa Water Atlas*. UNEP/Earthprint.

UNEP-WCMC. 2019a. *Protected Area Profile for Algeria from the World Database of Protected Areas.* Protected Planet. https://www.protectedplanet.net/country/DZ (accessed 8.16.19).

UNEP-WCMC. 2019b. *Protected Area Profile for Benin from the World Database of Protected Areas*. Protected Planet. https://www.protectedplanet.net/country/BJ (accessed 8.16.19).

UNEP-WCMC. 2019c. *Protected Area Profile for Burkina Faso from the World Database of Protected Areas.* Protected Planet. https://www.protectedplanet.net/country/BF (accessed 8.16.19).

UNEP-WCMC. 2019d. *Protected Area Profile for Chad from the World Database of Protected Areas.* Protected Planet. https://www.protectedplanet.net/country/TD (accessed 8.16.19).

UNEP-WCMC. 2019e. *Protected Area Profile for Cameroon from the World Database of Protected Areas.* Protected Planet. https://www.protectedplanet.net/country/CM (accessed 8.16.19).

UNEP-WCMC. 2019f. Protected Area Profile for Guinea from the World Database of Protected Areas. Protected Planet. https://www.protectedplanet.net/country/GN (accessed 8.16.19).

UNEP-WCMC. 2019g. Protected Area Profile for Côte D'Ivoire from the World Database of Protected Areas. Protected Planet. https://www.protectedplanet.net/country/CI (accessed 8.16.19).

UNEP-WCMC. 2019h. *Protected Area Profile for Niger from the World Database of Protected Areas*. Prot. Planet. https://www.protectedplanet.net/country/NE (accessed 8.16.19).

UNEP-WCMC. 2019i. *Protected Area Profile for Nigeria from the World Database of Protected Areas.* Protected Planet. https://www.protectedplanet.net/country/NG (accessed 8.16.19).

UNEP-WCMC. 2019j. *Protected Area Profile for Mali from the World Database of Protected Areas.* Protected Planet. https://www.protectedplanet.net/country/ML (accessed 8.16.19).

UN-SPIDER. 2020. *Step-by-Step: Recommended Practice: Flood Mapping and Damage Assessment using Sentinel-1 SAR data in Google Earth Engine*. UN-SPIDER knowledge portal. http://www.un-spider.org/advisory-support/recommended-practices/recommended-practice-google-earth-engine-flood-mapping/step-by-step (accessed 3.9.20).

Vandersypen, K., Bengaly, K., Keita, A.C.T., Sidibe, S., Raes, D., Jamin, J.-Y. 2006. Irrigation performance at tertiary level in the rice schemes of the Office du Niger (Mali): Adequate water delivery through over-supply. *Agricultural Water Management.* 83, 144–152. https://doi.org/10.1016/j.agwat.2005.11.003

Viergever, K. 2020. *Question about land use map Inner Niger Delta*.

Werth, S., White, D., Bliss, D.W. 2017. GRACE Detected Rise of Groundwater in the Sahelian Niger River Basin. *Journal of Geophysical Research: Solid Earth*. 122, 10,459-10,477. https://doi.org/10.1002/2017JB014845

Wetlands International, Altenburg & Wymenga consultants. 2017. OPIDIN - Floodviewer. https://www.opidin.org/en/floodviewer/floodviewer (accessed 4.6.20).

Yang, Y., Donohue, R.J., McVicar, T.R. 2016. Global estimation of effective plant rooting depth: Implications for hydrological modeling. *Water Resources Research.* 52, 8260–8276. https://doi.org/10.1002/2016WR019392

Zwart, S.J., Leclert, L.M.C. 2010. A remote sensing-based irrigation performance assessment: a case study of the Office du Niger in Mali. *Irrigation Science*. 28, 371–385. https://doi.org/10.1007/s00271-009-0199-3

Zwarts, L., Beukering, P.V., Koné, B., Wymenga, E., Taylor, D. 2006. The Economic and Ecological Effects of Water Management Choices in the Upper Niger River: Development of Decision Support Methods. *International Journal of Water Resources Development*. 22, 135–156. https://doi.org/10.1080/07900620500405874

Zwarts, L., Beukering, P. van, Bakary Kone, Eddy Wymenga. 2005. *The Niger, a lifeline. Effective water management of the Upper Niger Basin.*

Zwarts, L., Bijlsma, R.G., van der Kamp, J., Wymenga, E. 2009. *Living on the edge: Wetlands and birds in a changing Sahel*. KNNV Publishing, Zeist, The Netherlands.

Zwarts, L., van der Kamp, J. 2013. *Does the Inner Niger Delta suffer from a reduced river flow in the dry season?* (No. 1938), A&W-report. Altenburg & Wymenga Ecological consultants, Feanwâlden, the Netherlands.

Annexes

Annex I. Office du Niger production zones and expansion[1]

There are currently seven production zones in Office du Niger with total irrigated area of about 1,173 km² (Table A-1). The production zones of Office du Niger were developed around an ancient tributary of the Niger, which is nowadays connected with the mainstream through a system of canals stemming from Markala dam (Figure A-1).

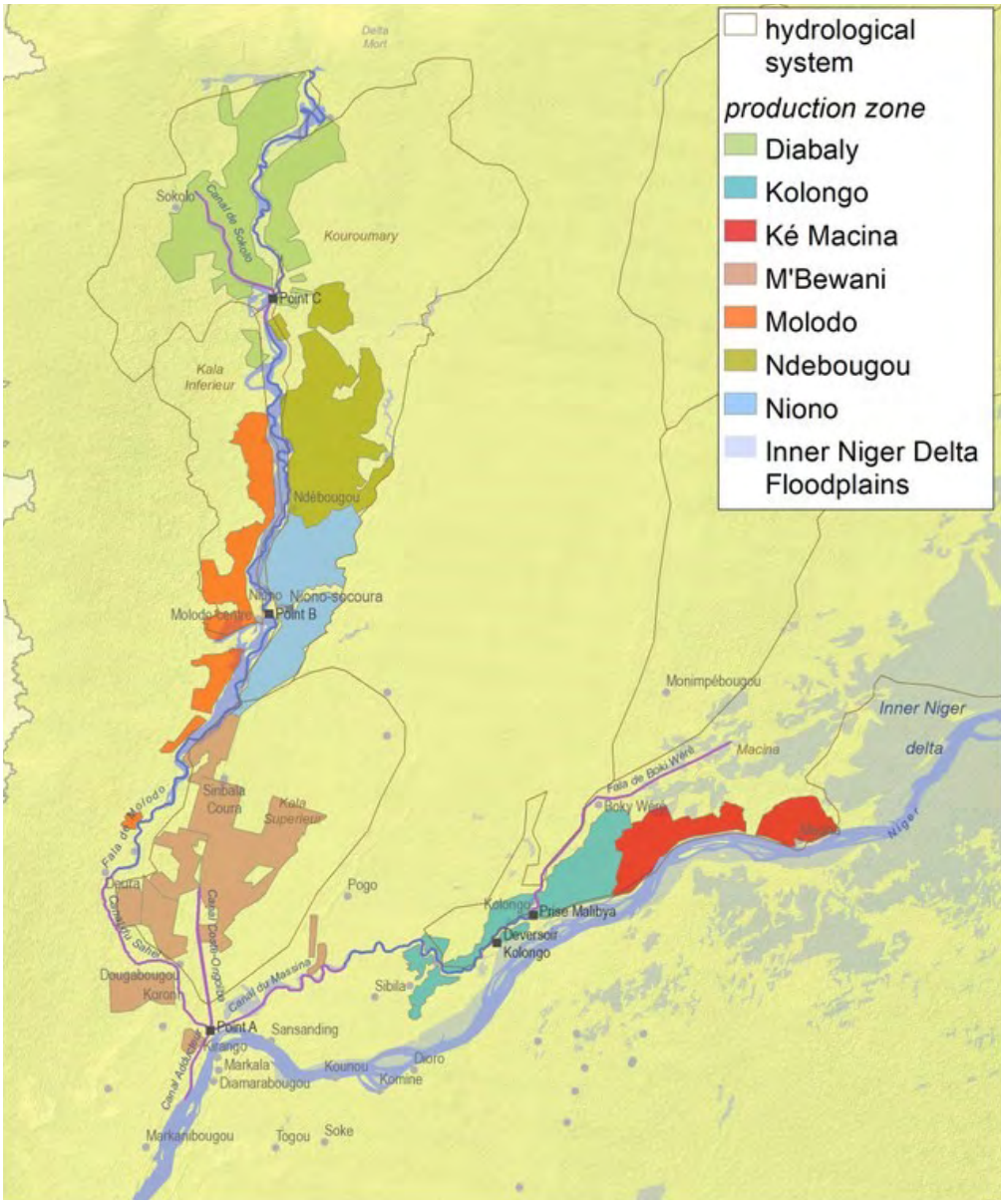

Figure A-1: Current production zone of Office du Niger

Table A-1: Area of production zones in Office du Niger as reported in 2018. Source: on-mali.org, May 2018

Production zone	Current Area (km²)	Potential Area (km²)
Niono	193.55	28.85
N'Débougou	117.57	97.16
Molodo	84.98	55.0
Kolongo	203.0	N/A
Ké-Macina	181.87	N/A
M'Béwani	51.28	N/A
Kouroumari/Diabaly	340.59	N/A
Total	**1,172.84**	**N/A**

The irrigated areas in Office du Niger have been continuously expanding (Figure A-2) with an average extension rate of 27 km²/year between 2000 and 2015 (BRLi & BETICO, 2015). Under the PA-HA-project (Étude du Programme d'Aménagement Hydro-agricole de la zone Office du Niger, 2014-2016) initiated by the Malian government, many scenarios have been developed to plan for the further extension of Office du Niger into the Inner Niger Delta. According the chosen scenario for long term development (2035), 3,300 km² will be added to the currently irrigated area of 1,200 km², which will encompass 1,850 km² of small producers and family farms (Figure A-3).

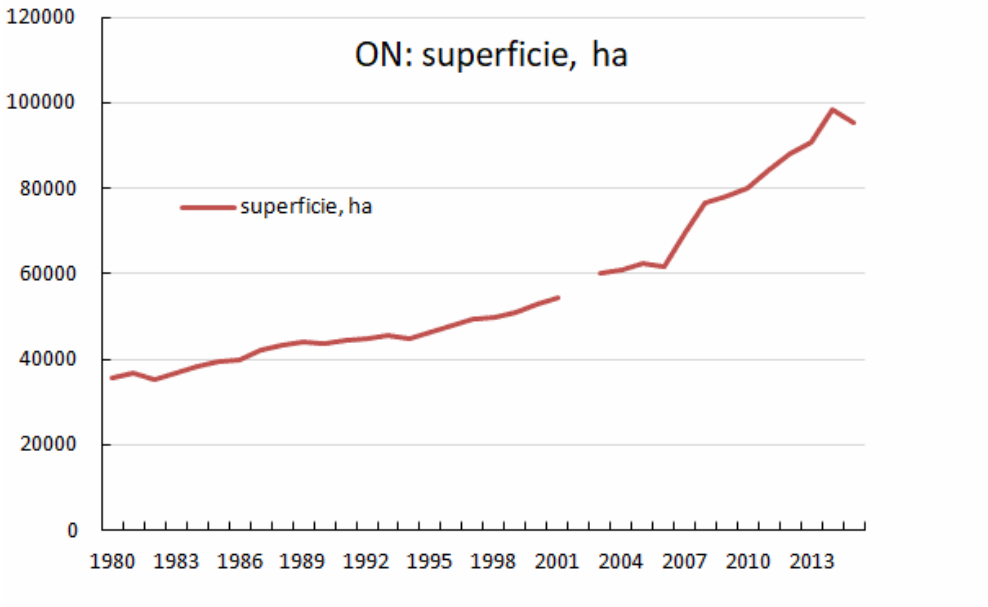

Figure A-2: Development of the surface area under irrigation in the Irrigation zone of Office du Niger between 1980 – 2015. Data: Office du Niger.

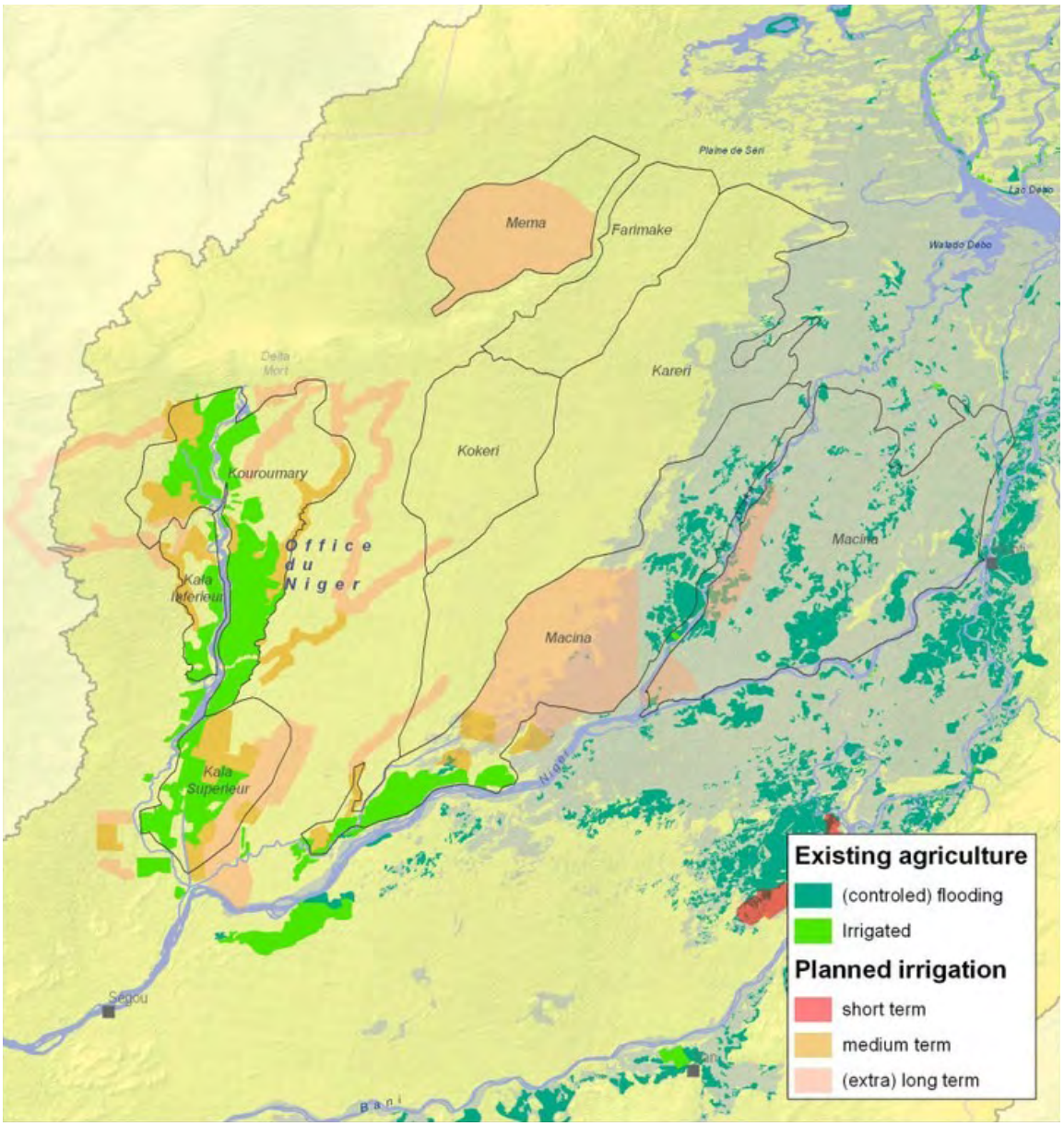

Figure A-3: Existing and planned extensions of the Irrigation zone of Office du Niger. Note that the extensions are planned on a short (2025), medium (2035) and very long term (2045). Source: BRLi & BETICO (2016).

References

BRLi & BETICO. 2016. Projet d'accroisement de la productivité agricole au Mali (PAPAM). *Étude du Programme d'Aménagement Hydro-Agricole (PAHA) de la zone Office du Niger (ON)*. Rapport de Phase 3. Concertation et choix du scenario.

BRLi & BETICO. 2015. Projet d'accroisement de la productivité agricole au Mali (PAPAM). *Étude du Programme d'Aménagement Hydro-Agricole (PAHA) de la zone Office du Niger (ON)*. Rapport de Phase 1. Etat des lieux. Volume 2. Aménagements hydrauliques.

Annex II. Annual Precipitation (P) of individual years

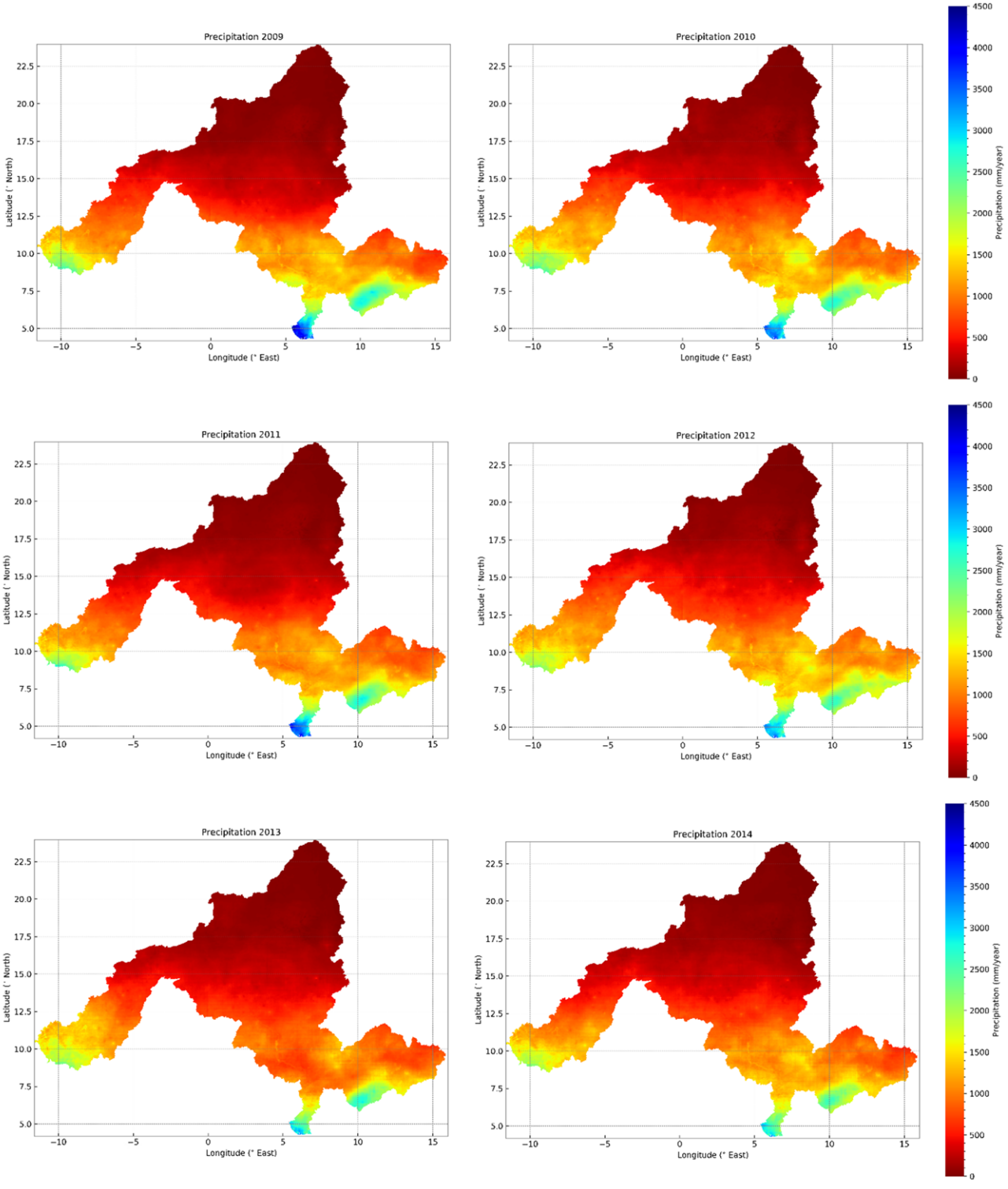

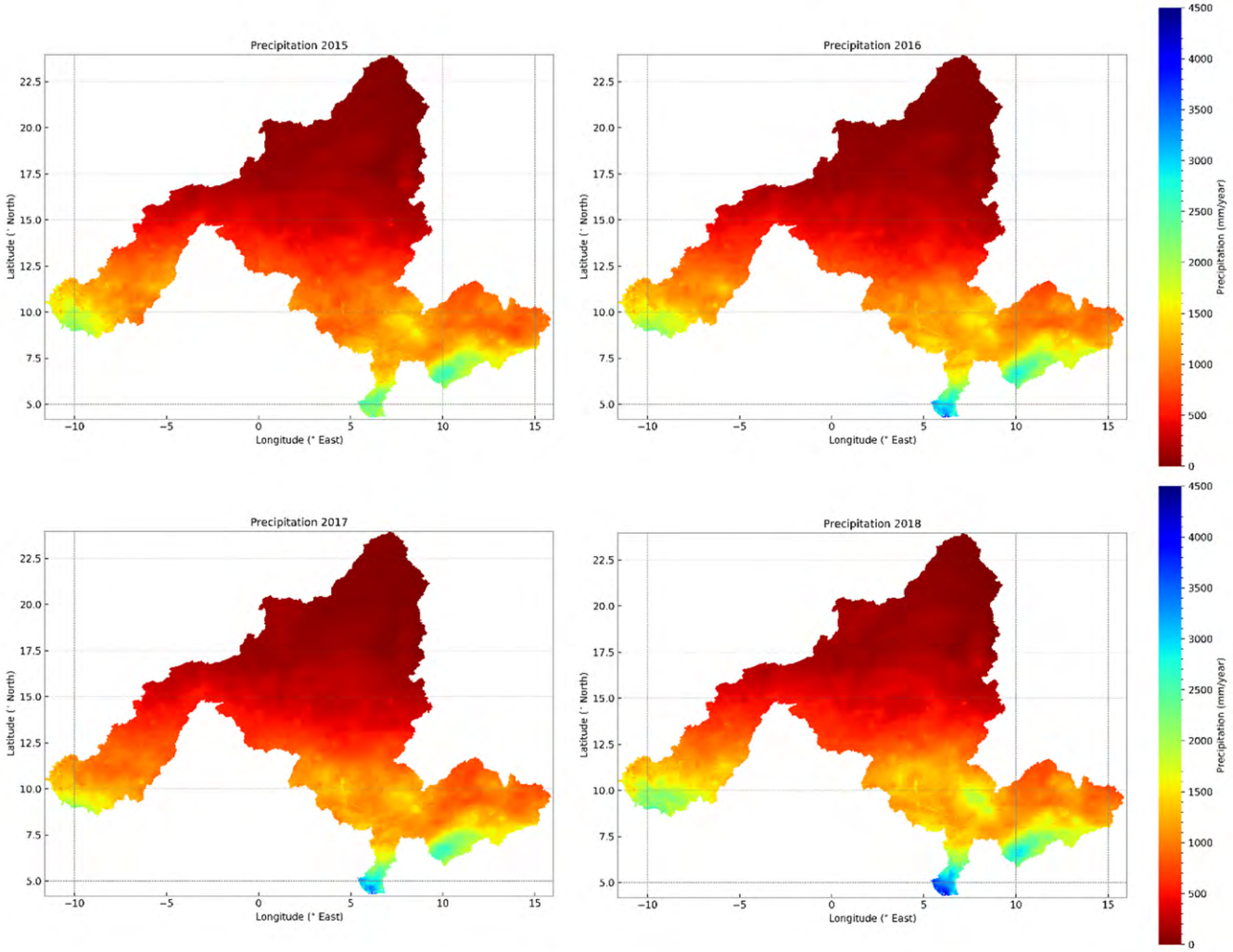
Precipitation 2015
Precipitation 2016
Precipitation 2017
Precipitation 2018
Latitude (° North)
Longitude (° East)
Precipitation (mm/year)
22.5
20.0
17.5
15.0
12.5
10.0
7.5
5.0
−10
−5
0
5
10
15
4500
4000
3500
3000
2500
2000
1500
1000
500
0

Annex III. Annual actual evapotranspiration (ET_a) of individual years

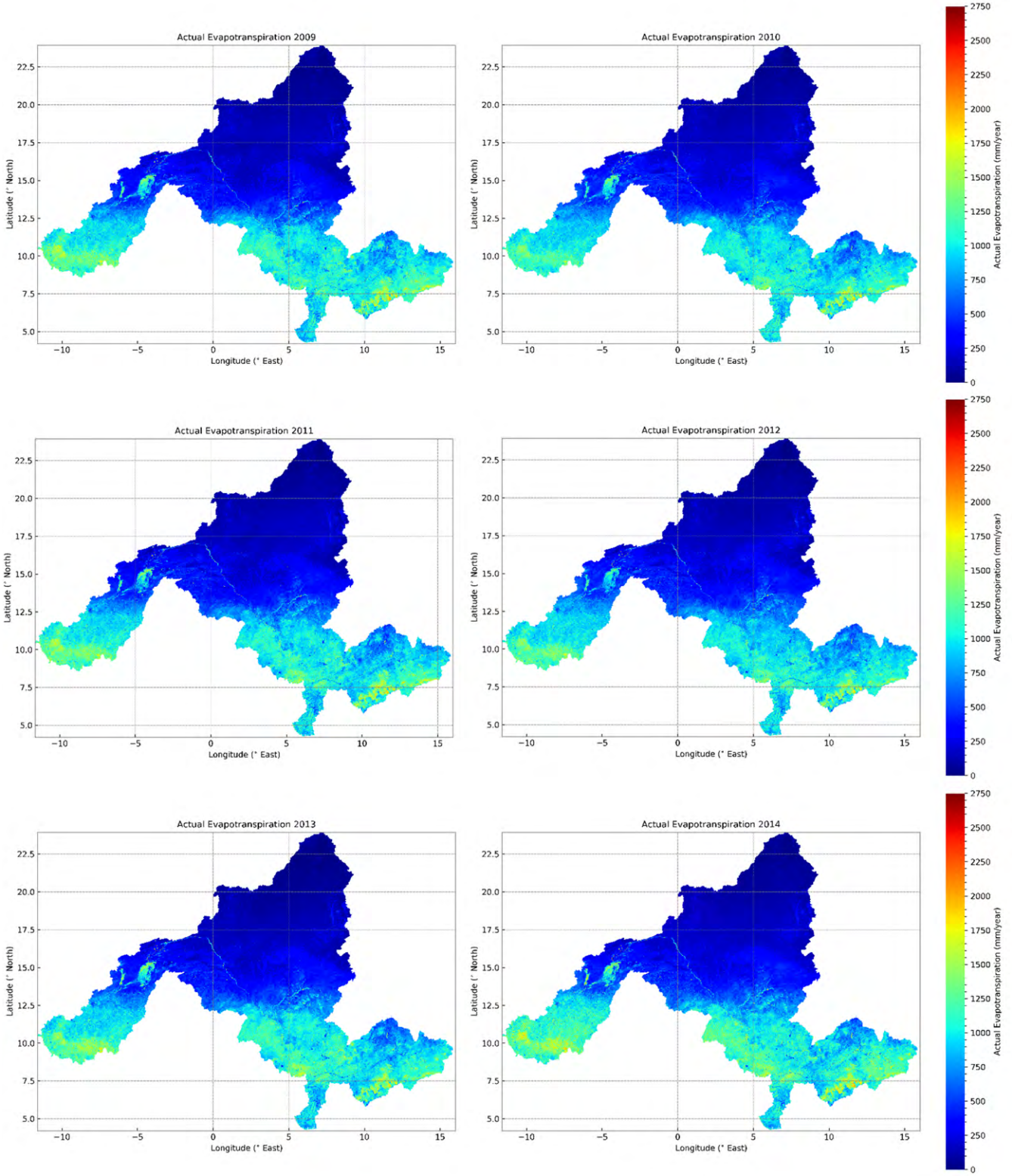

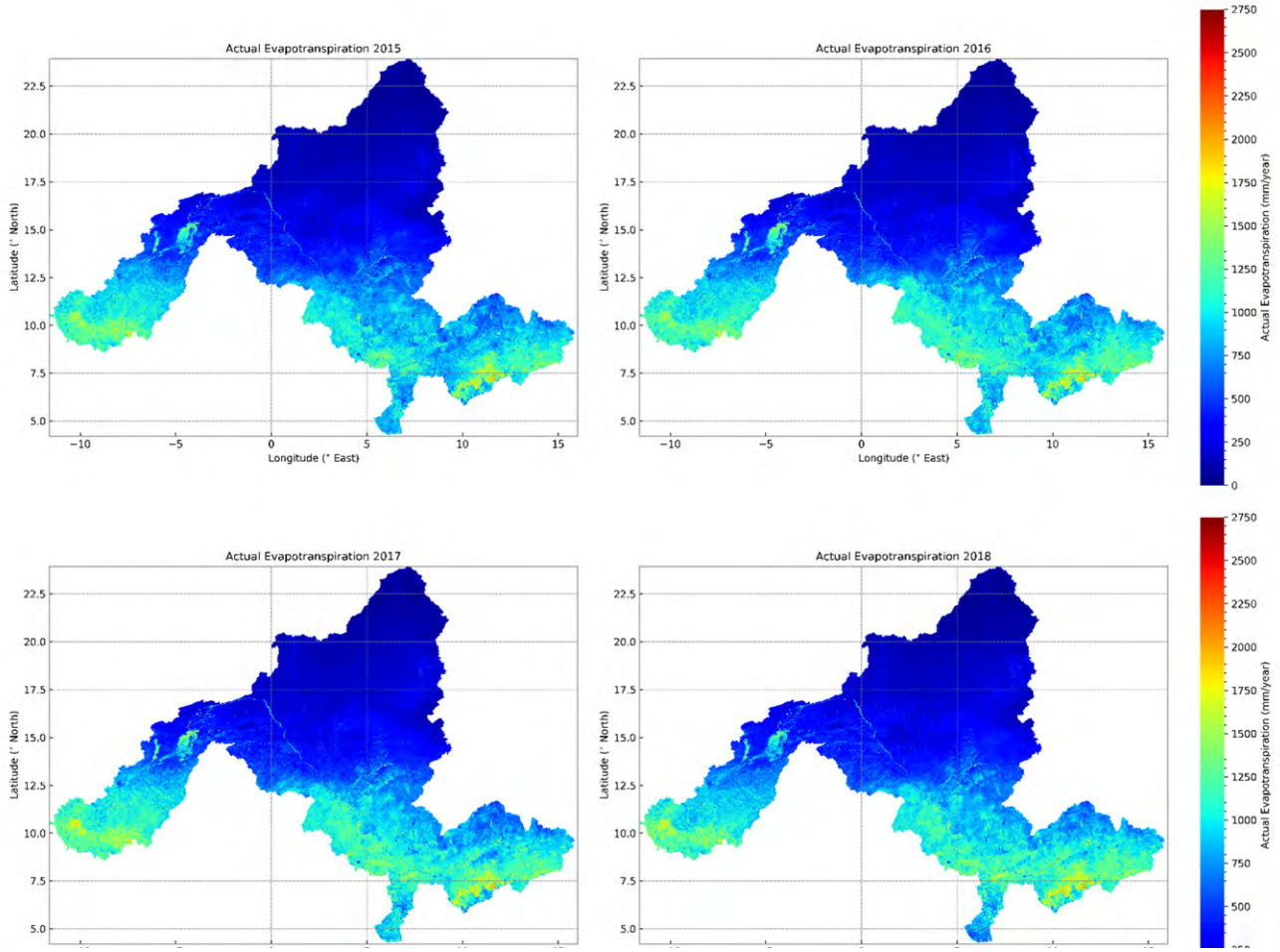
Actual Evapotranspiration 2015
Actual Evapotranspiration 2016
Actual Evapotranspiration 2017
Actual Evapotranspiration 2018
Latitude (° North)
Longitude (° East)
Actual Evapotranspiration (mm/year)

Annex IV. Yearly WaPOR Land cover classification maps

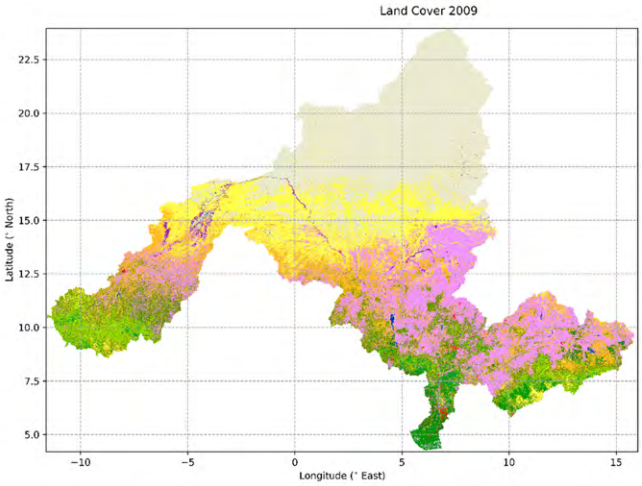

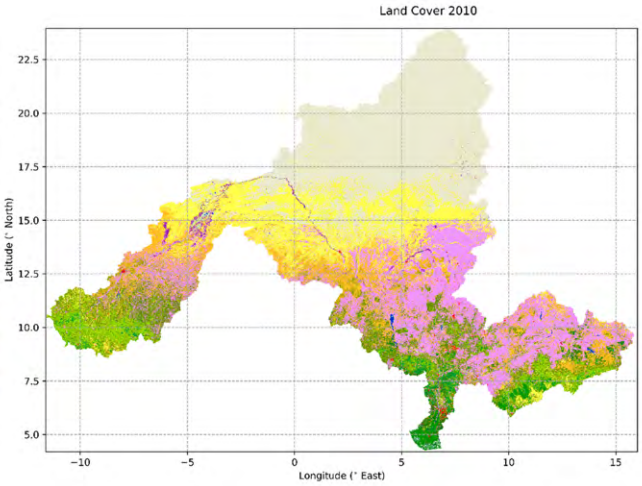

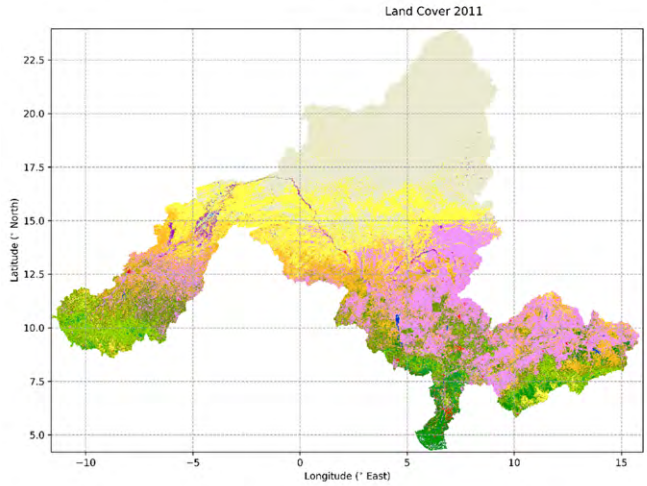

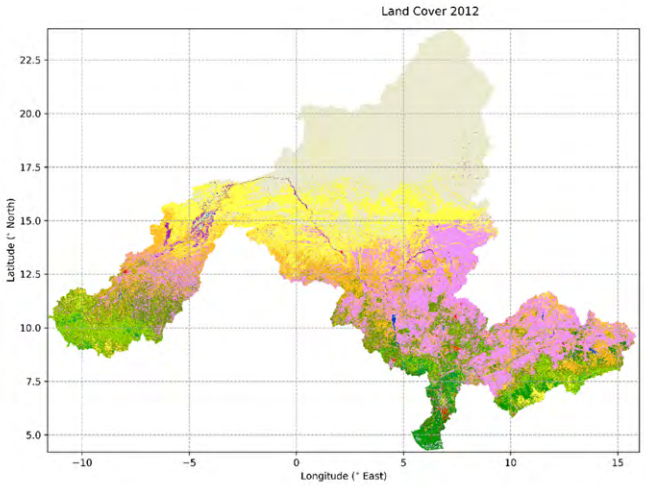

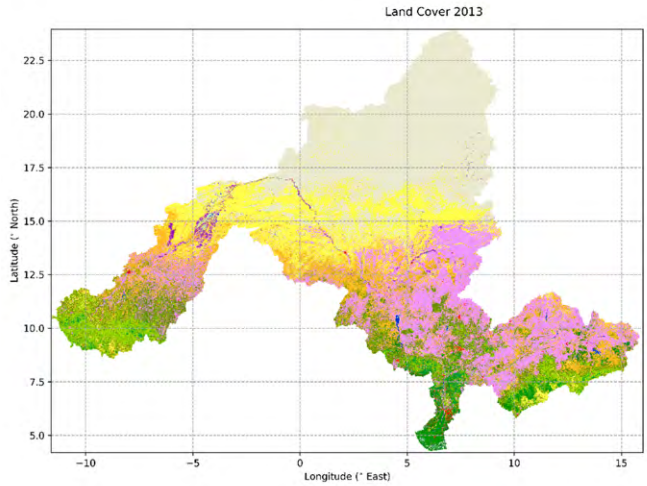

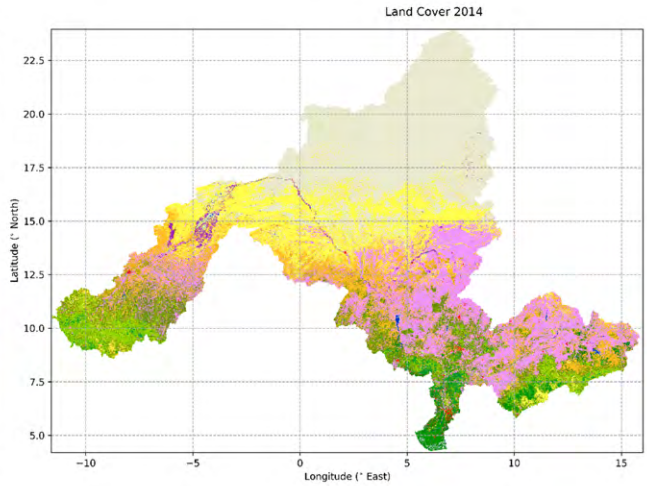

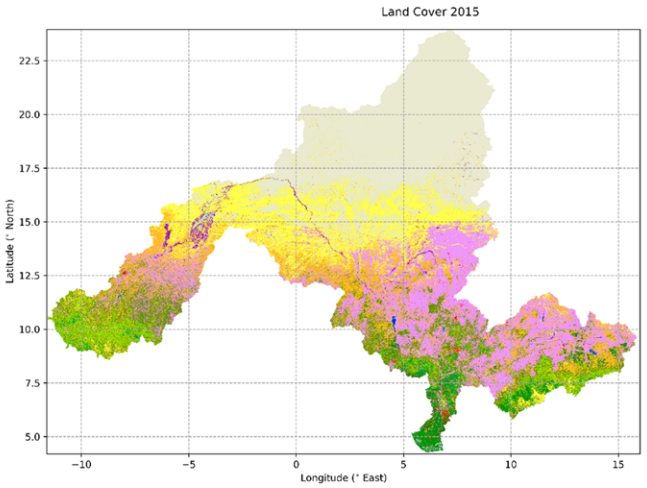
Land Cover 2015
Latitude (° North)
Longitude (° East)

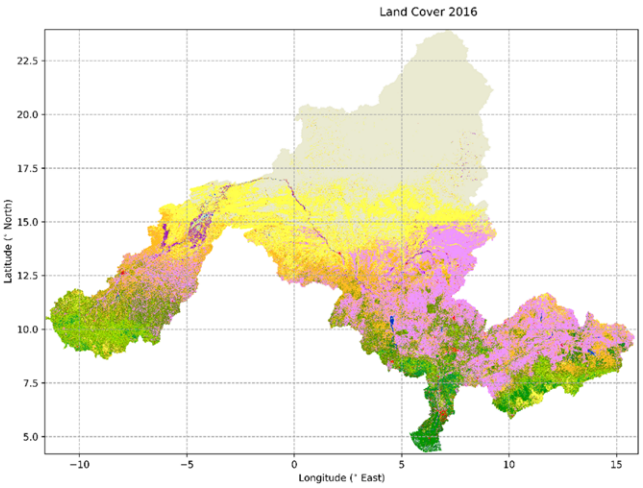
Land Cover 2016
Latitude (° North)
Longitude (° East)

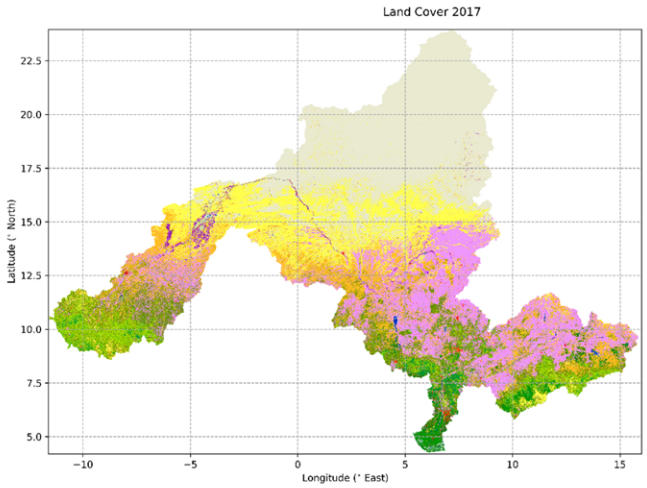
Land Cover 2017
Latitude (° North)
Longitude (° East)

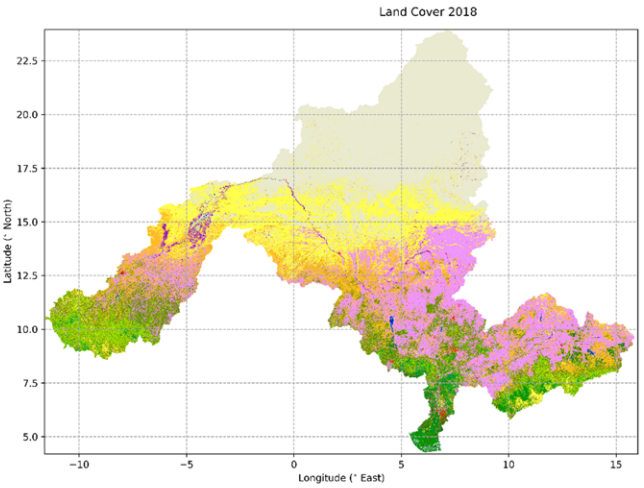
Land Cover 2018
Latitude (° North)
Longitude (° East)


Shrub or herbaceous cover, flooded
Tree cover: open, deciduous broadleaved
Tree cover: open, deciduous needle-leaved
Tree cover: open, evergreen broadleaved
Tree cover: open, evergreen needle-leaved
Tree cover: closed, deciduous broadleaved
Tree cover: closed, evergreen broadleaved
Tree cover: closed, evergreen needle-leaved
Sea water
Temporary water bodies
Water bodies
Permament snow / ice
Tree cover: open, unknown type
Tree cover: open, mixed type
Tree cover: closed, unknown type
Tree cover: closed, mixed type
Bare / sparse vegetation
Built-up
Cropland, fallow
Cropland, irrigated or under water management
Cropland, rainfed
Grassland
Shrubland
n.a

Annex V. Annual P - ET_a of individual years

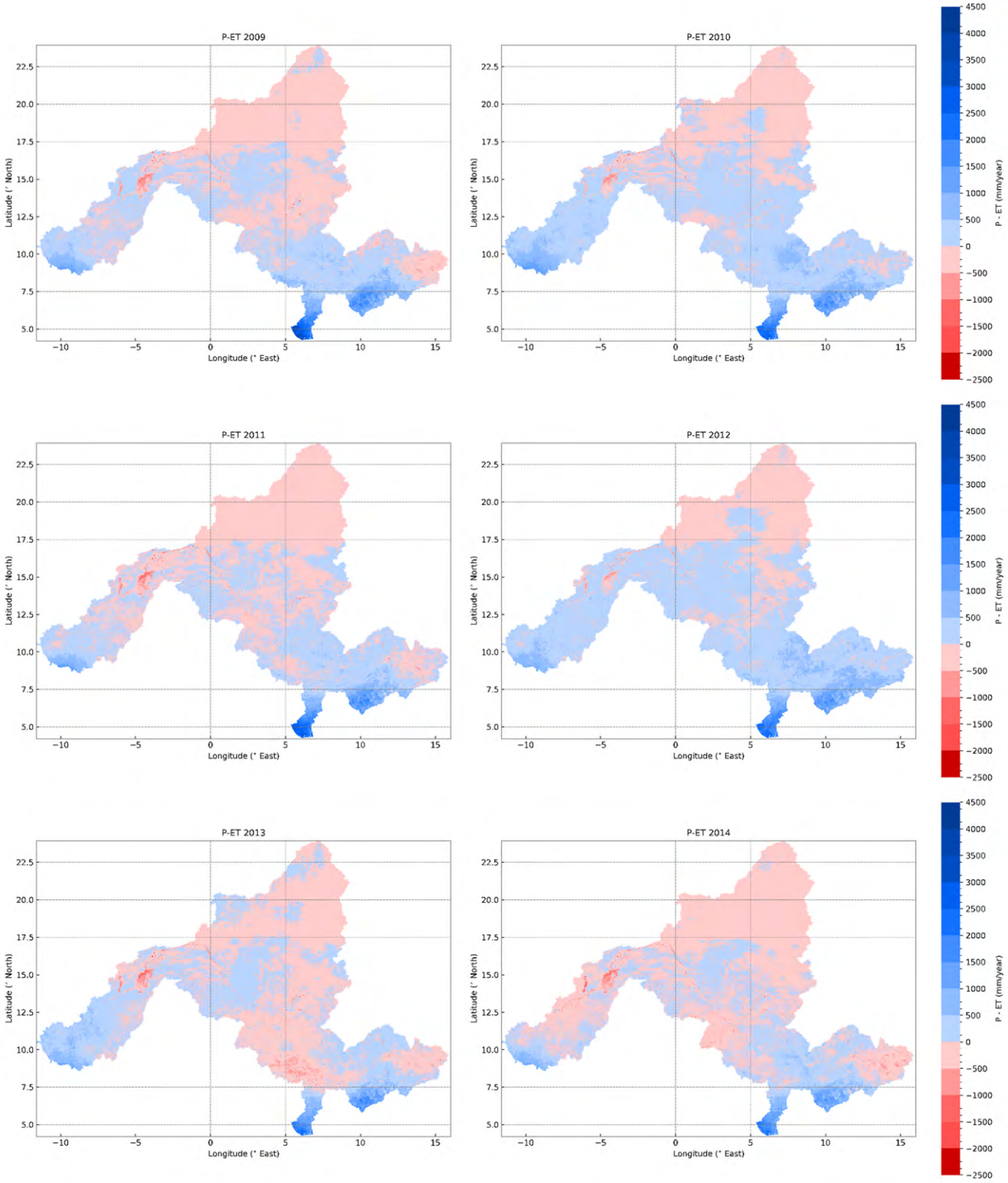

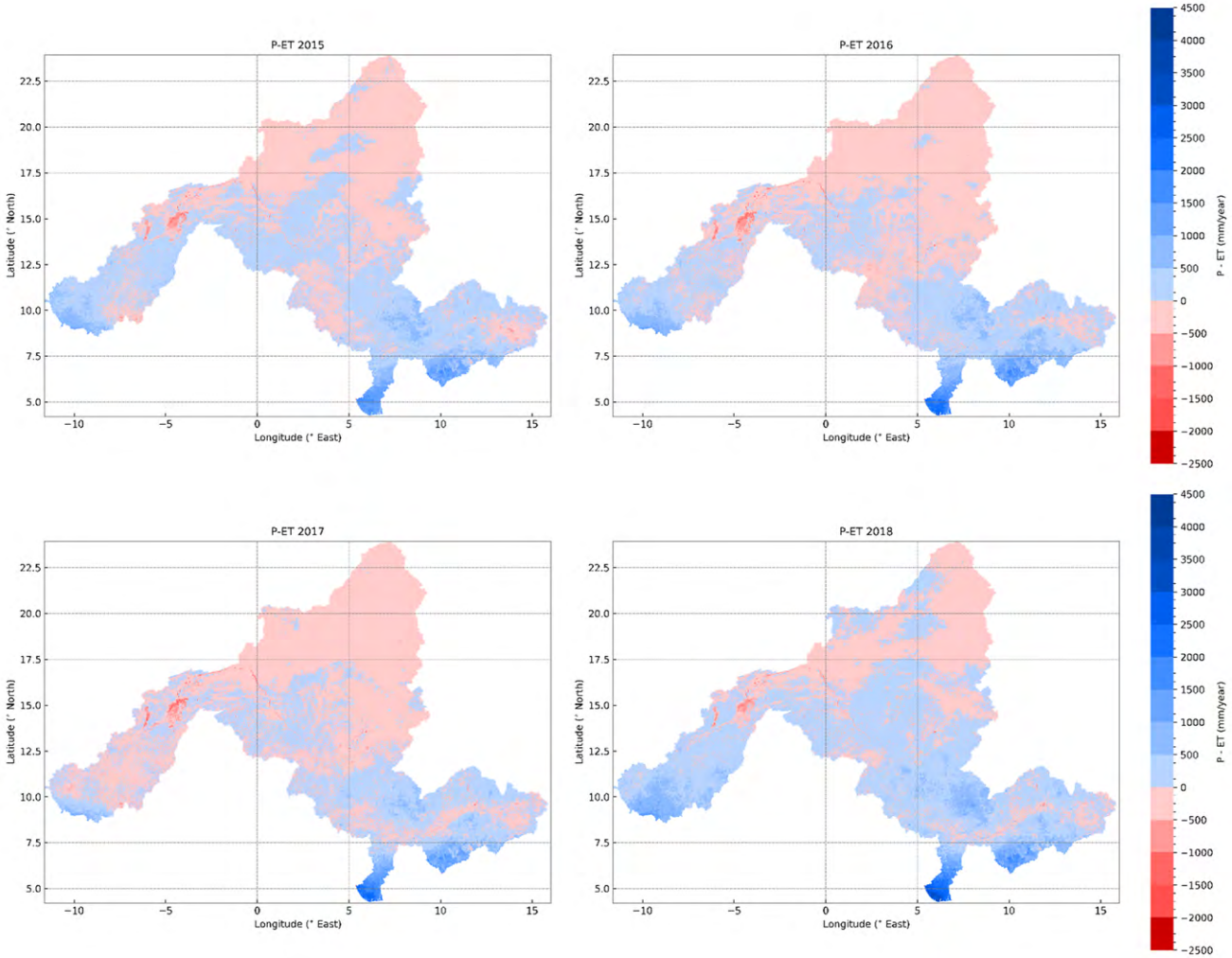
P-ET 2015
P-ET 2016
P-ET 2017
P-ET 2018
Latitude (° North)
Longitude (° East)
P - ET (mm/year)
4500
4000
3500
3000
2500
2000
1500
1000
500
0
−500
−1000
−1500
−2000
−2500
22.5
20.0
17.5
15.0
12.5
10.0
7.5
5.0
−10
−5
0
5
10
15

Annex VI. Yearly hydrographs at monitoring stations

Lokoja

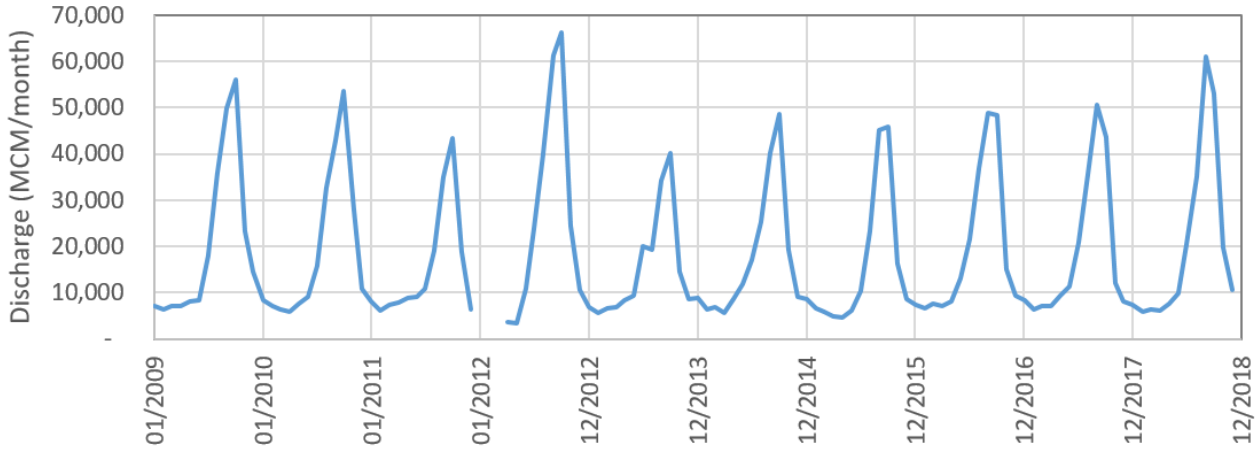

Jidere Boda

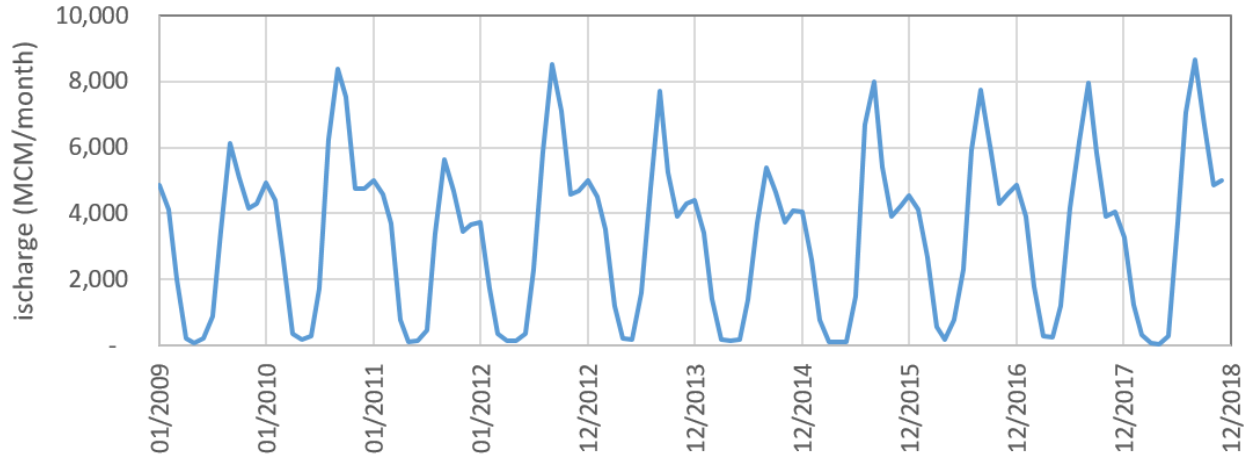

Kende

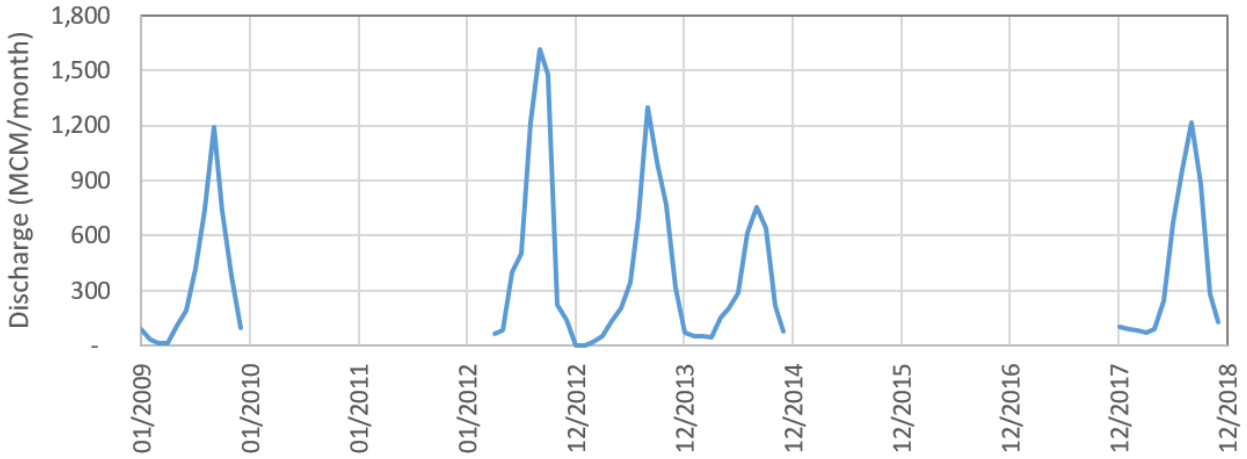

Mopti

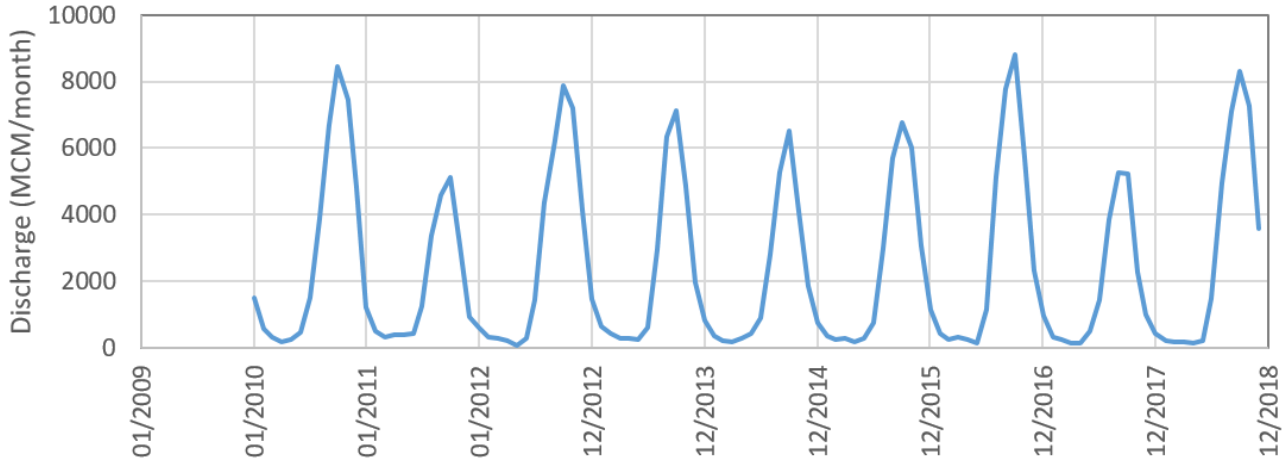
Discharge (MCM/month)
10000
8000
6000
4000
2000
0
01/2009
01/2010
01/2011
01/2012
12/2012
12/2013
12/2014
12/2015
12/2016
12/2017
12/2018

Akka

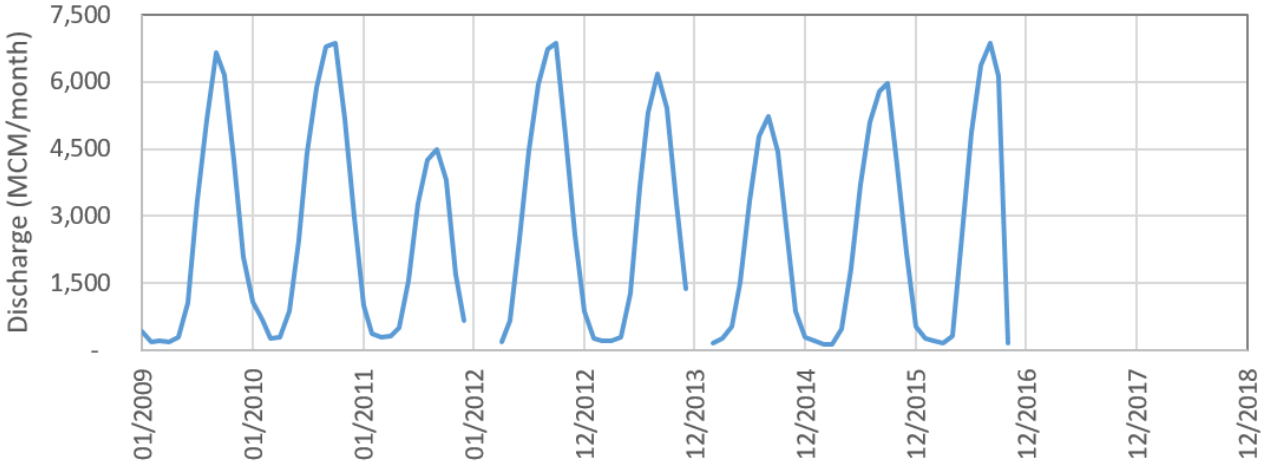
Discharge (MCM/month)
7,500
6,000
4,500
3,000
1,500
-
01/2009
01/2010
01/2011
01/2012
12/2012
12/2013
12/2014
12/2015
12/2016
12/2017
12/2018

Annex VII. Sub-catchment scale water balance of selected monitoring stations

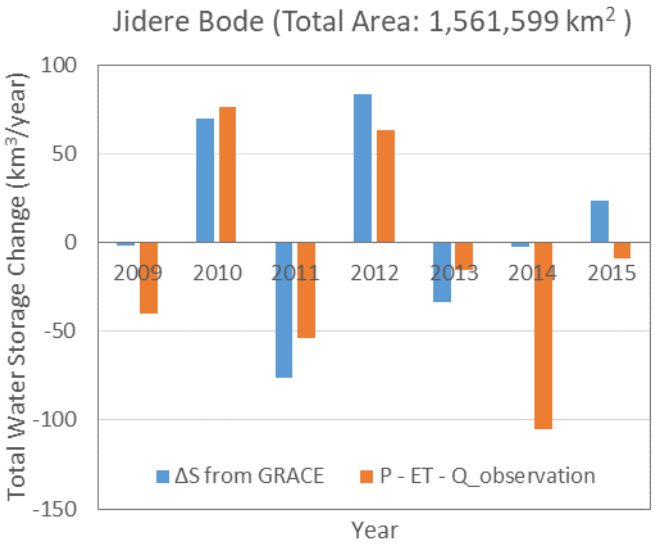

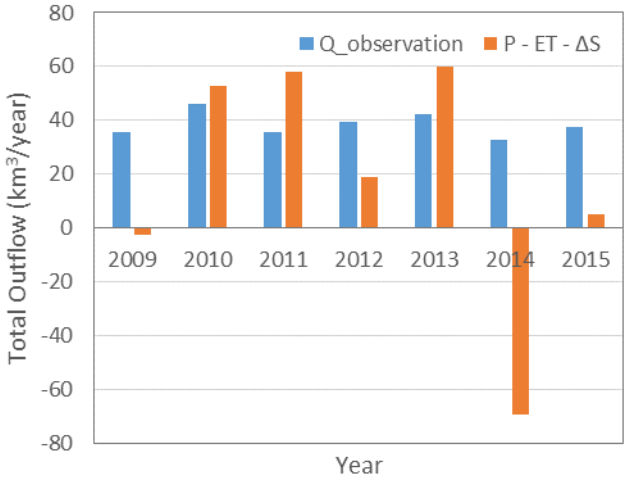

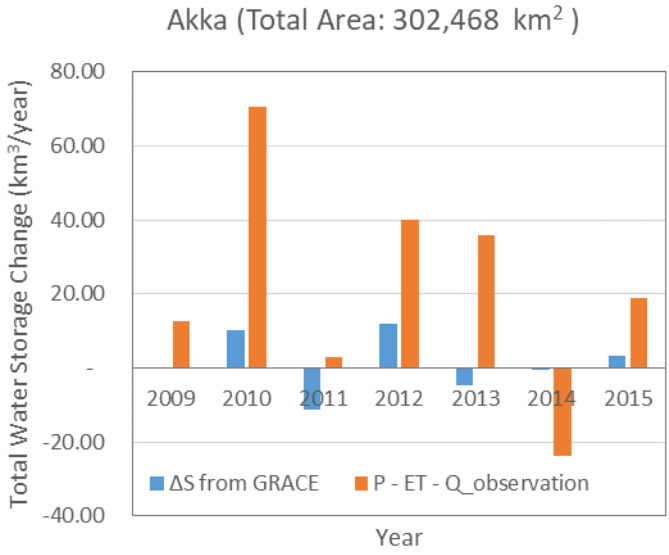

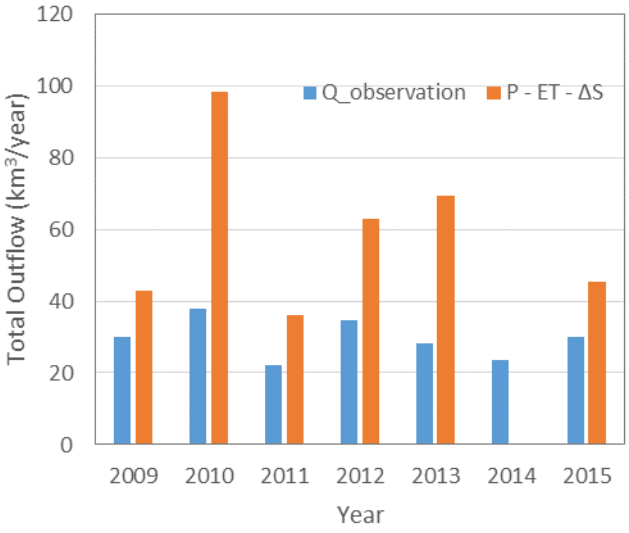

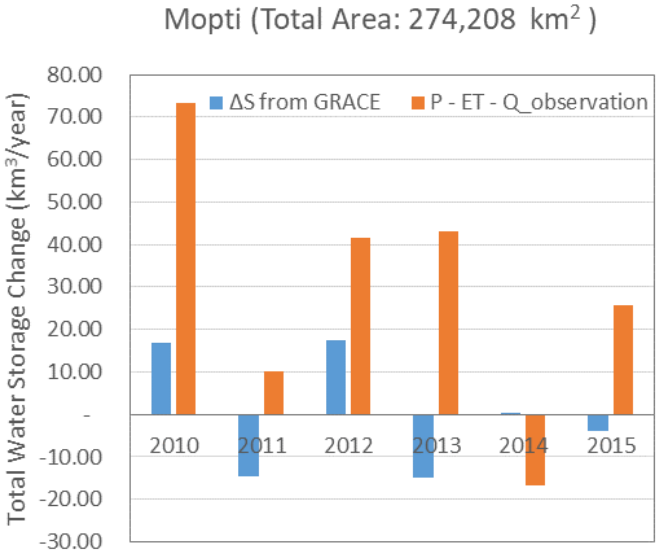

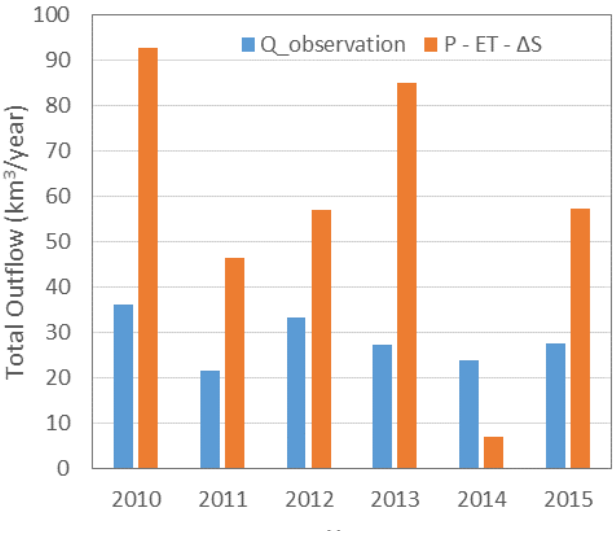

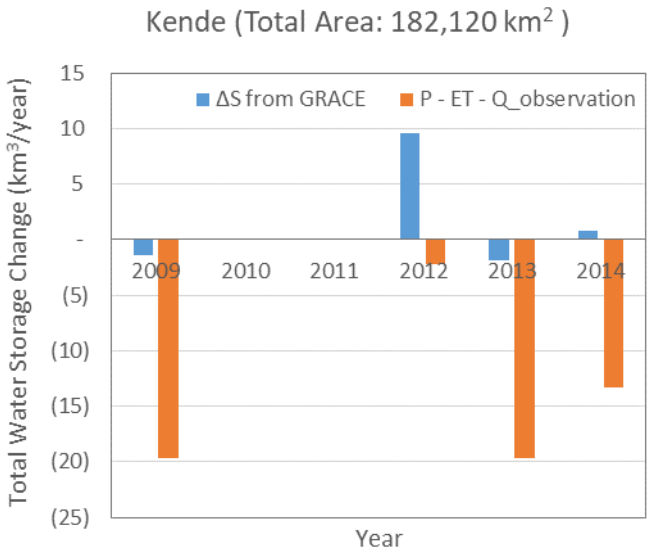
Kende (Total Area: 182,120 km2)
Total Water Storage Change (km3/year)
15
10
5
-
(5)
(10)
(15)
(20)
(25)
ΔS from GRACE
P - ET - Q_observation
2009
2010
2011
2012
2013
2014
Year

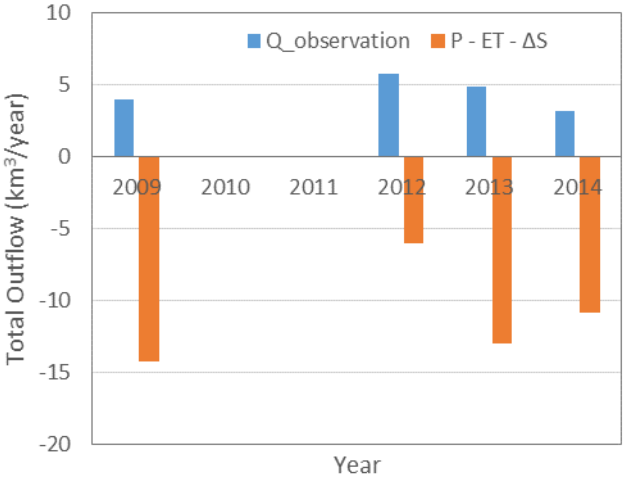
Total Outflow (km3/year)
10
5
0
-5
-10
-15
-20
Q_observation
P - ET - ΔS
2009
2010
2011
2012
2013
2014
Year

Annex VIII. Correlation between total water storage change estimations of selected monitoring stations

Akka Station

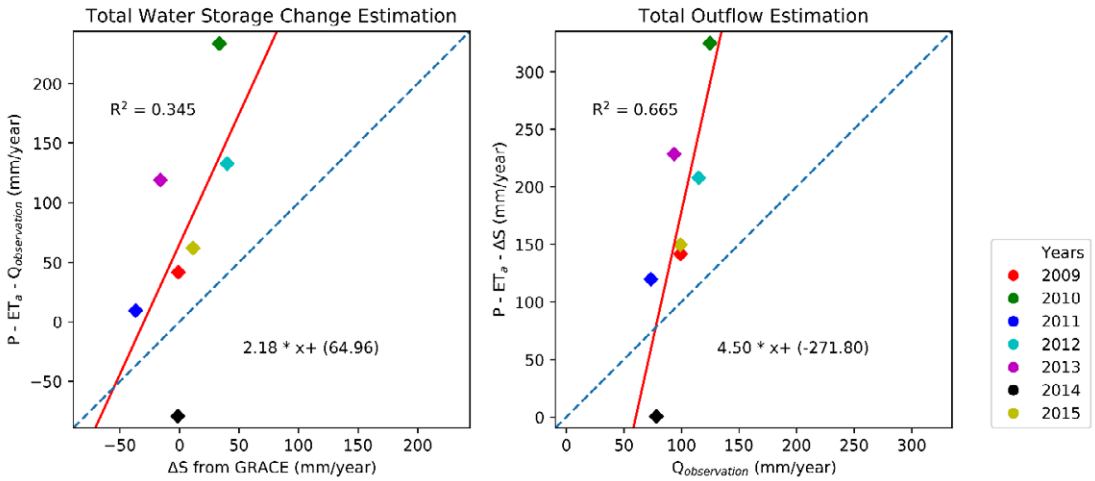

Kende Station

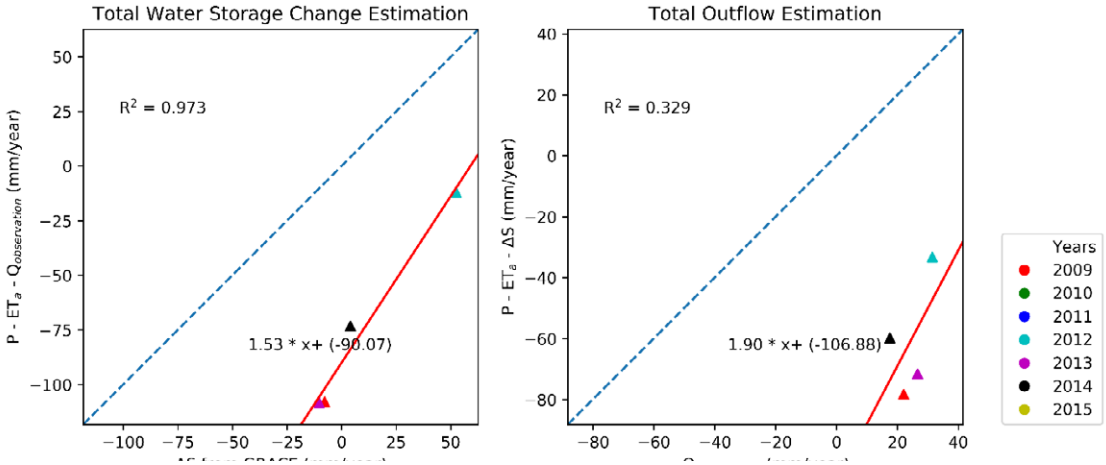

Mopti Station

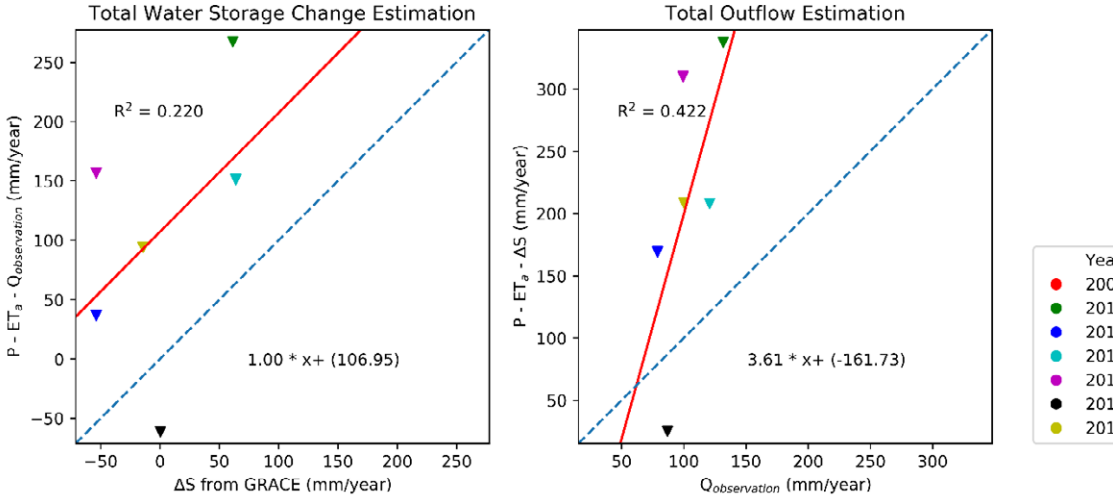

Annex IX. Yearly WA+ Land use classification maps

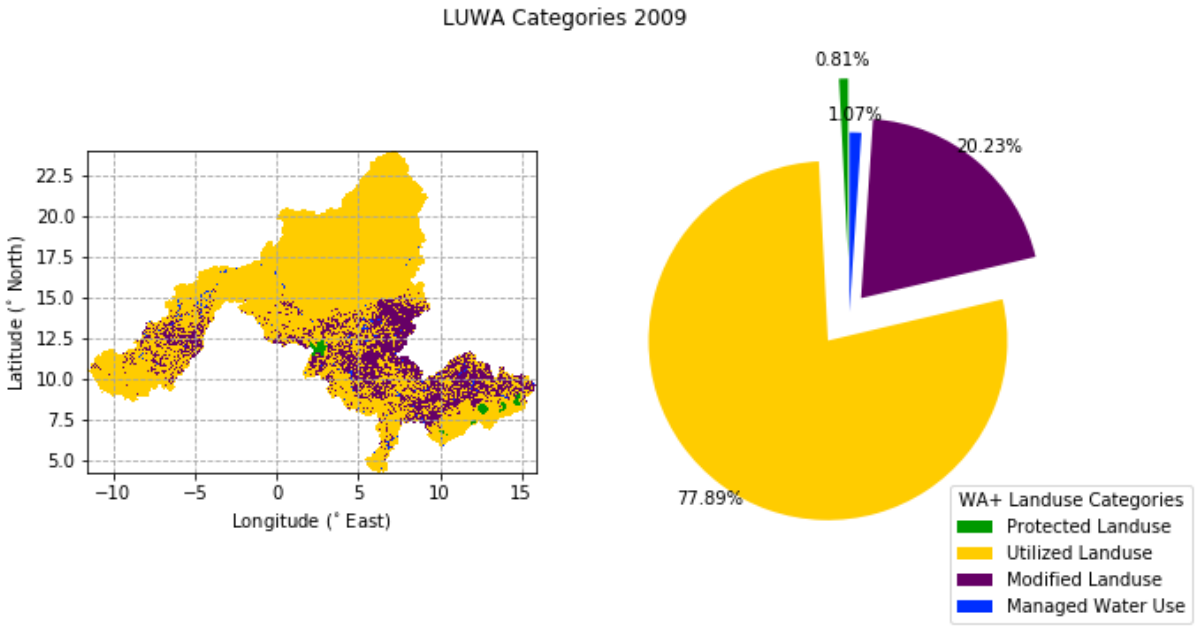

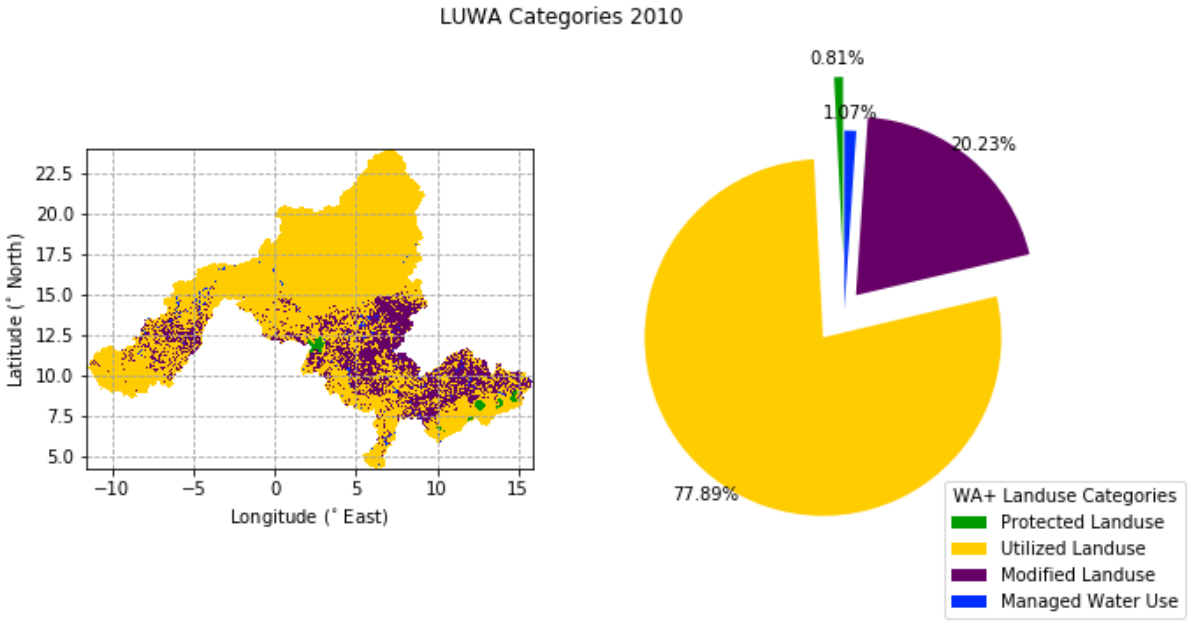

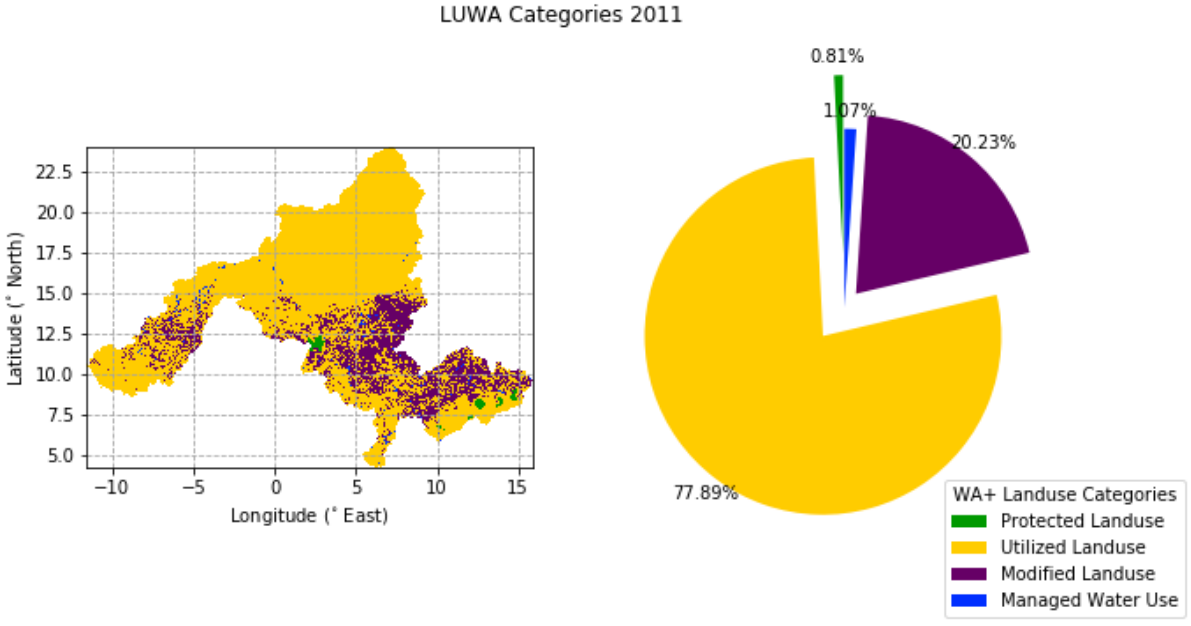

LUWA Categories 2012

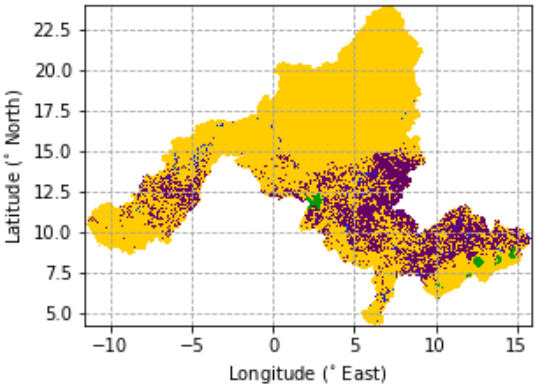

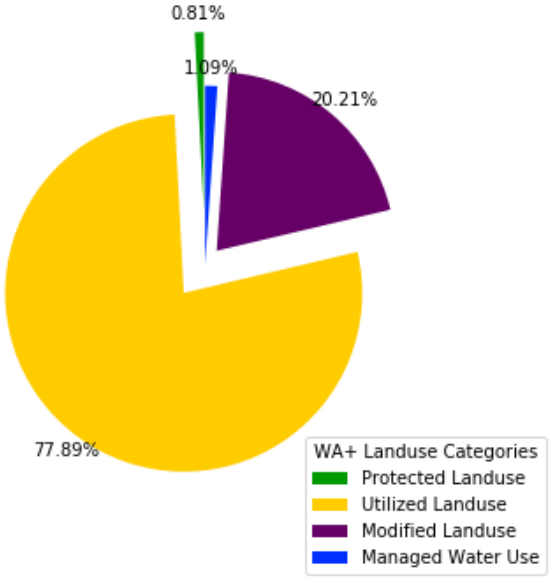

LUWA Categories 2013

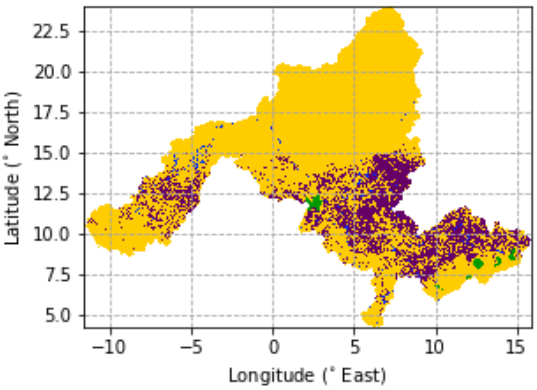

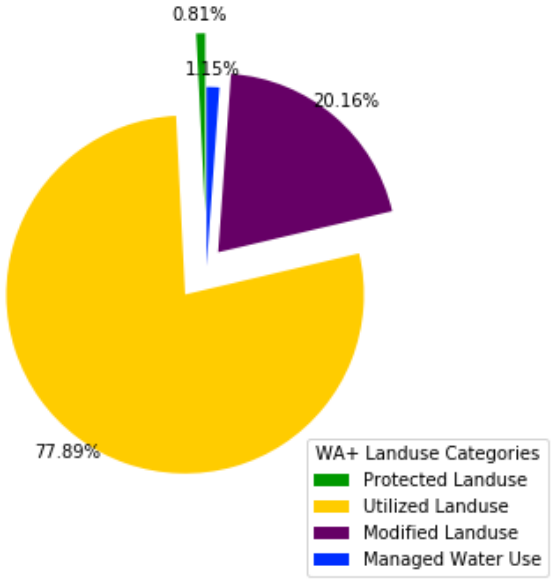

LUWA Categories 2014

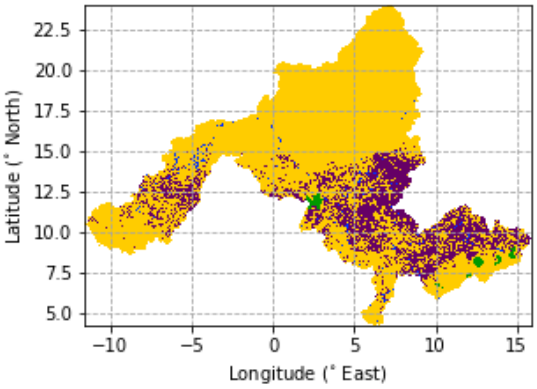

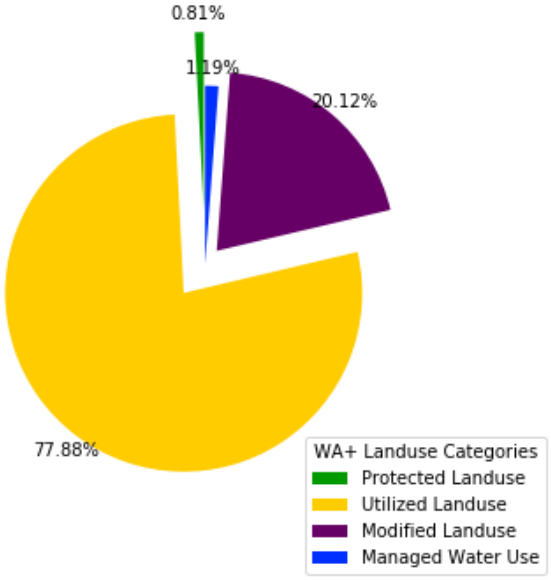

LUWA Categories 2015

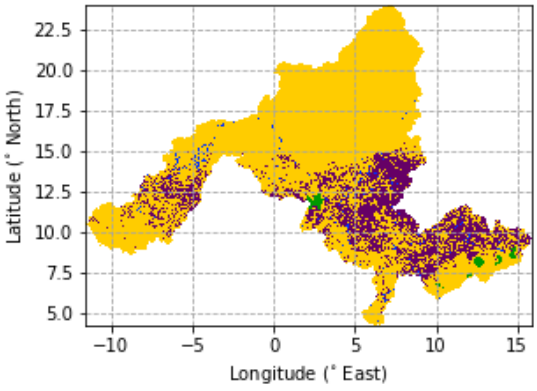

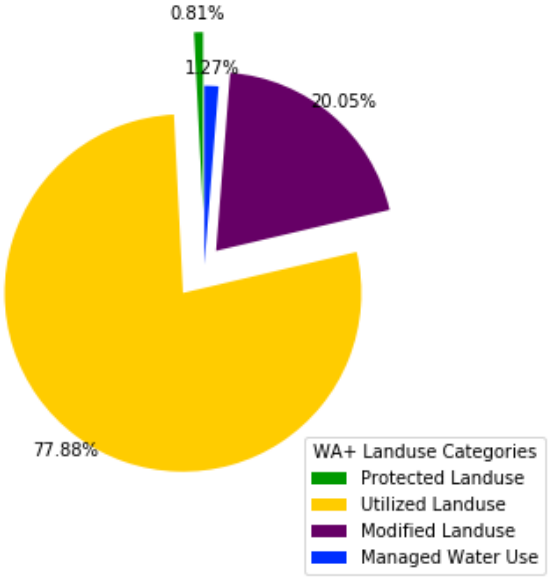

LUWA Categories 2016

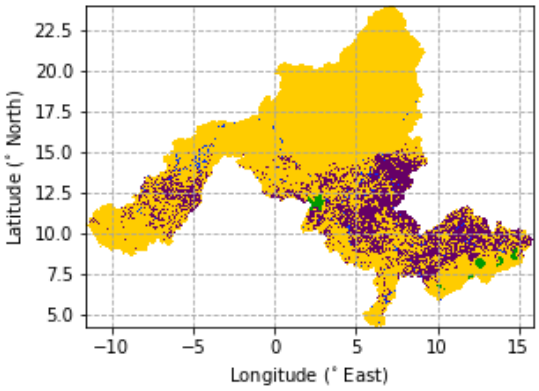

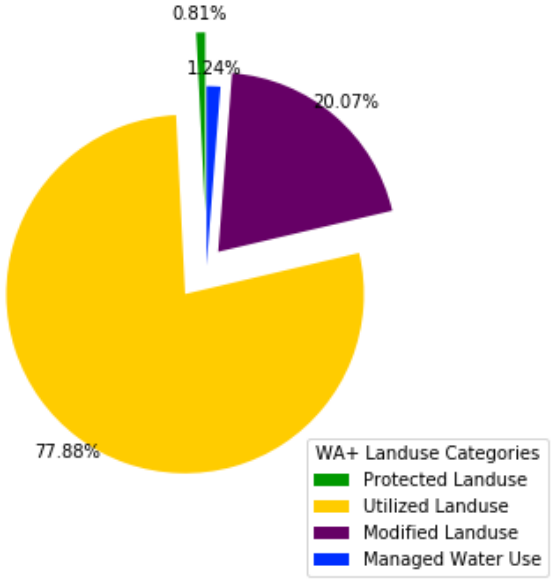

LUWA Categories 2017

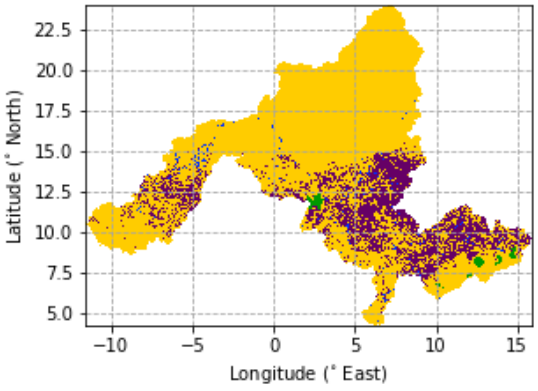

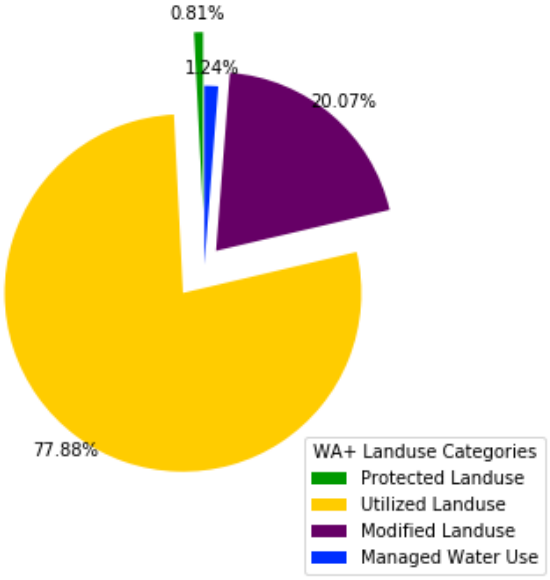

Annex X. Annual estimated Incremental ET (ET_{incr}) of individual years

2010

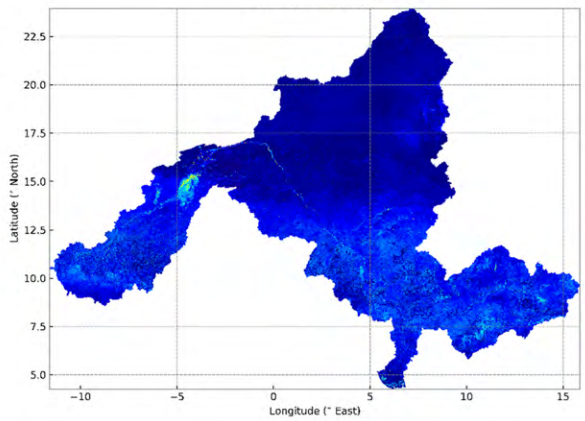

2011

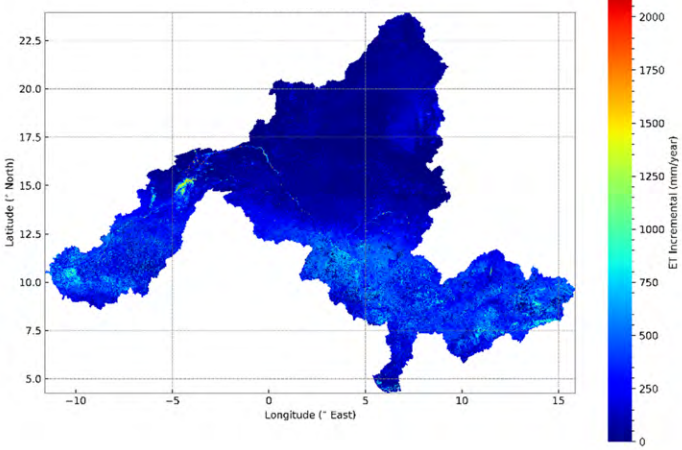

2012

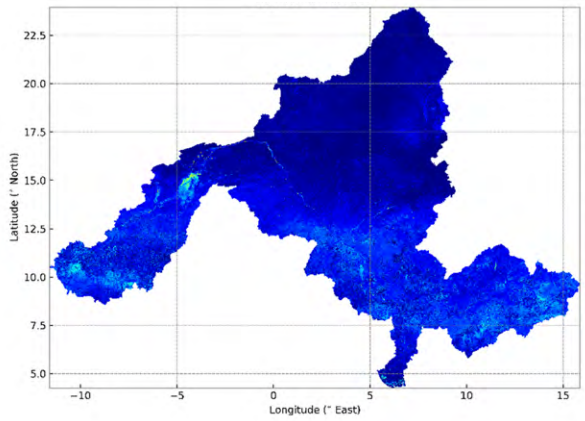

2013

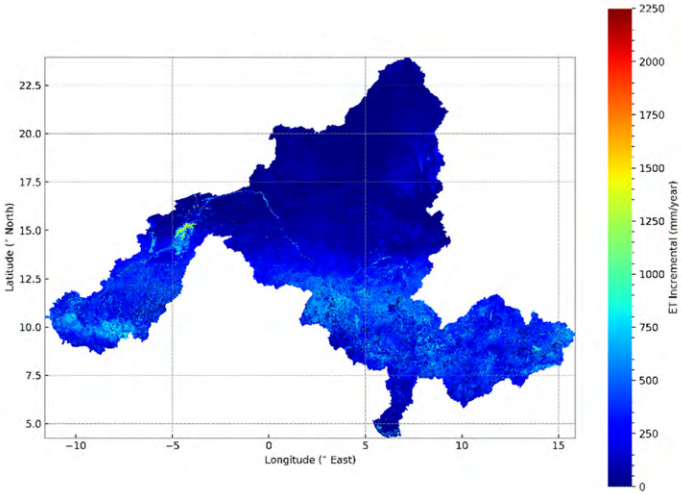

2014

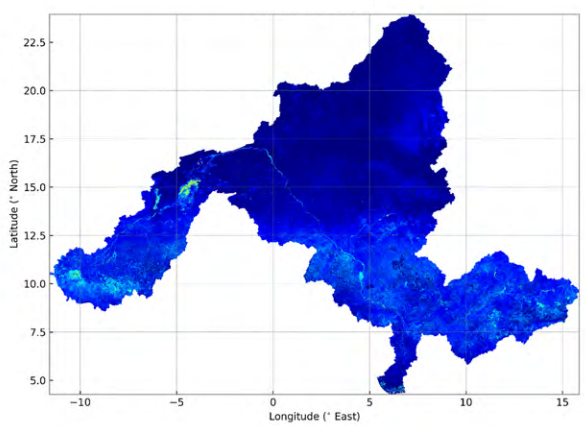

2015

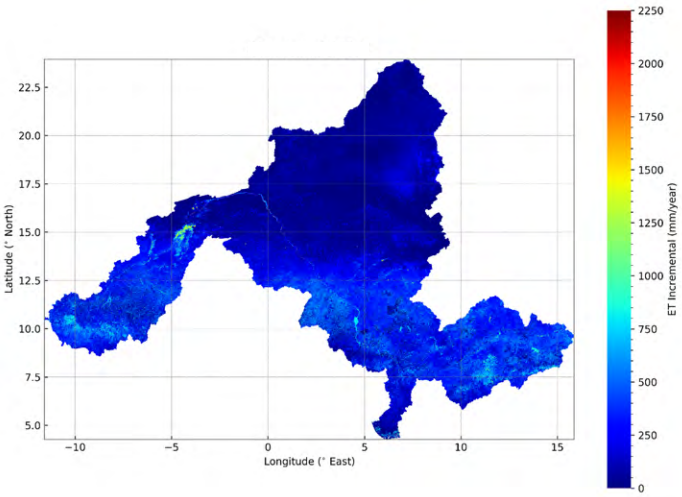

2016

2017

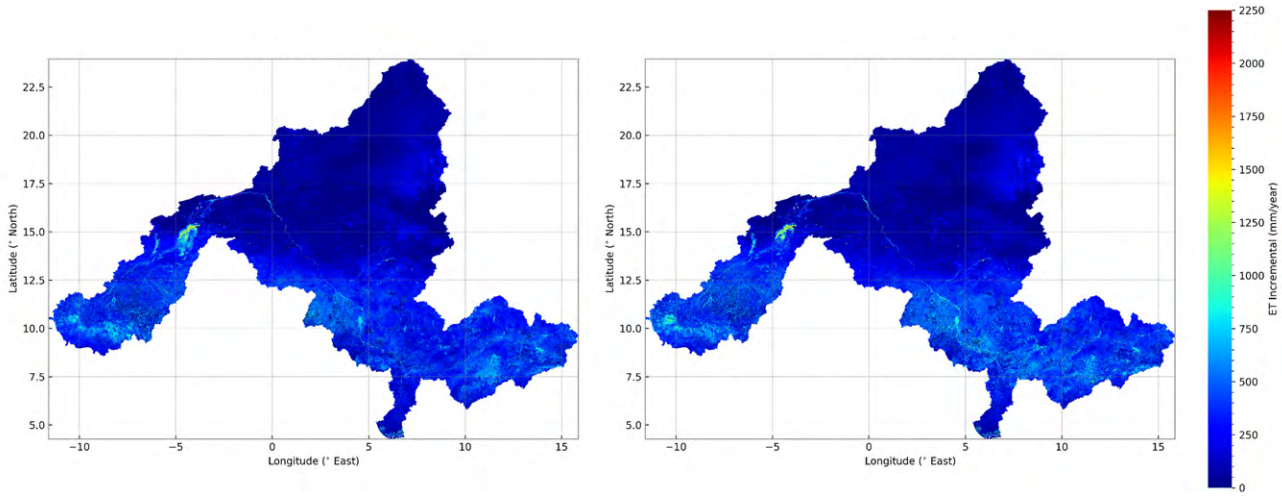

2018

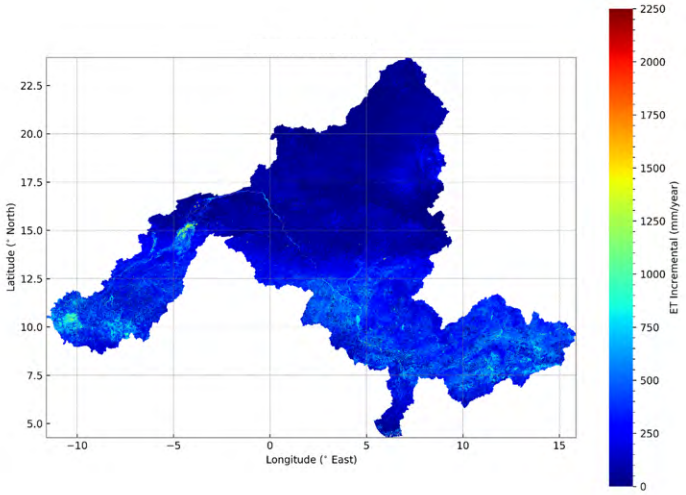

Annex XI. Annual estimated Rainfall ET (ET_{rain}) of individual years

2010

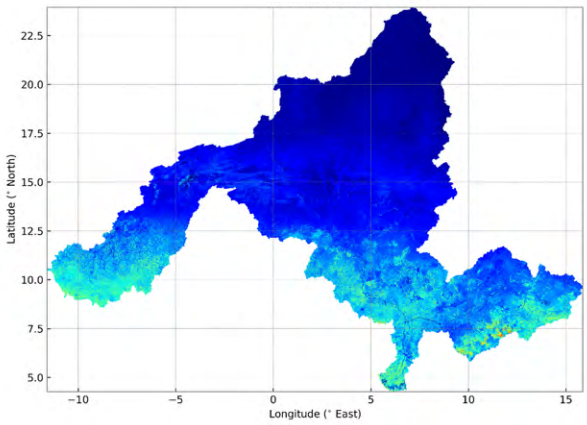

2011

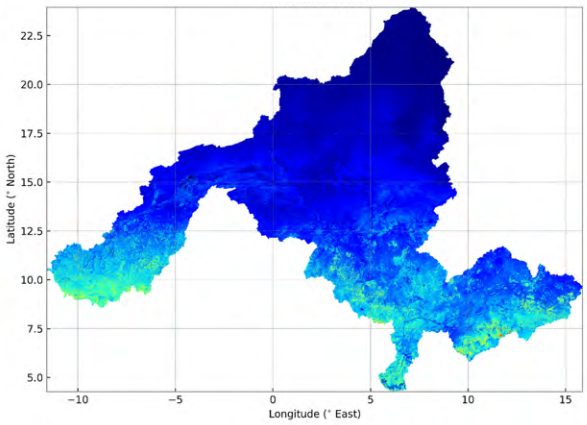

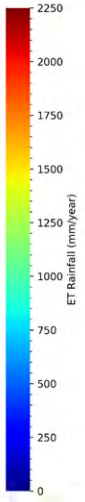

2012

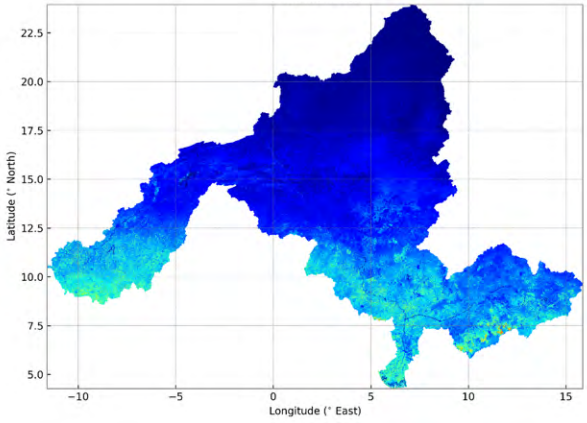

2013

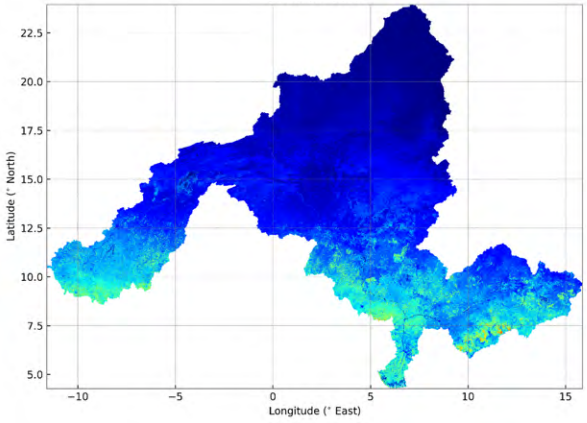

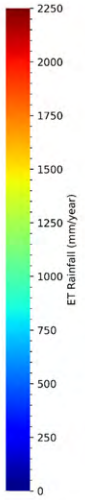

2014

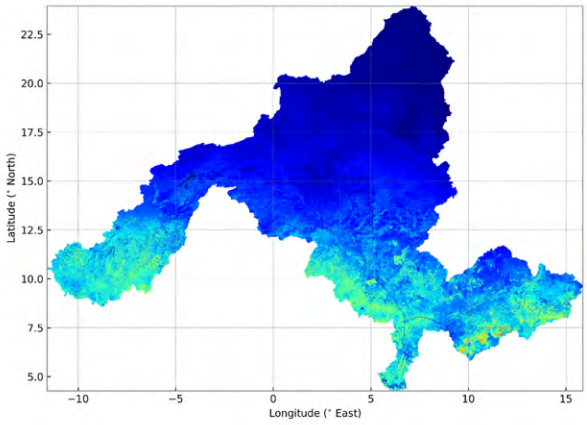

2015

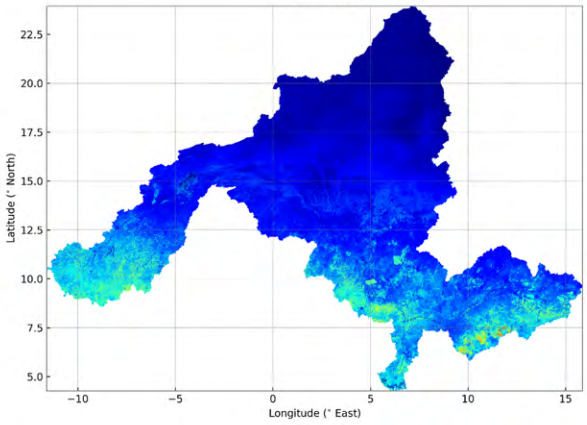

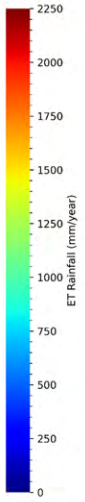

2016

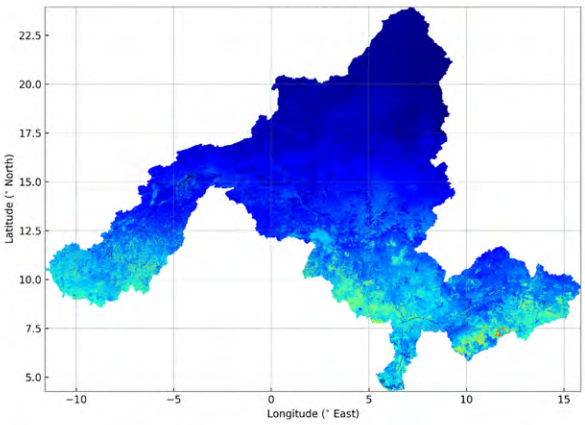

2017

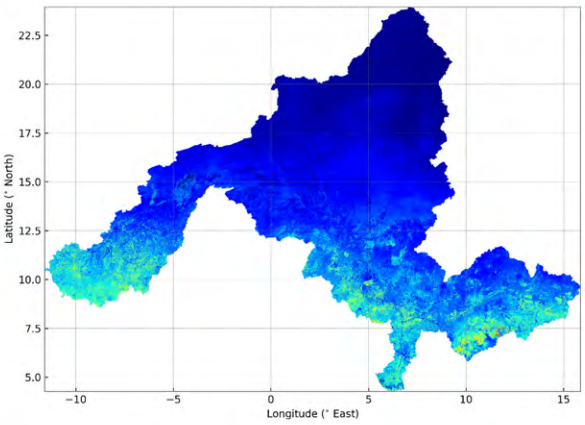

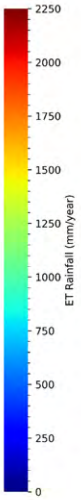

2018

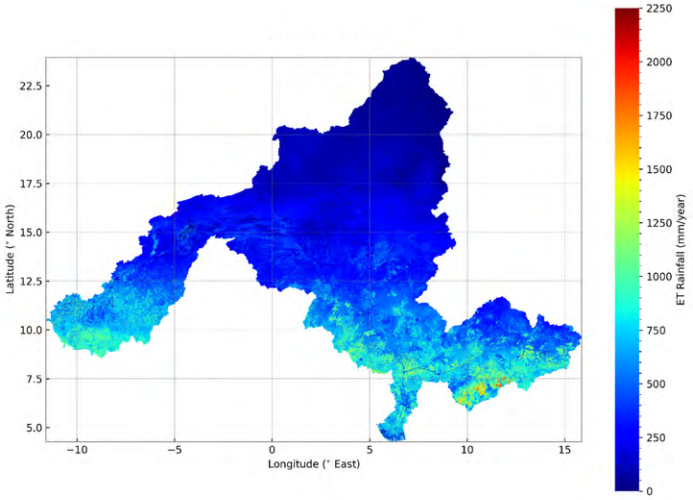

Annex XII. Water level in Akka[2]

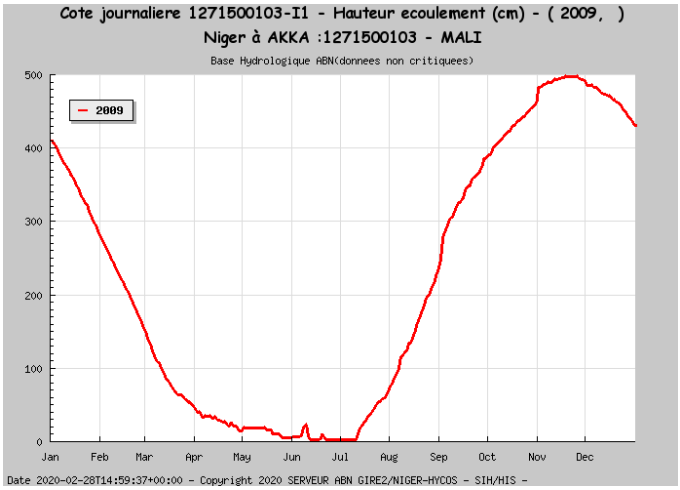

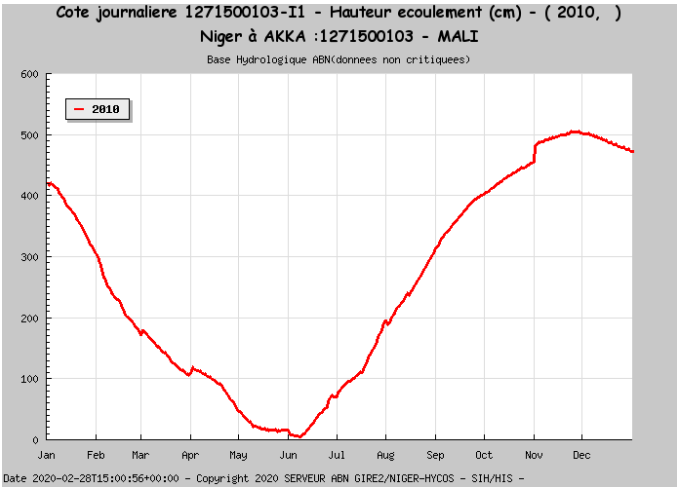

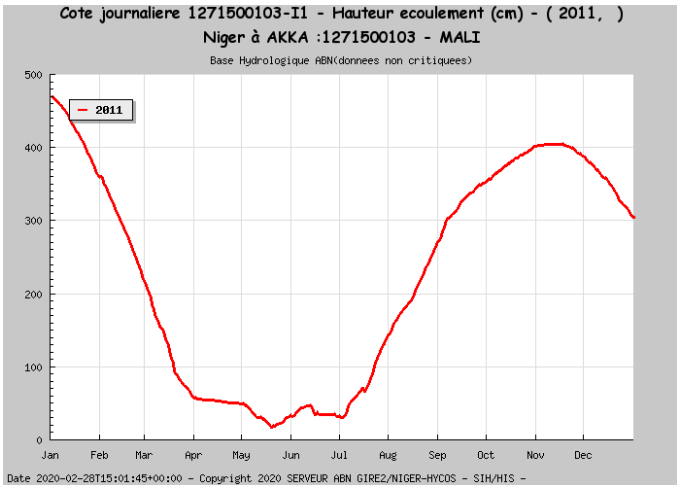

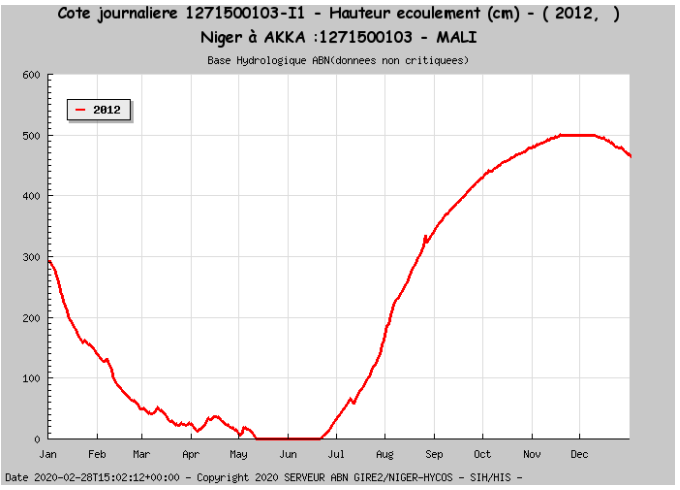

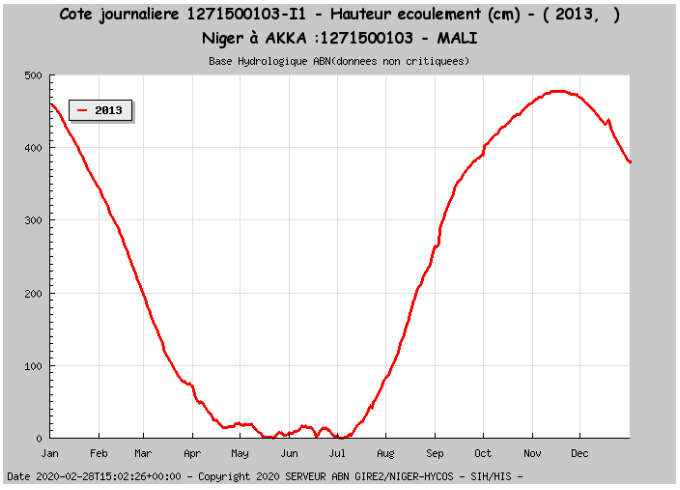

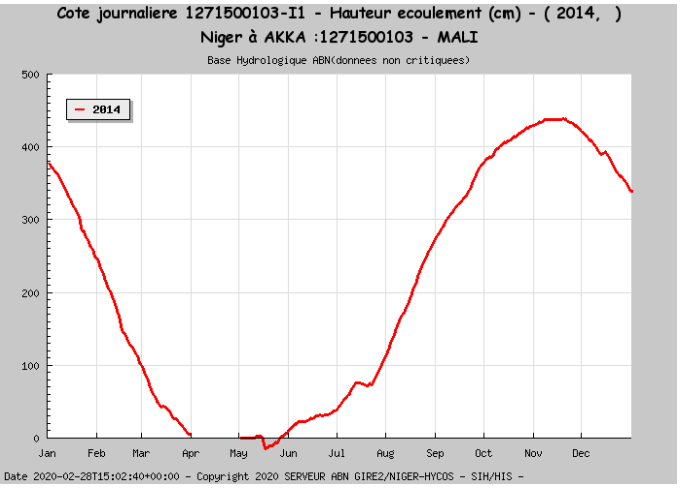

2 Source: http://nigerhycos.abn.ne/

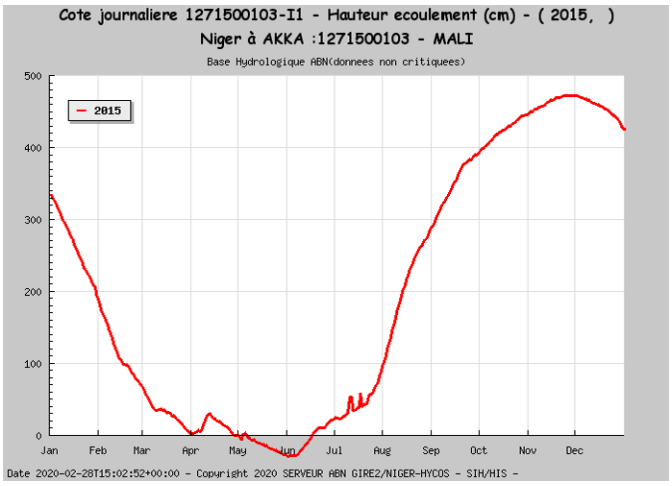
Cote journaliere 1271500103-I1 - Hauteur ecoulement (cm) - (2015,)
Niger à AKKA :1271500103 - MALI
Base Hydrologique ABN(donnees non critiquees)
2015
Jan Feb Mar Apr May Jun Jul Aug Sep Oct Nov Dec
Date 2020-02-28T15:02:52+00:00 - Copyright 2020 SERVEUR ABN GIRE2/NIGER-HYCOS - SIH/HIS -

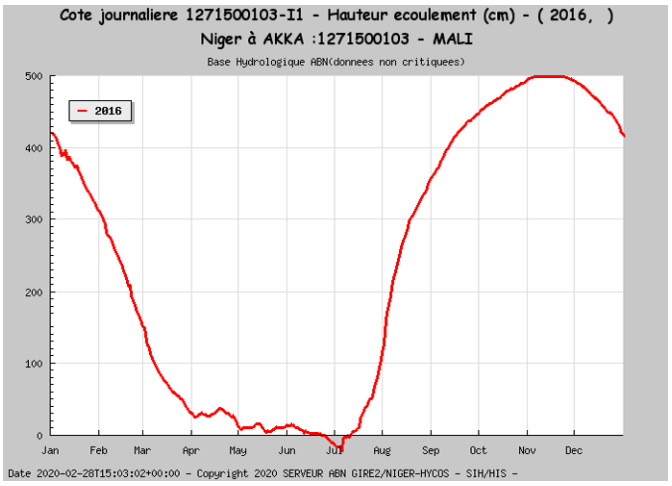
Cote journaliere 1271500103-I1 - Hauteur ecoulement (cm) - (2016,)
Niger à AKKA :1271500103 - MALI
Base Hydrologique ABN(donnees non critiquees)
2016
Jan Feb Mar Apr May Jun Jul Aug Sep Oct Nov Dec
Date 2020-02-28T15:03:02+00:00 - Copyright 2020 SERVEUR ABN GIRE2/NIGER-HYCOS - SIH/HIS -

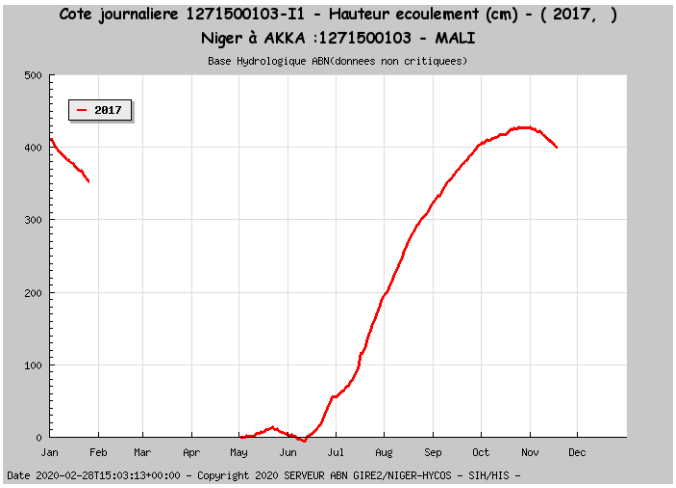
Cote journaliere 1271500103-I1 - Hauteur ecoulement (cm) - (2017,)
Niger à AKKA :1271500103 - MALI
Base Hydrologique ABN(donnees non critiquees)
2017
Jan Feb Mar Apr May Jun Jul Aug Sep Oct Nov Dec
Date 2020-02-28T15:03:13+00:00 - Copyright 2020 SERVEUR ABN GIRE2/NIGER-HYCOS - SIH/HIS -

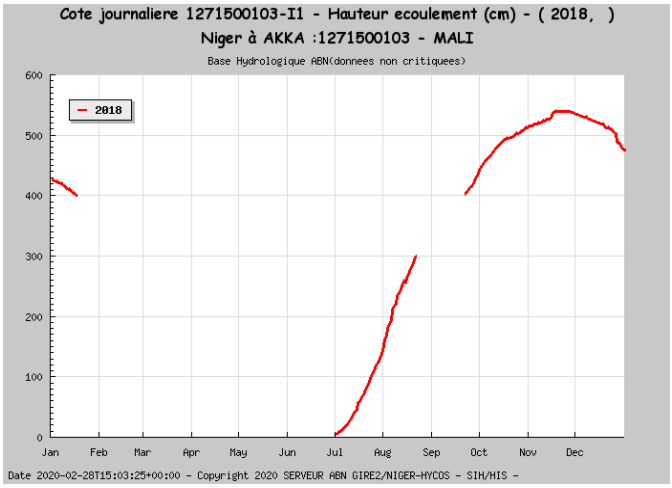
Cote journaliere 1271500103-I1 - Hauteur ecoulement (cm) - (2018,)
Niger à AKKA :1271500103 - MALI
Base Hydrologique ABN(donnees non critiquees)
2018
Jan Feb Mar Apr May Jun Jul Aug Sep Oct Nov Dec
Date 2020-02-28T15:03:25+00:00 - Copyright 2020 SERVEUR ABN GIRE2/NIGER-HYCOS - SIH/HIS -

Annex XIII. Other methods for delineate flood extent in the Inner Delta Niger

XIII.1. Using JRC global surface water extent

Global maps of surface water such as the JRC Monthly Water History (v1.1) dataset contains global maps of surface water from 1984 to 2018 (Pekel et al., 2016). The JRC maps are based on the whole archive of Landsat 5, 7 and 8 satellite imagery. Figure A-4 shows the variations of the surface water in the Inner Niger Delta based on the JRC data for the period 2009-2018. The largest surface water area is found in December. Inter-annual variability of the maximum flood extent is large, with the 2011 peak less than 40% of the maximum observed peak in 2010.

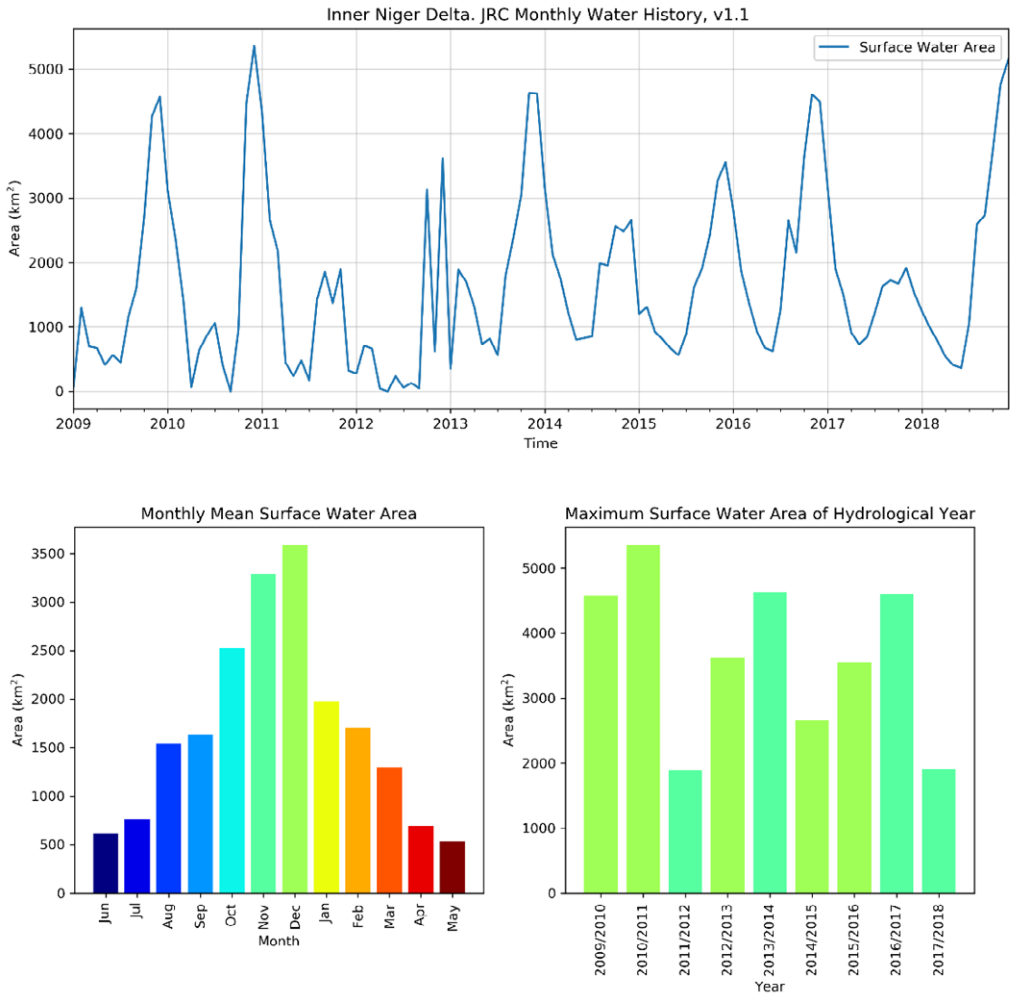

Figure A-4: Surface water area in the Inner Niger Delta extracted from JRC Monthly Water History v1.1 data. The bar color in the lower right plot indicates the month in the respective hydrological year where peak surface water area occurs.

The JRC maps, however, only capture surface water and are not able to detect flooded area under the vegetation canopy, especially in the Southern part of the delta during flood season months. As can be seen in the monthly recurrence percentage, these areas have close to zero % of flooded occurrence (Figure A-5).

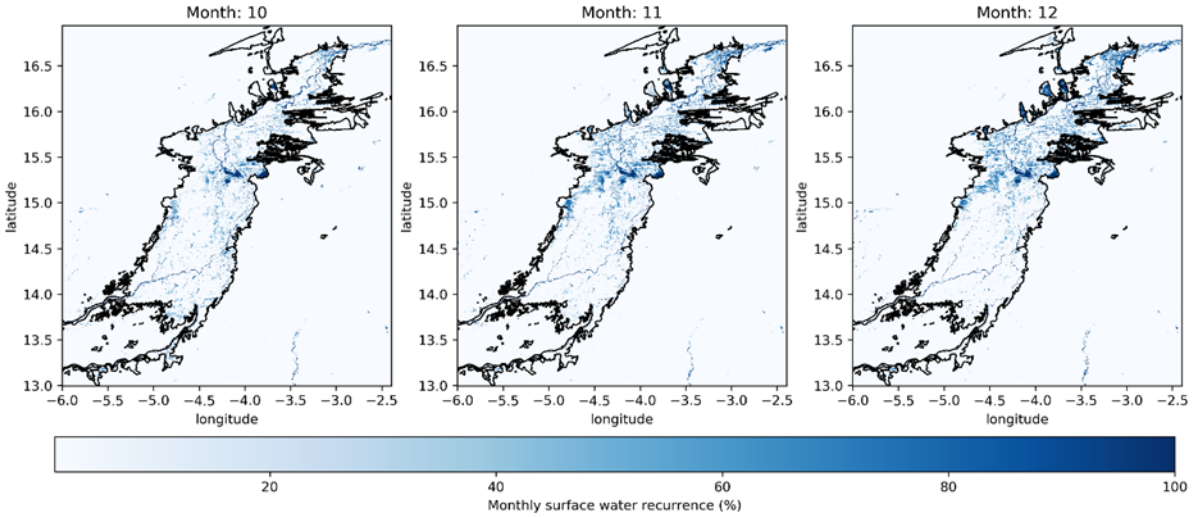

Figure A-5: JRC monthly surface water recurrence of all years (1984 -2018) as percentage of the flooding season months in the Inner Niger Delta. Black line represents the boundary of Inner Niger Delta.

References

Pekel, J.-F., Cottam, A., Gorelick, N., Belward, A.S. 2016. High-resolution mapping of global surface water and its long-term changes. *Nature*. 540, 418–422. https://doi.org/10.1038/nature20584

XIII.2. Using relationship between peak flood level in Akka and the corresponding flood extent in the Inner Niger Delta from literature[3]

"A high inflow of the Bani and Niger Rivers not only produce a high flood level, but also floods a more extensive area. The higher the maximum flood level, the larger the area (see viewer). In a dry year (as 1984), just one third of the Delta became inundated; the northern Delta was not even reached by the flood. In a wet year (such as 1999) though, the southern Delta was fully flooded, as well as a large part of the northern Delta including several of the lakes just north of the Delta. Zwarts & Grigoras (2005) used a polynomial to describe the relationship between the peak flood level in Akka and the corresponding flood extent:

$$\text{maximum flood extent } (km^2) = 0.099 * x^2 - 35.521x + 8727$$

where x = water level in Akka (cm).

The function is based on water maps for which the water level in Akka was up to 511 cm, but in the past, peak flood level in Akka has been as high as 625 cm. Extrapolating this function for these higher water levels, the flood extent would arrive at 25,000 km² when the water level in Akka would be 625 cm in Akka (as was the case in 1956). This is still substantially less than the total surface of the floodplains as shown on

the Institut Géographique National (IGN) maps (31,000 km²). This apparent discrepancy is caused by the northward mild slope of the floodplain that delays flooding in the north with two-three months; by that time the southern floodplain has already been drained of water.

Using the function given above, the variation in flood extent can be shown for all years since 1907:

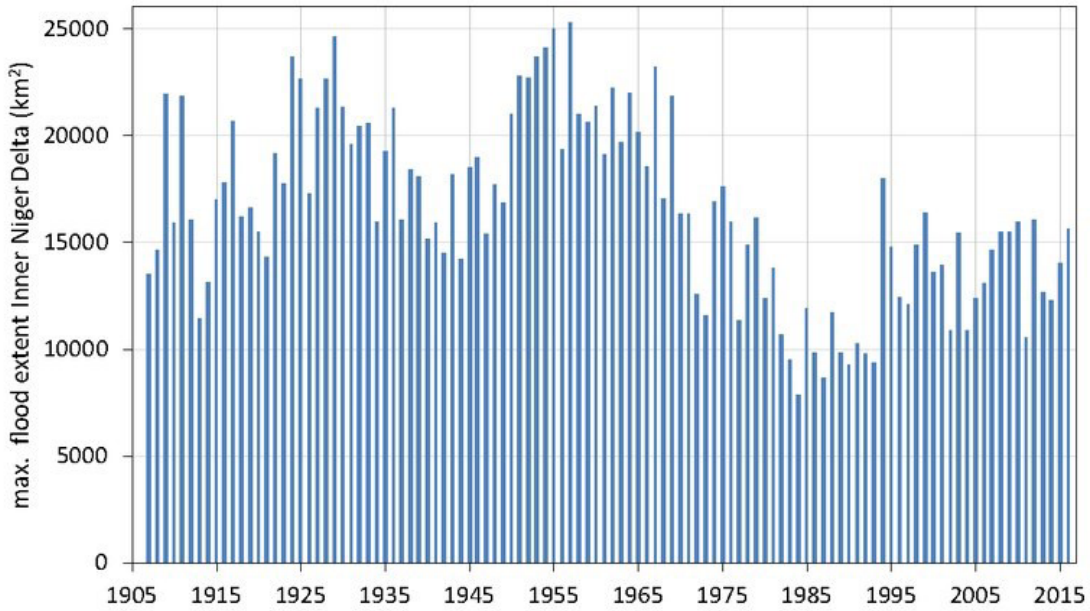

Figure A-6: The flood extent of the Inner Niger Delta derived from the annual peak flood level in Akka

Combining the data given above, it is also possible to show the relation between the total inflow of Bani and Niger Rivers and the flood extent in the same year:

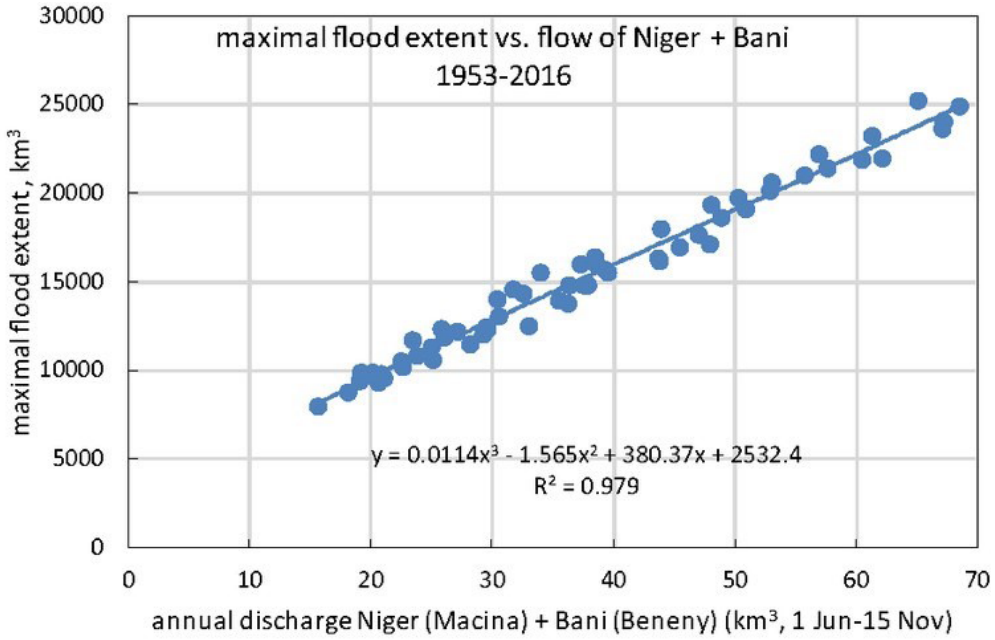

Figure A-7: The maximal flood extent of the Inner Niger Delta as a function of the annual inflow of Niger and Bani during incoming water.

The water maps given by Zwarts & Hoekema (2013) are intended to show the inundation at different water levels during the peak flood, but may also be used to show the change in the water cover

during incoming water. The maps cannot be used, however, to show the water cover as a function of the water level during the deflooding when a large part of the inundated area lost its connection to the river system. The higher the flood, the more isolated lakes come into existence and the larger the fraction of inundated area being unconnected to the river. Hence, during the deflooding it is not the water level in the river, but the maximal water level, as well as the time passed since the water level has reached its peak, which determines where isolated and temporary lakes with water can be found. This is true for small depressions of some ha of shallow water, but also for Lac Faquibine and the other, large lakes west and east of the Inner Niger Delta."

References

Zwarts, L & Hoekema, F.S. 2013. *Atlas: les plaines inondables du Delta Intérieur du Niger*. Altenburg & Wymenga, ecological consultants, Feanwâlden.

Zwarts, L., Grigoras, I. 2005. Chapter 3: Flooding of the Inner Niger Delta, in: The Niger, a Lifeline. *Effective Water Management in the Upper Niger Basin*. RIZA, Lelystad / Wetlands International, Sévaré / Institute for Environmental studies (IVM), Amsterdam / A&W ecological consultants, Veenwouden., Mali / the Netherlands, pp. 43–77.

XIII.3. Using Sentinel-1 C-band SAR data change detection4

XIII.3.1. Data collection

The imagery in the Google Earth Engine 'COPERNICUS/S1_GRD' Sentinel-1 Synthetic Aperture Radar (SAR) C-band collection was used to provide additional reference maps of the flooded area in the Inner Niger Delta wetland. This imagery consists of Level-1 Ground Range Detected (GRD) scenes processed to backscatter coefficient (σ°) in decibels (dB) by applying the following pre-processing steps (as implemented in the Sentinel-1 Toolbox):

- Apply orbit file
- GRD border noise removal
- Thermal noise removal
- Radiometric calibration
- Terrain correction

The 'COPERNICUS/S1_GRD' *ImageCollection* in Google Earth Engine is filtered by the region of

4 This annex follows the practice recommended by UN-SPIDER at: http://www.un-spider.org/advisory-support/recommended-practices/recommended-practice-google-earth-engine-flood-mapping/step-by-step

the Inner Niger Delta. Furthermore, the collection is filtered by instrument mode, orbit pass, and polarization for relative change calculation of the imagery before and after the peak flood.

```
var roi = ee.Table('users/username/InnerDelta')//shapefile of Inner Delta
var collection = ee.ImageCollection('COPERNICUS/S1_GRD')
.filter(ee.Filter.eq('instrumentMode', 'IW'))
.filter(ee.Filter.eq('orbitProperties_pass', 'ASCENDING'))
.filterMetadata('resolution_meters', 'equals' , 10)
.filterBounds(roi)
.select('VV', 'VH');
```

The selected collection is further filtered by periods of 15 days before and during peak flood in order to capture the difference of backscatter coefficient of the vegetated surface due to flooding while reducing the influence of quick change in vegetation cover.

```
var before_start= '2018-11-08';

var before_end=  '2018-11-23';



var after_start= '2018-11-24';

var after_end=  '2018-12-09' ;

var before = collection.filterDate(before_start, before_end).mosaic();
var after = collection.filterDate(after_start, after_end).mosaic();
```

The list of selected S1A_IW_GRDH_1SDV scenes are provided in the table below.

Date	system:id	relativeOrbitNumber_start
16/10/2016	COPERNICUS/S1_GRD/S1A_IW_GRDH_1SDV_20161016T182017_20161016T182042_013519_015A01_092E	147
	COPERNICUS/S1_GRD/S1A_IW_GRDH_1SDV_20161016T182042_20161016T182107_013519_015A01_E0EB	147
	COPERNICUS/S1_GRD/S1A_IW_GRDH_1SDV_20161016T182107_20161016T182132_013519_015A01_C7CF	147
21/10/2016	COPERNICUS/S1_GRD/S1A_IW_GRDH_1SDV_20161021T182759_20161021T182824_013592_015C4B_7F68	45
	COPERNICUS/S1_GRD/S1A_IW_GRDH_1SDV_20161021T182824_20161021T182849_013592_015C4B_E58C	45
	COPERNICUS/S1_GRD/S1A_IW_GRDH_1SDV_20161021T182849_20161021T182914_013592_015C4B_BA97	45
	COPERNICUS/S1_GRD/S1A_IW_GRDH_1SDV_20161021T182914_20161021T182939_013592_015C4B_E3A7	45
26/10/2016	COPERNICUS/S1_GRD/S1A_IW_GRDH_1SDV_20161026T183622_20161026T183647_013665_015E84_8D70	118
28/10/2016	COPERNICUS/S1_GRD/S1A_IW_GRDH_1SDV_20161028T182017_20161028T182042_013694_015F6B_57F2	147
	COPERNICUS/S1_GRD/S1A_IW_GRDH_1SDV_20161028T182042_20161028T182107_013694_015F6B_4E54	147
	COPERNICUS/S1_GRD/S1A_IW_GRDH_1SDV_20161028T182107_20161028T182132_013694_015F6B_1A7D	147
02/11/2016	COPERNICUS/S1_GRD/S1A_IW_GRDH_1SDV_20161102T182759_20161102T182824_013767_0161B0_3F4B	45
	COPERNICUS/S1_GRD/S1A_IW_GRDH_1SDV_20161102T182824_20161102T182849_013767_0161B0_E4DE	45
	COPERNICUS/S1_GRD/S1A_IW_GRDH_1SDV_20161102T182849_20161102T182914_013767_0161B0_A661	45
	COPERNICUS/S1_GRD/S1A_IW_GRDH_1SDV_20161102T182914_20161102T182939_013767_0161B0_FB3A	45
07/11/2016	COPERNICUS/S1_GRD/S1A_IW_GRDH_1SDV_20161107T183622_20161107T183647_013840_0163FC_8768	118
09/11/2016	COPERNICUS/S1_GRD/S1A_IW_GRDH_1SDV_20161109T182017_20161109T182042_013869_0164EE_7B0C	147
	COPERNICUS/S1_GRD/S1A_IW_GRDH_1SDV_20161109T182042_20161109T182107_013869_0164EE_F7D0	147
	COPERNICUS/S1_GRD/S1A_IW_GRDH_1SDV_20161109T182107_20161109T182132_013869_0164EE_B032	147
14/11/2016	COPERNICUS/S1_GRD/S1A_IW_GRDH_1SDV_20161114T182759_20161114T182824_013942_016731_0E56	45
	COPERNICUS/S1_GRD/S1A_IW_GRDH_1SDV_20161114T182824_20161114T182849_013942_016731_1BA3	45
	COPERNICUS/S1_GRD/S1A_IW_GRDH_1SDV_20161114T182849_20161114T182914_013942_016731_A173	45
	COPERNICUS/S1_GRD/S1A_IW_GRDH_1SDV_20161114T182914_20161114T182939_013942_016731_11E0	45
19/11/2016	COPERNICUS/S1_GRD/S1A_IW_GRDH_1SDV_20161119T183622_20161119T183647_014015_016965_8C53	118
21/11/2016	COPERNICUS/S1_GRD/S1A_IW_GRDH_1SDV_20161121T182017_20161121T182042_014044_016A45_8C32	147
	COPERNICUS/S1_GRD/S1A_IW_GRDH_1SDV_20161121T182042_20161121T182107_014044_016A45_66EE	147
	COPERNICUS/S1_GRD/S1A_IW_GRDH_1SDV_20161121T182107_20161121T182132_014044_016A45_2D66	147

26/11/2016	COPERNICUS/S1_GRD/S1A_IW_GRDH_1SDV_20161126T182759_20161126T182824_014117_016C82_6D18	45
	COPERNICUS/S1_GRD/S1A_IW_GRDH_1SDV_20161126T182824_20161126T182849_014117_016C82_782D	45
	COPERNICUS/S1_GRD/S1A_IW_GRDH_1SDV_20161126T182849_20161126T182914_014117_016C82_CBC6	45
	COPERNICUS/S1_GRD/S1A_IW_GRDH_1SDV_20161126T182914_20161126T182939_014117_016C82_B2CA	45
27/09/2017	COPERNICUS/S1_GRD/S1A_IW_GRDH_1SDV_20170927T183622_20170927T183647_018565_01F4A7_12DE	118
	COPERNICUS/S1_GRD/S1A_IW_GRDH_1SDV_20170927T183647_20170927T183712_018565_01F4A7_1C64	118
29/09/2017	COPERNICUS/S1_GRD/S1A_IW_GRDH_1SDV_20170929T182025_20170929T182050_018594_01F587_40D8	147
	COPERNICUS/S1_GRD/S1A_IW_GRDH_1SDV_20170929T182050_20170929T182115_018594_01F587_1A19	147
04/10/2017	COPERNICUS/S1_GRD/S1A_IW_GRDH_1SDV_20171004T182808_20171004T182833_018667_01F7BF_8D7B	45
	COPERNICUS/S1_GRD/S1A_IW_GRDH_1SDV_20171004T182833_20171004T182858_018667_01F7BF_3DF4	45
	COPERNICUS/S1_GRD/S1A_IW_GRDH_1SDV_20171004T182858_20171004T182923_018667_01F7BF_DF9D	45
09/10/2017	COPERNICUS/S1_GRD/S1A_IW_GRDH_1SDV_20171009T183622_20171009T183647_018740_01F9F7_E218	118
	COPERNICUS/S1_GRD/S1A_IW_GRDH_1SDV_20171009T183647_20171009T183712_018740_01F9F7_4789	118
11/10/2017	COPERNICUS/S1_GRD/S1A_IW_GRDH_1SDV_20171011T182026_20171011T182051_018769_01FAD7_E379	147
	COPERNICUS/S1_GRD/S1A_IW_GRDH_1SDV_20171011T182051_20171011T182116_018769_01FAD7_DBD5	147
16/10/2017	COPERNICUS/S1_GRD/S1A_IW_GRDH_1SDV_20171016T182808_20171016T182833_018842_01FD1B_39C3	45
	COPERNICUS/S1_GRD/S1A_IW_GRDH_1SDV_20171016T182833_20171016T182858_018842_01FD1B_8F10	45
	COPERNICUS/S1_GRD/S1A_IW_GRDH_1SDV_20171016T182858_20171016T182923_018842_01FD1B_BDAD	45
21/10/2017	COPERNICUS/S1_GRD/S1A_IW_GRDH_1SDV_20171021T183623_20171021T183648_018915_01FF5C_BCE7	118
	COPERNICUS/S1_GRD/S1A_IW_GRDH_1SDV_20171021T183648_20171021T183713_018915_01FF5C_1B72	118
23/10/2017	COPERNICUS/S1_GRD/S1A_IW_GRDH_1SDV_20171023T182026_20171023T182051_018944_020039_E165	147
	COPERNICUS/S1_GRD/S1A_IW_GRDH_1SDV_20171023T182051_20171023T182116_018944_020039_A97A	147
28/10/2017	COPERNICUS/S1_GRD/S1A_IW_GRDH_1SDV_20171028T182808_20171028T182833_019017_020269_8EFB	45
	COPERNICUS/S1_GRD/S1A_IW_GRDH_1SDV_20171028T182833_20171028T182858_019017_020269_D7B7	45
	COPERNICUS/S1_GRD/S1A_IW_GRDH_1SDV_20171028T182858_20171028T182923_019017_020269_335B	45
02/11/2017	COPERNICUS/S1_GRD/S1A_IW_GRDH_1SDV_20171102T183623_20171102T183648_019090_0204AB_B08A	118
	COPERNICUS/S1_GRD/S1A_IW_GRDH_1SDV_20171102T183648_20171102T183713_019090_0204AB_47D0	118
04/11/2017	COPERNICUS/S1_GRD/S1A_IW_GRDH_1SDV_20171104T182026_20171104T182051_019119_02058F_BB4D	147
	COPERNICUS/S1_GRD/S1A_IW_GRDH_1SDV_20171104T182051_20171104T182116_019119_02058F_BFB2	147

09/11/2017	COPERNICUS/S1_GRD/S1A_IW_GRDH_1SDV_20171109T182807_20171109T182832_019192_0207CF_281F	45
	COPERNICUS/S1_GRD/S1A_IW_GRDH_1SDV_20171109T182832_20171109T182857_019192_0207CF_ECB5	45
	COPERNICUS/S1_GRD/S1A_IW_GRDH_1SDV_20171109T182857_20171109T182922_019192_0207CF_73BD	45
28/10/2018	COPERNICUS/S1_GRD/S1A_IW_GRDH_1SDV_20181028T183629_20181028T183654_024340_02AA42_2A86	118
	COPERNICUS/S1_GRD/S1A_IW_GRDH_1SDV_20181028T183654_20181028T183719_024340_02AA42_ADBC	118
30/10/2018	COPERNICUS/S1_GRD/S1A_IW_GRDH_1SDV_20181030T182032_20181030T182102_024369_02AB27_959F	147
04/11/2018	COPERNICUS/S1_GRD/S1A_IW_GRDH_1SDV_20181104T182814_20181104T182839_024442_02ADC6_A2FA	45
	COPERNICUS/S1_GRD/S1A_IW_GRDH_1SDV_20181104T182839_20181104T182904_024442_02ADC6_E58E	45
	COPERNICUS/S1_GRD/S1A_IW_GRDH_1SDV_20181104T182904_20181104T182929_024442_02ADC6_90CC	45
09/11/2018	COPERNICUS/S1_GRD/S1A_IW_GRDH_1SDV_20181109T183629_20181109T183654_024515_02B07C_D790	118
	COPERNICUS/S1_GRD/S1A_IW_GRDH_1SDV_20181109T183654_20181109T183719_024515_02B07C_339B	118
11/11/2018	COPERNICUS/S1_GRD/S1A_IW_GRDH_1SDV_20181111T182032_20181111T182057_024544_02B182_7789	147
	COPERNICUS/S1_GRD/S1A_IW_GRDH_1SDV_20181111T182057_20181111T182122_024544_02B182_2DB6	147
16/11/2018	COPERNICUS/S1_GRD/S1A_IW_GRDH_1SDV_20181116T182814_20181116T182839_024617_02B42B_2F51	45
	COPERNICUS/S1_GRD/S1A_IW_GRDH_1SDV_20181116T182839_20181116T182904_024617_02B42B_90A0	45
	COPERNICUS/S1_GRD/S1A_IW_GRDH_1SDV_20181116T182904_20181116T182929_024617_02B42B_AA3B	45
21/11/2018	COPERNICUS/S1_GRD/S1A_IW_GRDH_1SDV_20181121T183629_20181121T183654_024690_02B6EC_662A	118
	COPERNICUS/S1_GRD/S1A_IW_GRDH_1SDV_20181121T183654_20181121T183719_024690_02B6EC_8F6F	118
23/11/2018	COPERNICUS/S1_GRD/S1A_IW_GRDH_1SDV_20181123T182032_20181123T182057_024719_02B7F2_0DEF	147
	COPERNICUS/S1_GRD/S1A_IW_GRDH_1SDV_20181123T182057_20181123T182122_024719_02B7F2_D94C	147
28/11/2018	COPERNICUS/S1_GRD/S1A_IW_GRDH_1SDV_20181128T182814_20181128T182839_024792_02BA98_D4F9	45
	COPERNICUS/S1_GRD/S1A_IW_GRDH_1SDV_20181128T182839_20181128T182904_024792_02BA98_7016	45
	COPERNICUS/S1_GRD/S1A_IW_GRDH_1SDV_20181128T182904_20181128T182929_024792_02BA98_5937	45
03/12/2018	COPERNICUS/S1_GRD/S1A_IW_GRDH_1SDV_20181203T183628_20181203T183653_024865_02BCFB_4F68	118
	COPERNICUS/S1_GRD/S1A_IW_GRDH_1SDV_20181203T183653_20181203T183718_024865_02BCFB_60FD	118
05/12/2018	COPERNICUS/S1_GRD/S1A_IW_GRDH_1SDV_20181205T182031_20181205T182102_024894_02BDDA_F833	147

XIII.3.2. Processing steps

Since the imagery provided on Google Earth Engine is already pre-processed, only a smoothing filter was applied to reduce the speckle-effect of radar imagery:

```
var SMOOTHING_RADIUS = 50;


var before_filtered = before.focal_mean(SMOOTHING_RADIUS, 'circle','meters');
var after_filtered = after.focal_mean(SMOOTHING_RADIUS, 'circle','meters');
```

A difference threshold method can be used:

```
var DIFF_UPPER_THRESHOLD = -2;
var diff_smoothed = after_filtered.subtract(before_filtered);
var diff_thresholded = diff_smoothed.lt(DIFF_UPPER_THRESHOLD);
var selected_diff= diff_thresholded.select('VV').eq(1)
.multiply(diff_thresholded.select('VH').eq(0));
```

Or a ratio threshold method:

```
var RATIO_UPPER_THRESHOLD=1.2;
var polarization='VV';
var ratio = after_filtered.divide(before_filtered);
var ratio_thresholded = ratio.select(polarization)
.gt(RATIO_UPPER_THRESHOLD);
```

After that, the resulted maps need to be refined to avoid disconnected pixels and high slope pixels to be flooded. This can be done using the method:

```
var MAX_SLOPE=5; //parameter
var MIN_NEIGHBOURS=8; //parameter

var JRC = ee.ImageCollection('JRC/GSW1_1/MonthlyHistory')
.filterDate(before_start, after_end).first();

var swater_mask=JRC.eq(2).updateMask(JRC.eq(2));
var flooded_mask = selected.where(swater_mask,1);
var flooded= flooded_mask.updateMask(flooded_mask);

//Selected only pixels in IND
var ind_mask = ee.Image.constant(1).clip(ind).mask();
var flooded= flooded.updateMask(ind_mask);

//filter slope less than SLOPE_LOWER_THRESHOLD
var DEM = ee.Image('WWF/HydroSHEDS/03VFDEM');
var terrain = ee.Algorithms.Terrain(DEM);
var slope = terrain.select('slope');
var flooded = flooded.updateMask(slope.lt(MAX_SLOPE));

// Compute connectivity of pixels to eliminate those connected to MIN_
NEIGHBOURS or fewer neighbours
var connections = flooded.connectedPixelCount();
var flooded = flooded.updateMask(connections.gte(MIN_NEIGHBOURS));
```

XIII.3.3. Parameter sensitivity

XIII.3.3.1. Threshold and before flood window period

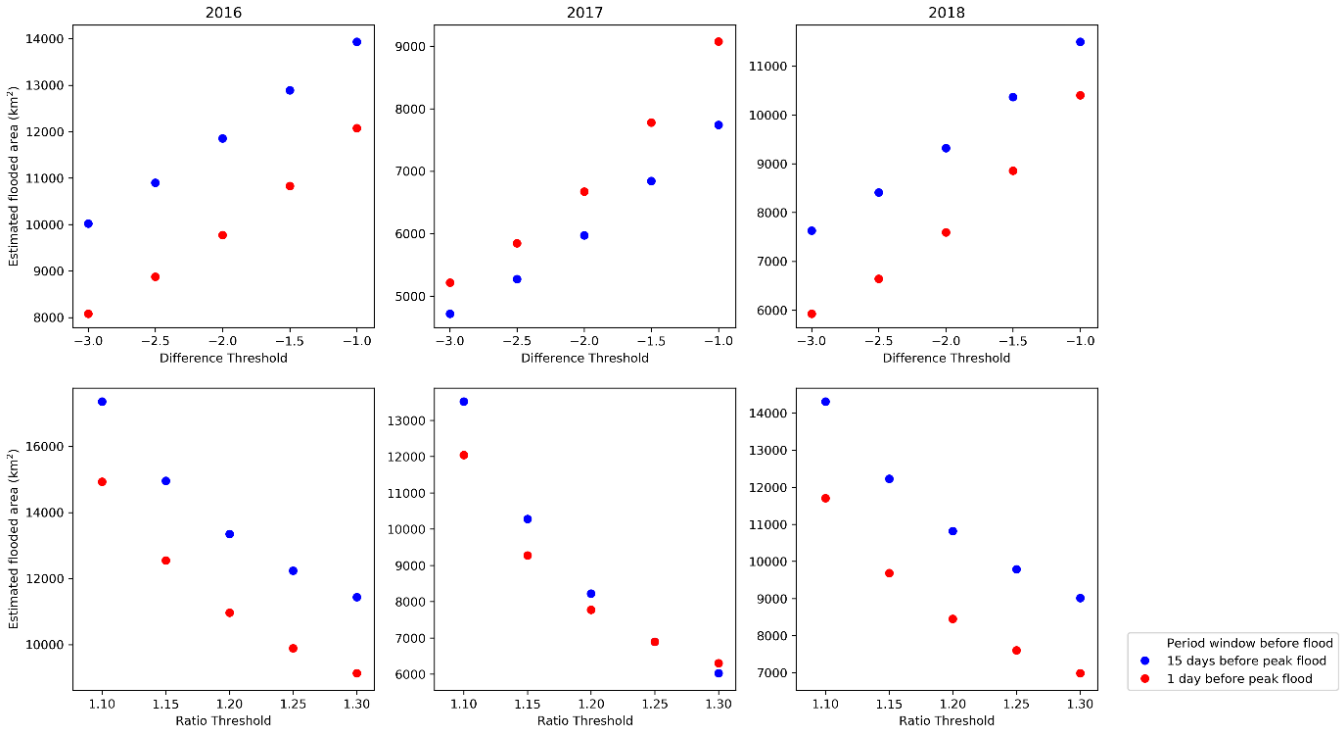

Figure A-8: Sensitivity of estimated flooded area to selection of SAR change detection method and the period window before flood moment

The selected method and threshold influence greatly the estimated flooded area. As can be seen in Figure A-8, the estimated flooded area varies in a range of up to 7,000 km² difference for ratio threshold from 1.1 to 1.3 and 6,000 km² for difference threshold from -3 to -1. The dependence on threshold is different between wet and dry years. As can be seen in Figure A-9, the estimated flooded area as a function of threshold is more linear in wet years (2016 and 2018) than in dry year (2017).

Choosing earlier before-flood window result in much higher total flooded area, the different can be up to more than 2,000 km². This is due to the fact that, the earlier the before-flood window, the drier the mosaic is compared to the one of the period after peak flood. The difference between two methods varies from dry to wet years, with smaller difference in the dry year (2017).

XIII.3.3.2. Refining parameters

There are two types of threshold used to refine the flood map: maximum slope and minimum number of neighbour pixels. The impact of refining parameters are less significant than that of difference and ratio threshold. Figure A-9 shows that the higher maximum slope is, the larger the estimated flooded area is. However, it does not matter much from slope above 6%, and the difference of resulted flooded area compared to 3% slope is only from 200 to 400 km² depending on years. In case of minimum number

of neighbours, the estimated flooded area decrease with increasing this number. For minimum number of neighbours from 4 to 8, the estimated flooded area decrease by 100 to 200 km². In the dry year (2017), the minimum number of neighbours has greater impact on the results, while in wet years (2016 and 2018), the estimated flooded area is more influenced by the maximum slope.

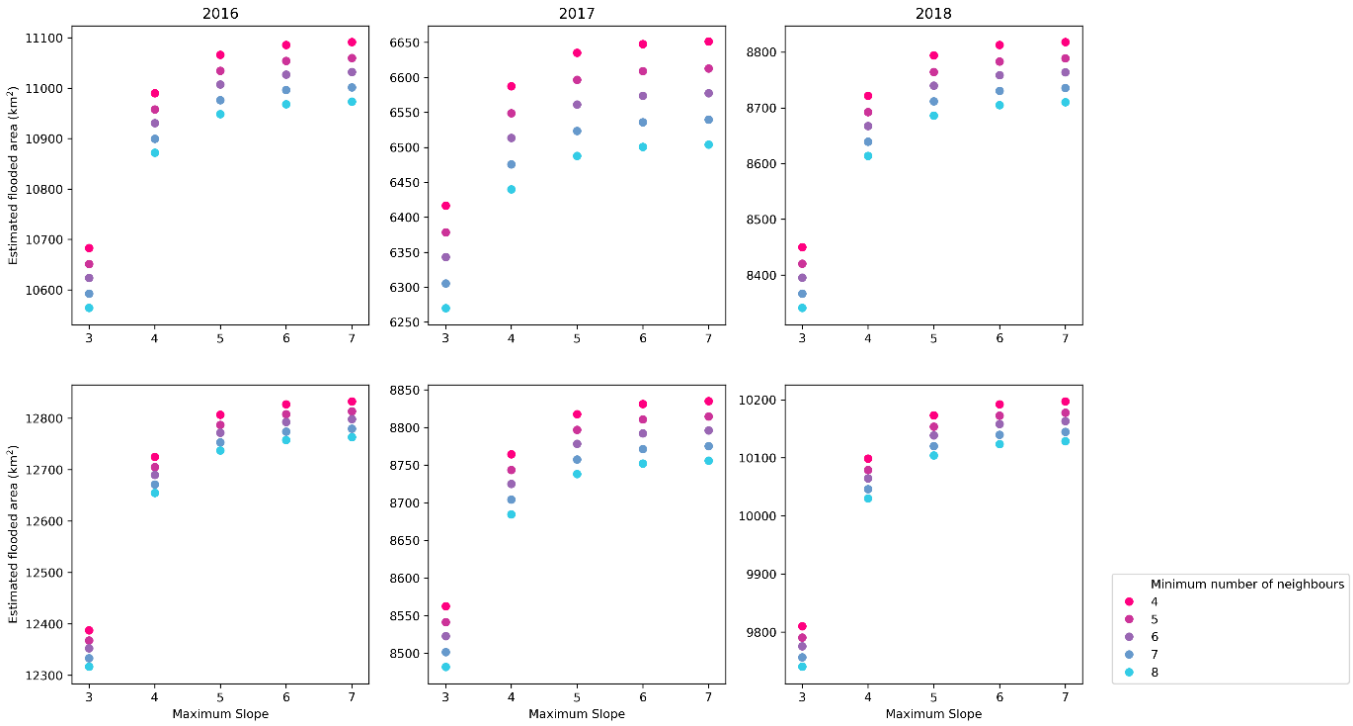

Figure A-9: Sensitivity of estimated flooded area to flood map refining parameters

Annex XIV. Yearly WA+ Sheet 1 Resource Base

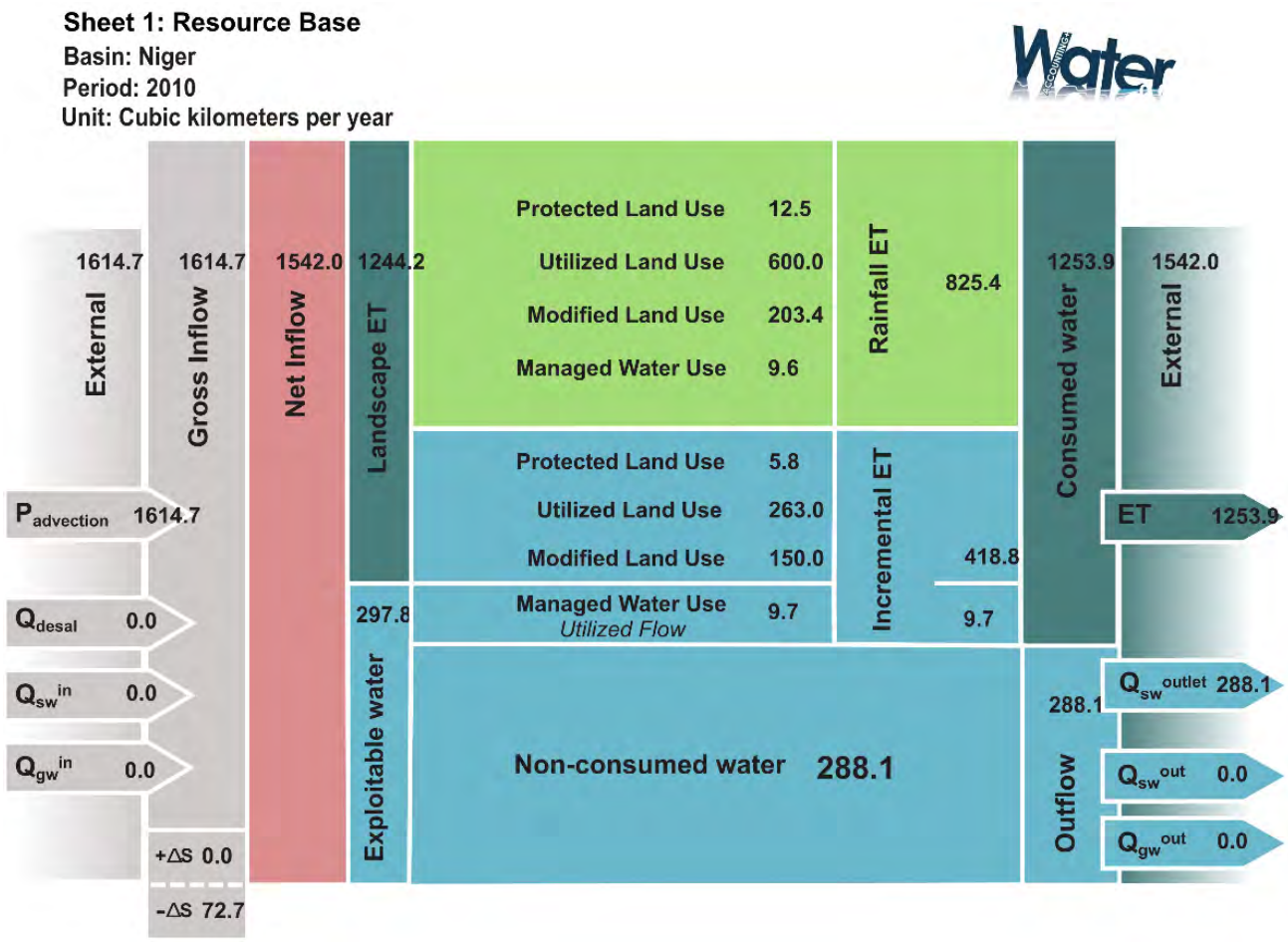

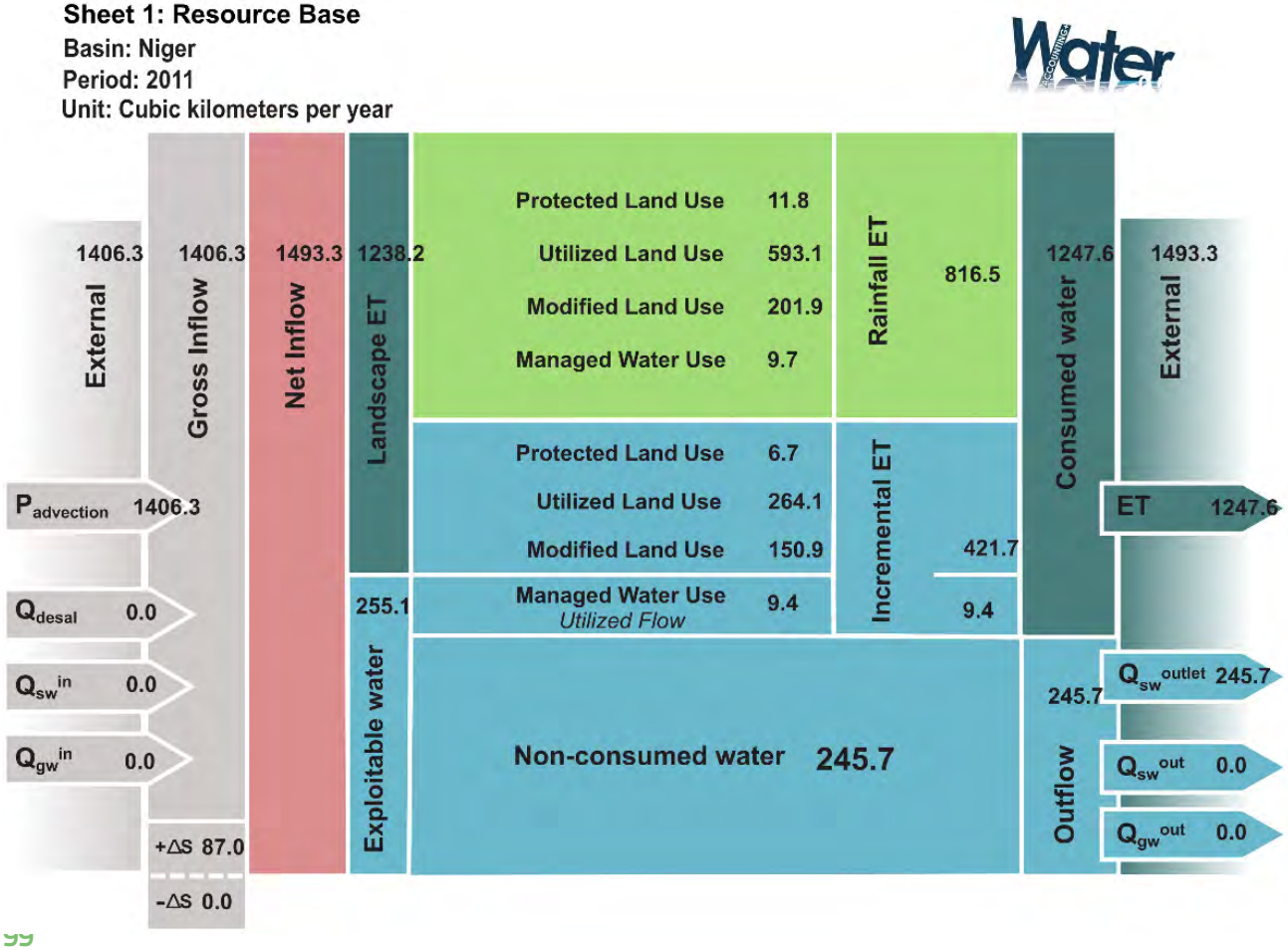

Sheet 1: Resource Base
Basin: Niger
Period: 2012
Unit: Cubic kilometers per year

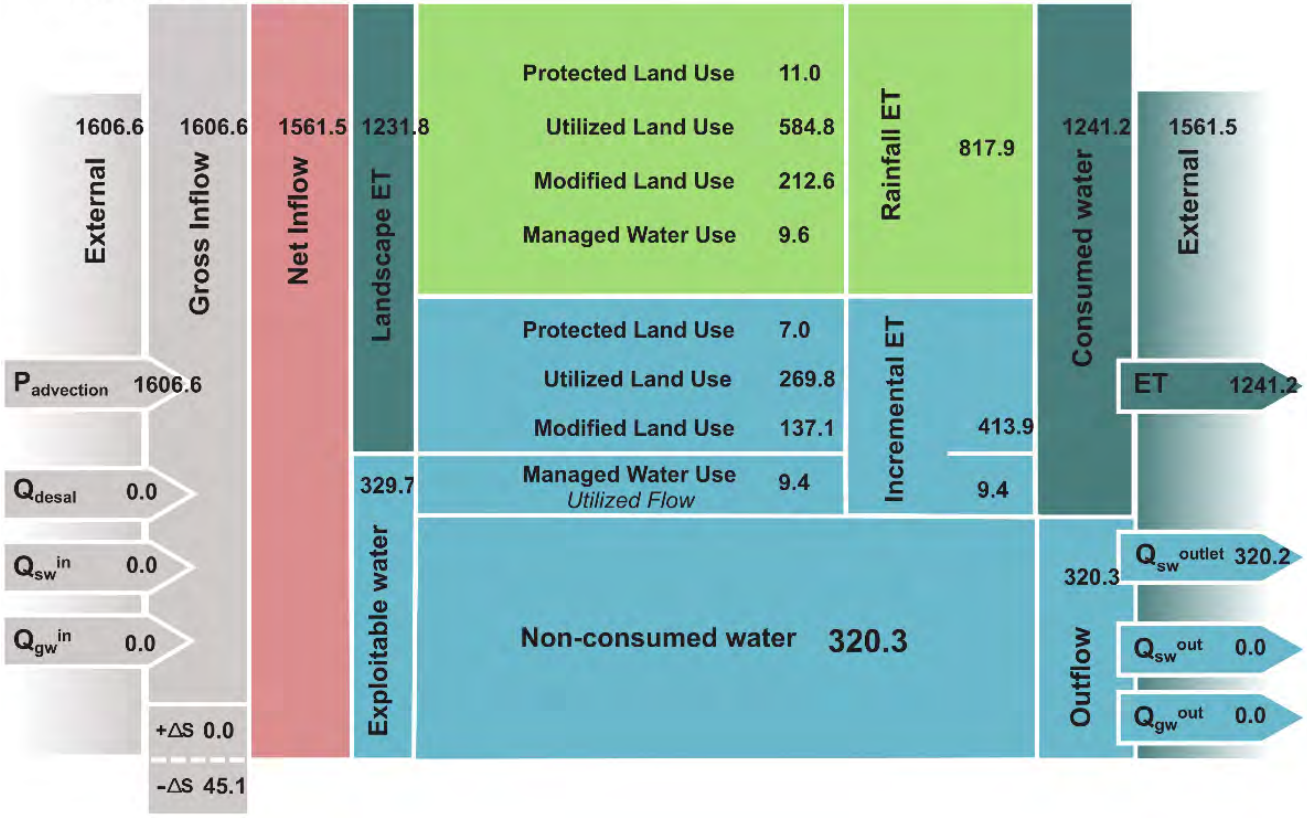

Sheet 1: Resource Base
Basin: Niger
Period: 2013
Unit: Cubic kilometers per year

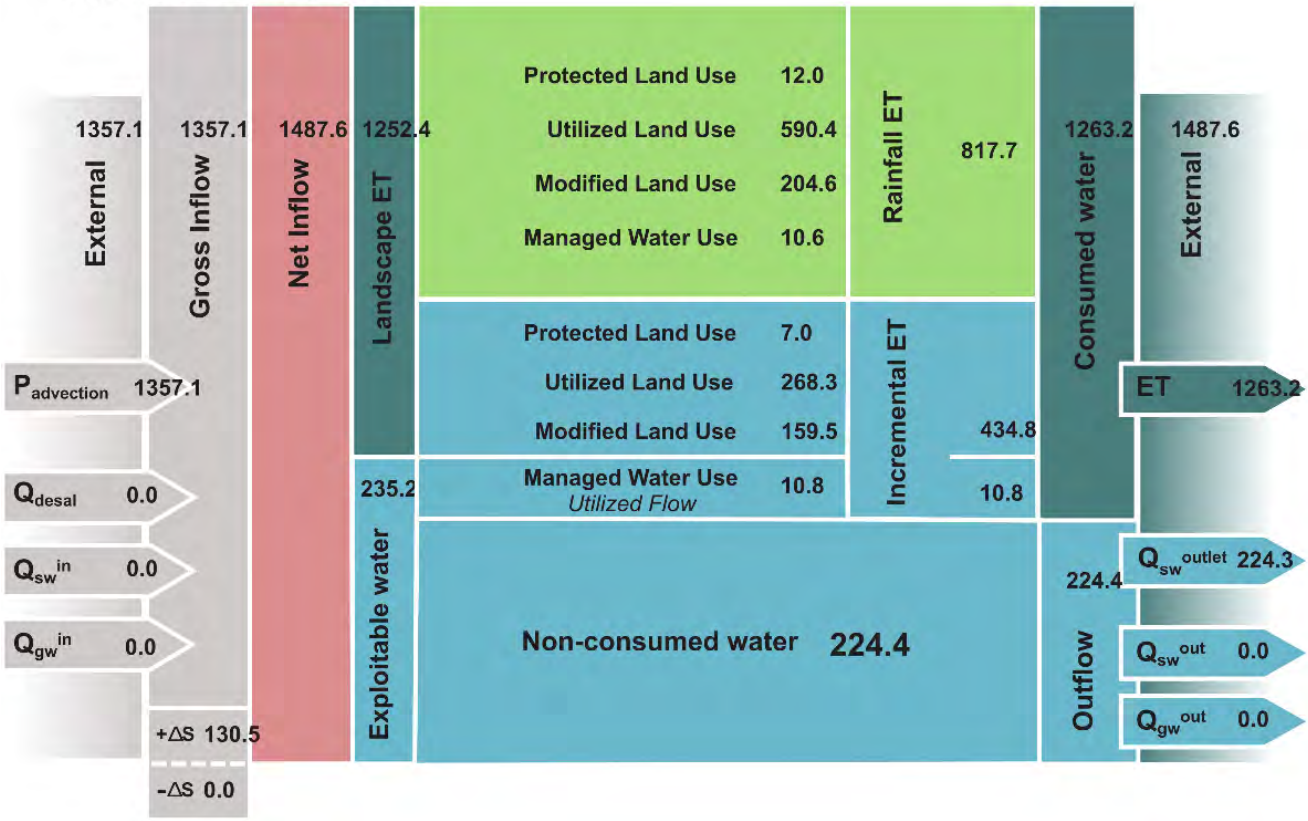

Sheet 1: Resource Base
Basin: Niger
Period: 2014
Unit: Cubic kilometers per year

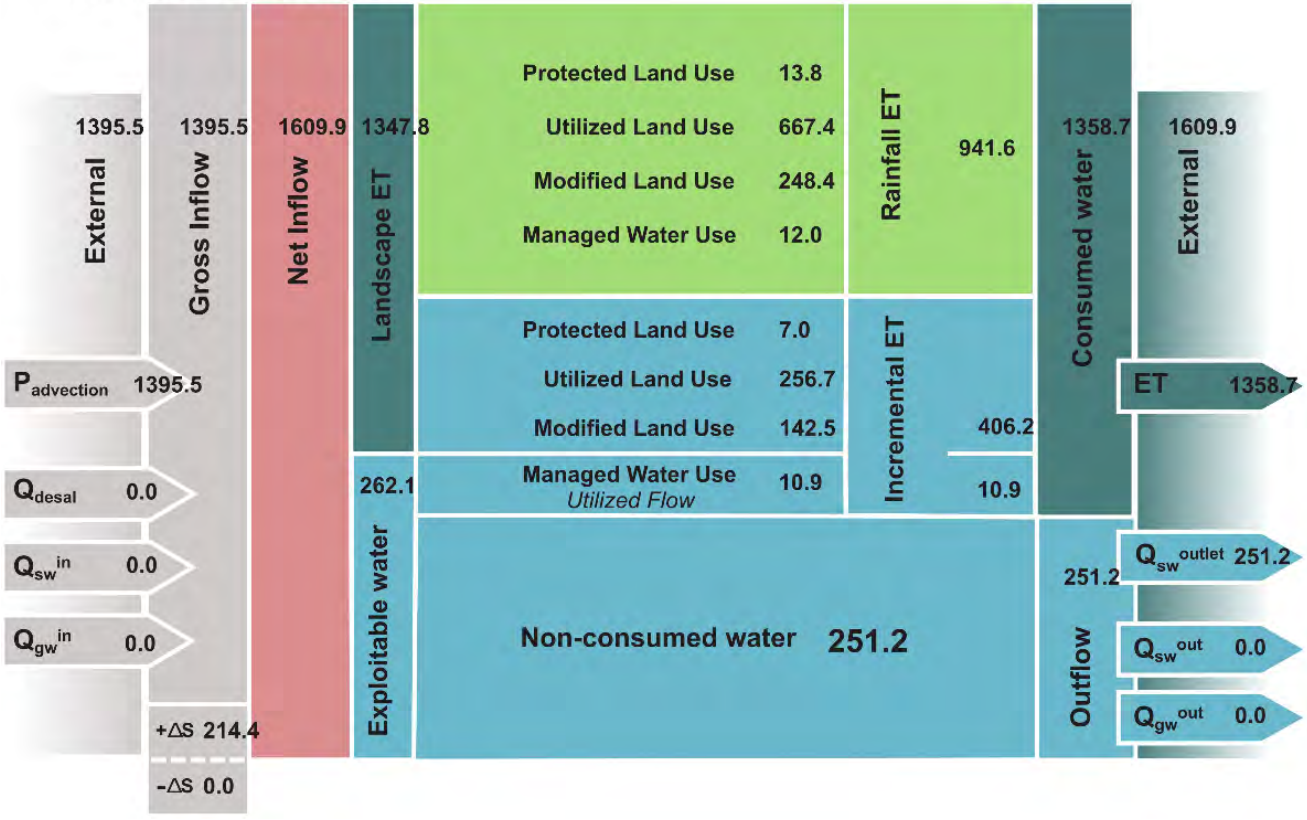

Sheet 1: Resource Base
Basin: Niger
Period: 2015
Unit: Cubic kilometers per year

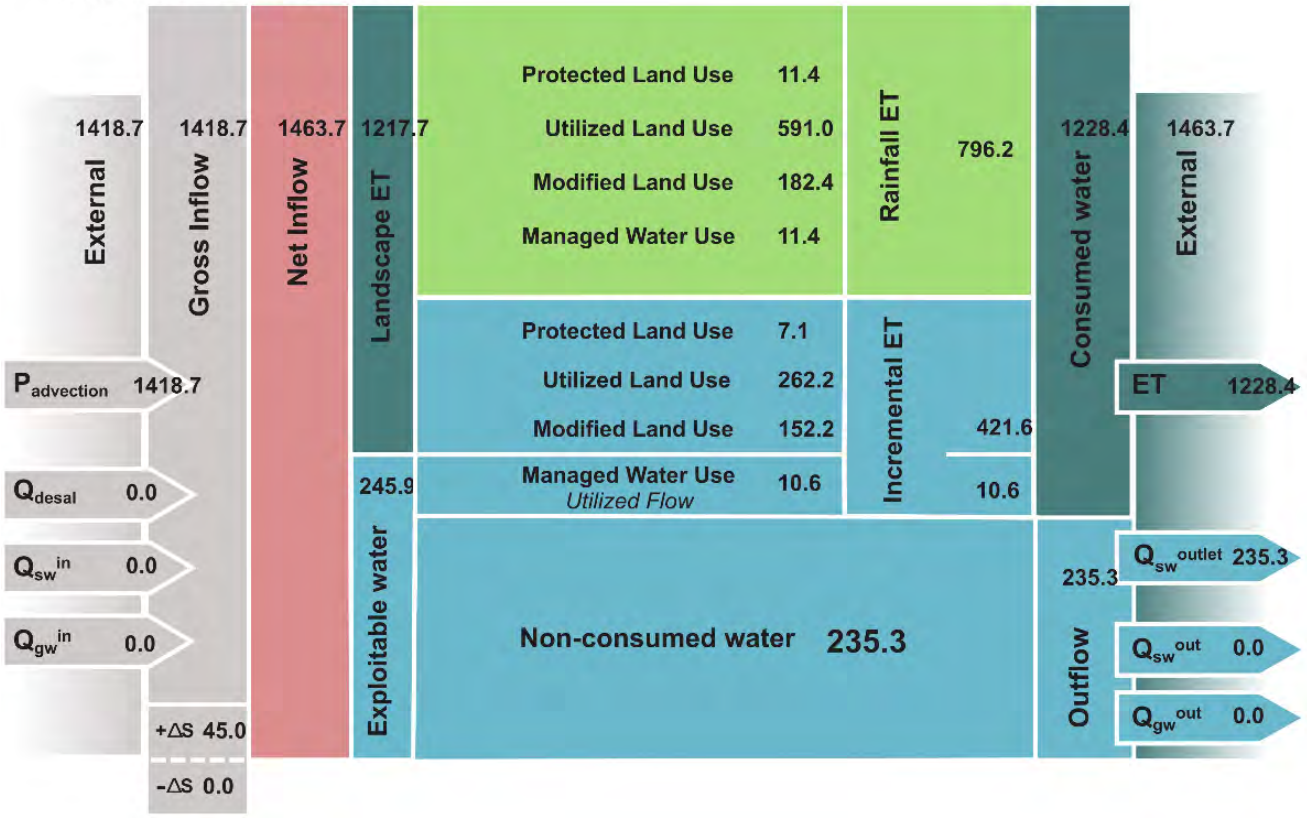

Sheet 1: Resource Base
Basin: Niger
Period: 2016
Unit: Cubic kilometers per year

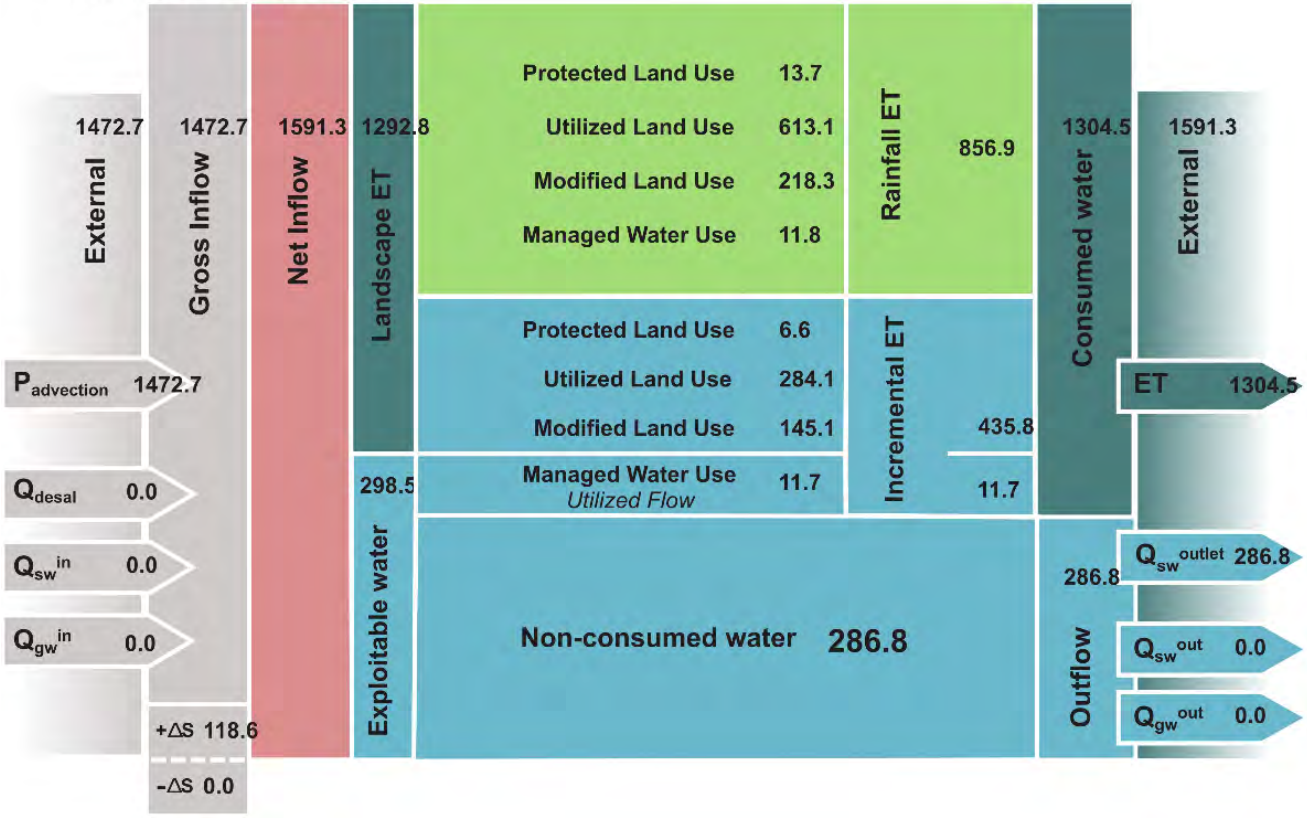

Sheet 1: Resource Base
Basin: Niger
Period: 2017
Unit: Cubic kilometers per year

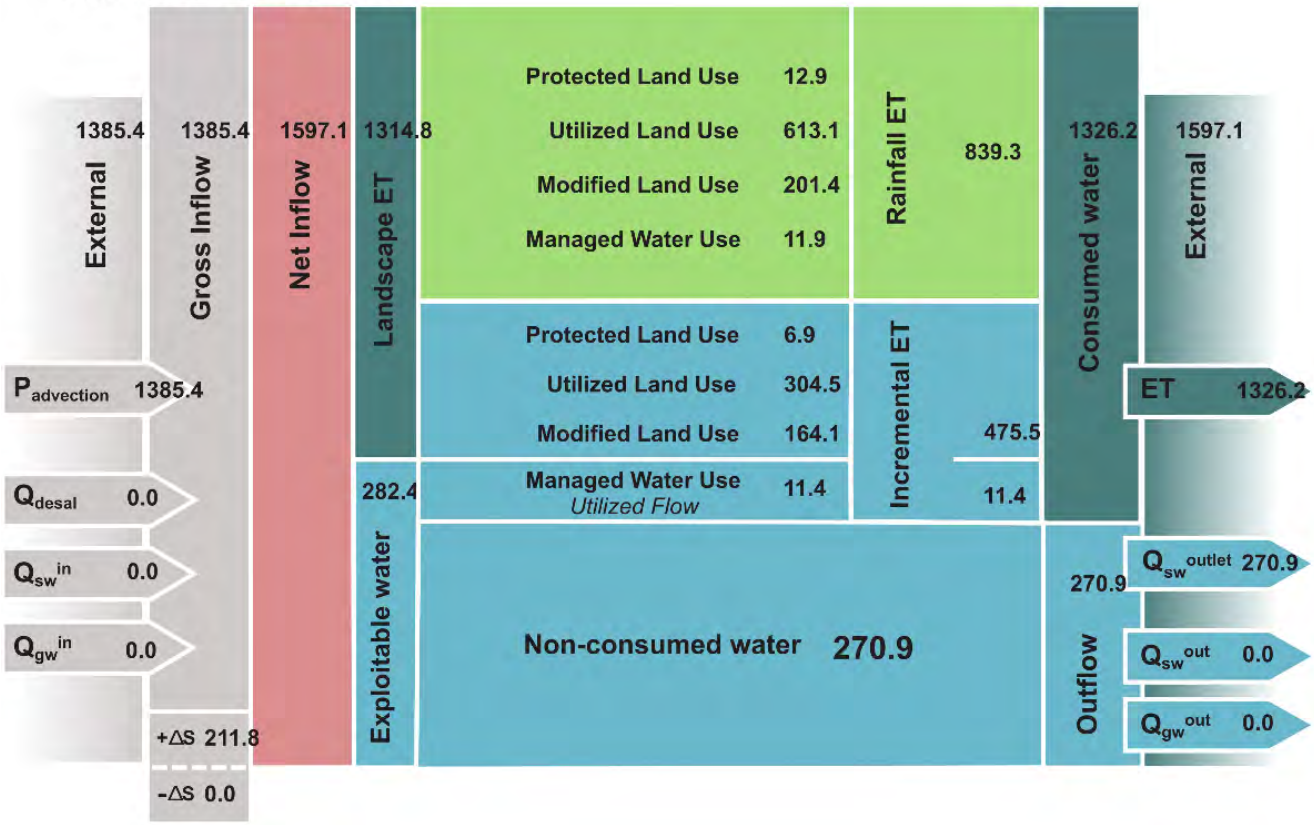

Sheet 1: Resource Base
Basin: Niger
Period: 2018
Unit: Cubic kilometers per year

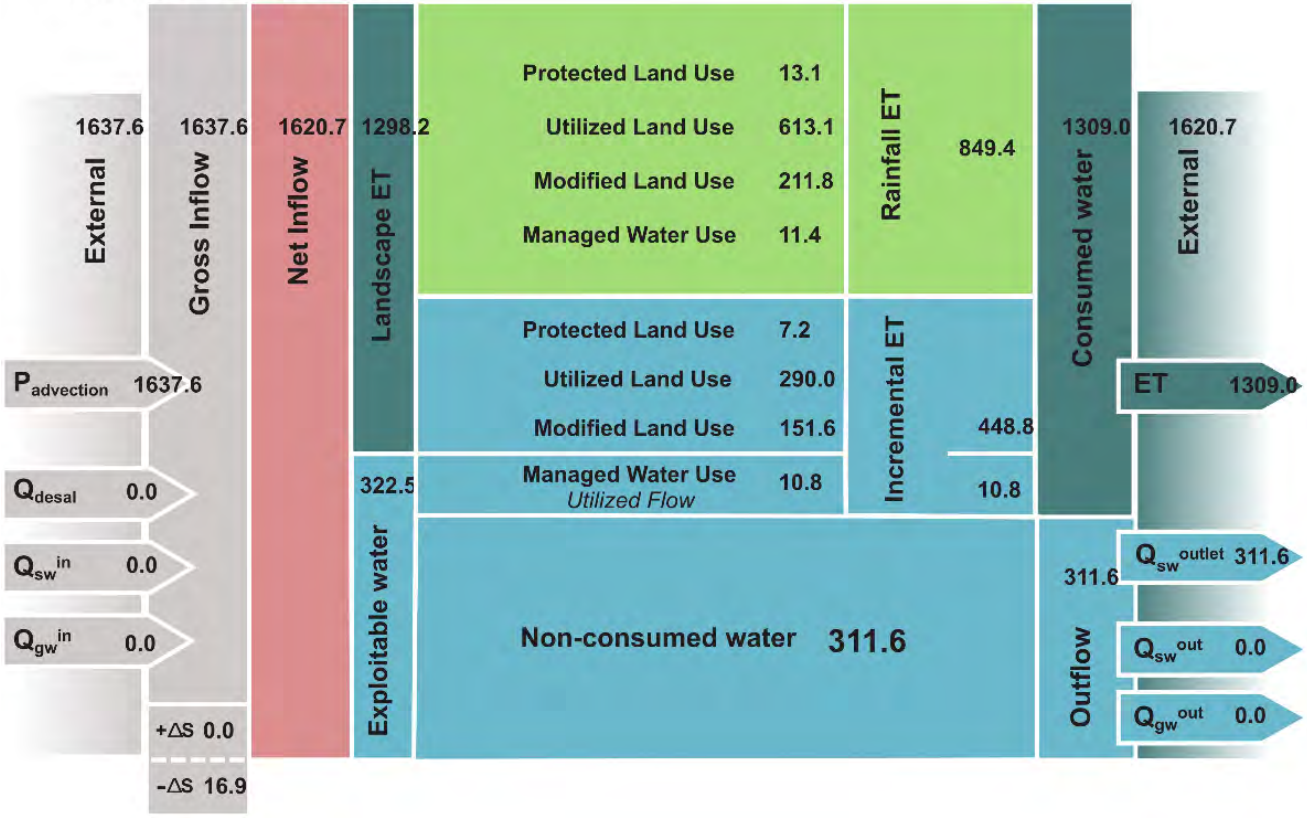

Water Accounting in the Niger River Basin

This report describes the water accounting study for the Niger River Basin carried out by IHE-Delft using the Water Productivity (WaPOR) data portal of the Food and Agricultural Organization (FAO).

The Niger River Basin is a transboundary basin covering nine riparian countries to the Niger River that are increasingly putting pressure on the available water resources as their populations expand. Yet, the nine countries are also among the poorest in the world and adequate exploitation of the water of the basin could be part of a broader strategy for poverty reduction in these countries. Major challenges to that end are the lacking water infrastructure and growing vulnerability to extreme weather hazards as the climate changes. In that context, a better understanding of the state of water resources in the basin is a crucial departure point for any measures towards the sustainable use of water. The Water Accounting Plus (WA+) system designed by IHE Delft with its partners FAO and IWMI has been applied to gain full insights into the state of the water resources in the basin.

Funded by:

Ministry of Foreign Affairs of the Netherlands

Frame consortium:

eleaf FEED THE WORLD

ITC

vito vision on technology

UNIVERSITY OF TWENTE.

WATERWATCH FOUNDATION

ISBN 978-92-5-133378-5

9 789251 333785

CB1274EN/1/10.20